

Stony Brook University



OFFICIAL COPY

The official electronic file of this thesis or dissertation is maintained by the University Libraries on behalf of The Graduate School at Stony Brook University.

© All Rights Reserved by Author.

Host-Guest Approach for 1,6-Topochemical Polymerization of Triacetylenes

A Thesis Presented

by

Zhaobo Fan

to

The Graduate School

in Partial Fulfillment of the

Requirements

for the Degree of

Master of Science

in

Chemistry

Stony Brook University

May 2012

Copyright by
Zhaobo Fan
2012

Stony Brook University

The Graduate School

Zhaobo Fan

We, the thesis committee for the above candidate for the
Master of Science degree, hereby recommend
acceptance of this thesis.

**Dr. Frank W. Fowler – Thesis Advisor
Department of Chemistry**

**Dr. Joseph W. Lauher – Thesis Advisor
Department of Chemistry**

**Dr. Andreas Mayr – Chair
Department of Chemistry**

**Dr. Nancy S. Goroff – Third Member
Department of Chemistry**

This thesis is accepted by the Graduate School

Charles Taber
Interim Dean of the Graduate School

Abstract of the Thesis

Host-Guest Approach for 1,6-Topochemical Polymerization of Triacetylenes

by

Zhaobo Fan

Master of Science

in

Chemistry

Stony Brook University

2012

Since Shirakawa et al. discovered the promising electrical conductivity of polyacetylene in the 1970s, polyacetylenes and their analogues have been extensively explored as advanced materials. Among them, polytriacetylenes are a new class of conjugated polymers that can only be achieved by topochemical polymerization. Theoretically, topochemically polymerizing the triacetylene monomers is the most direct route to get polytriacetylene. However, the challenge in 1,6 polymerization is to get the suitable molecular spacing for the topochemical reaction.

Host-guest strategy was developed to achieve the specific spacing suitable for topochemical polymerizations, such as 1,4 and 1,6- polymerizations. After optimizing the previous synthesis route and crystal growing method, a quality co-crystals of 3-((3-(pyridin-4-yl)propyl)amino)cyclohex-2-enone and dodeca-4,6,8-triynedioic acid was successfully prepared. The co-crystal, with repeat distance of 7.25 Å, underwent a 100% polymerization at 115°C over 19 days. X-ray diffraction was used to characterize all monomer and polymer crystals.

Another attempt has been made to design and synthesize a triacetylene that assembled due to π - π interaction. This pyridyl-substituted triacetylene was successfully synthesized in a five-step route. X-ray diffraction was utilized to characterize the single crystal of octa-2,4,6-triyn-1,8-diyl dinicotinate which indicated the repeat distance of 7.408 Å. This value meets the ideal requirement for 1,6- polymerization.

Table of Contents

Table of Contents	iv
List of Figures	vi
List of Tables	viii
List of Schemes	ix
I. Introduction	1
1. Conjugated polymers (CPs)	1
1.1 Strategies to modify the effective conjugation	6
1.2 Synthetic Strategy to Linear π -Conjugated Polymers	7
1.3 Synthetic Strategy for the Non-linear π -Conjugated Polymer	11
2. Supramolecular Chemistry	12
3. Hydrogen Bonding--- A significant intermolecular interactions	14
II. Some applications of Supramolecular Chemistry	26
1. Topochemical reaction	27
2. Host-Guest Strategy	27
2.1 Synthesizing Polydiacetylene by using Host-Guest strategy	28
2.1.1 Pre-organization for Polytriacetylene (PTA)	31
2.1.2 Host-Guest Strategy in preparing PTA.	33
3. Research Goal	39
III. Results and Discussion	42
1. First Project: Preparing the Host and Guest for 1,6-Polymerization	42
1.1 Synthesis of Triacetylene Guest	42
1.2 Synthesis of Host	43
1.3 1,6-polymerization of triacetylene.	47
2. Second Project: Preparing the π - π stacking Triacetylene for 1,6- polymerization.	58
3. Conclusion	63
IV. Future Work	65
1. Removal of the Host from Polytriacetylene	65

2. Growing suitable single crystal of octa-2,4,6-triyn-1,8-diyl dinicotinate 20b	65
V. Experimental Section	67
1. The synthesis of the Guest molecule	67
2. The synthesis of the Host molecule	71
3. The synthesis of octa-2,4,6-triyn-1,8-diyl dinicotinate	73
4. Growing crystals	76
Reference	78
Appendix 1: Crystal Graphic Data	89
Appendix 2: NMR Spectra Data	111

List of Figures

Figure 1- 1 Structure of polyacetylenes.	1
Figure 1- 2 The structures of organic conjugated π -systems constructed with classic building block	2
Figure 1- 3 On the left: Tris(8-hydroxyquinoline) aluminum (Alq3); On the right: Poly(3,4-ethylenedioxythiophen)-polystyrenesulfonate (PEDOT: PSS)	4
Figure 1- 4 Linear Homologue of Graphite Ribbon ¹²	5
Figure 1- 5 Poly(benzobisimidazobenzophenanthroline) (BBL) ¹⁵ .	7
Figure 1- 6 Using Heck- Hagihara-Sonogashira approach to produce PPEs ¹⁹ .	8
Figure 1- 7 Using metathesis approach to produce PPEs.	9
Figure 1- 8 Using palladium catalyst to synthesize spiro with thiophene-based core ²¹ .	10
Figure 1- 9 Synthesis HT-P3HT ²² .	10
Figure 1- 10 The synthetic strategy of Diels-Alder Cycloaddition to get branched polyphenylenes	12
Figure 1- 11 Watson-Crick base pairing.	14
Figure 1- 12 Unsymmetrical and symmetric carboxylate anions.	15
Figure 1- 13 I, II, III illustrate the geometry of two, three, and four center hydrogen bonds, respectively.	18
Figure 1- 14 A) Carboxylic dimer B) Diaminopyridine ³² .	19
Figure 1- 15 Examples of one-dimensional network	20
Figure 1- 16 The Library of functionalities that self-assemble to one-dimensional π -networks.	21
Figure 1- 17 Malate anion generates β -network through hydrogen bond	22
Figure 1- 18 N, N'-disubstituted ureas generate a two-dimensional β -network.	23
Figure 1- 19 β -network is formed Pyridine-carboxylic acid hydrogen bonds	24
Figure 2- 1 Poly-acetylene, Poly-diacetylene, and Poly triacetylene	26
Figure 2-2 The spatial requirements for ideal topochemical polymerization of diacetylene ⁴³ .	29
Figure 2-3 On the left, the repeat distance of the co-crystal (oxalamide of glycine with a bis-pyridyl substituted diacetylene) is 4.97 Å. The tilt angle with respect to the axis is 43 ^{o38b} .	30
Figure 2-4 Polymerization of triacetylenes(PTA s)	33
Figure 2-5 Candidate system of aminobenzoquinone host and triacetylene guest	34
Figure 2-6 Candidate system of vinylogous amide host and triacetylene guest	35
Figure 2-7 Host-Guest structure for 1,6- polymerization	36
Figure 2-8 Vinylogous amide with succinic acid with repeating distance of 7.233 Å. Below: The observed molecular stacking of the monomer ⁴⁶ .	37
Figure 2-9 Vinylogous amide with adipic acid with packing distance of 7.26 Å. Below: The observed molecular stacking of the monomer ⁴⁶ .	38

Figure 2-10 Vinylogous amide with succinic acid with a packing distance 7.171Å. Below: The observed molecular stacking of the monomer ⁴⁶ .	39
Figure 2-11 Preparing the Host and Guest for 1,6- Polymerization	40
Figure 2-12 The pyridyl substituted triacetylenes could be assembled by π - π stacking	41
Figure 3- 1 The host molecules of Aminobenzoquinone (30a , 30b , 30c and 30d) and Vinylogous Amide (13a and 13b)	44
Figure 3- 2 (Photo) The light yellow crystal obtained from solvent (EA), evaporated very slowly. Crystal structure of vinylogous amide 13a .	46
Figure 3- 3 1,6-polymerization using first generation host 13b with two types of carboxylic acid triacetylenes 7a , 7b .	47
Figure 3- 4 Polymerization of triacetylene 7a , and vinylogous amide host 13a .	49
Figure 3- 5 No polymerization observed in the co-crystal of host 13a and triacetylene guest 7b .	50
Figure 3- 6 Co-crystal of 7a and 13a with crystal lattice data.	52
Figure 3- 7 Crystal-to-crystal 1,6-polymerization of triacetylene	53
Figure 3- 8 Molecular structure for co-crystal 7a-13a , before heating.	55
Figure 3- 9 Molecular structure for co-crystal 7a-13a , after heating 108 hours under the temperature of 115°C.	56
Figure 3-10 Molecular structure for co-crystal 7a-13a , after heating 456 hours under the temperature of 115°C	57
Figure 3- 11 (A) Molecular stacking pattern in the monomer. The repeat distance of 7.250 Å is shorter than the ideal polymerization value of 7.5 Å. (Photo) Freshly formed pink crystals of the monomer grown at room temperature (B) The repeat distance of 7.250 Å is close to the ideal distance, that allows the successful 1,6- topochemical polymerization. (Photo) Freshly formed crystals of the polymer formed through slowly annealing at 115° C.	58
Figure 3- 12 The X-ray crystal structure of 1 . The observed repeat distance is 7.252 Å, the tilt angle θ is 34°, the orientation angle ϕ is 68°, and a C1-to-C6 contact is 4.09 Å ⁴⁸ .	59
Figure 3- 13 Two forms of 3-pyridyl triacetylene 20b . On the left: 20b aggregated as a pink powder stick to the round flask. On the right: pink thin single crystal was obtained from the solvent (CH ₂ Cl ₂ /Hex=1/1).	63
Figure 4- 1 Low temperature condition for growing crystal	66

List of Tables

Table 1- 1 Hydrogen Bond Distance Observed from Purines, Pyrimidines, and Nucleosides ²⁶ .	17
Table 1- 2 The four fundamental supramolecular structures.	19
Table 2- 1 Three parameters for 1,4-topochemical polymerization	28
Table 3- 1 Crystal Lattice Data Change for the polymerization of co-crystal 7a-13a .	49
Table 3- 2 Crystal Lattice Data Change for Co-crystal of 7a-13a as Polymerization proceeds ⁴⁶	53
Table 3- 3 The change of crystal lattice data over 456 hours heating under 115°C.	54
Table 3- 4 The preliminary crystal data for compound 20b	63

List of Schemes

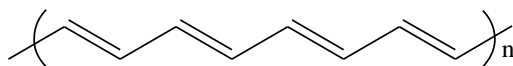
Scheme 2- 1 Synthesis of Polytriacetylene (PTA) by oxidative polymerization (TMS=trimethylsilyl, TIPS=triisopropylsilyl, TBDMS=tert-butyldimethylsilyl)	32
Scheme 3- 1 Synthesis of Triacetylene Carboxylic Acid Guest.	42
Scheme 3- 2 Synthesis of vinylogous amide host 13a .	44
Scheme 3- 3 Synthetic route for Triacetylene 20a , and 20b ⁵⁰ .	60
Scheme 3- 4 An unsuccessful attempt to optimize 3-pyridyl triacetylene 20b	61
Scheme 3- 5 The key step that cannot work out.	61
Scheme 3- 6 An alternative route for bipyridine substituted triacetylene 20b synthesis ⁵³	62

I. Introduction

1. Conjugated polymers (CPs)

Conjugated polymer materials have been studied as advanced materials for photonic and electronic applications¹. Physicists and materials scientists have discovered the extraordinary properties of conjugated compounds since the last century. In the 1970s, Shirakawa et al. reported a 10^{11} -fold increase of electrical conductivity for polyacetylene upon doping (Figure 1-1)². Nearly three decades later, for their great contribution in developing conjugated materials, Shirakawa, MacDiarmid and Heeger were awarded the 2000 Nobel Prize in Chemistry.

Figure 1- 1 Structure of polyacetylenes.

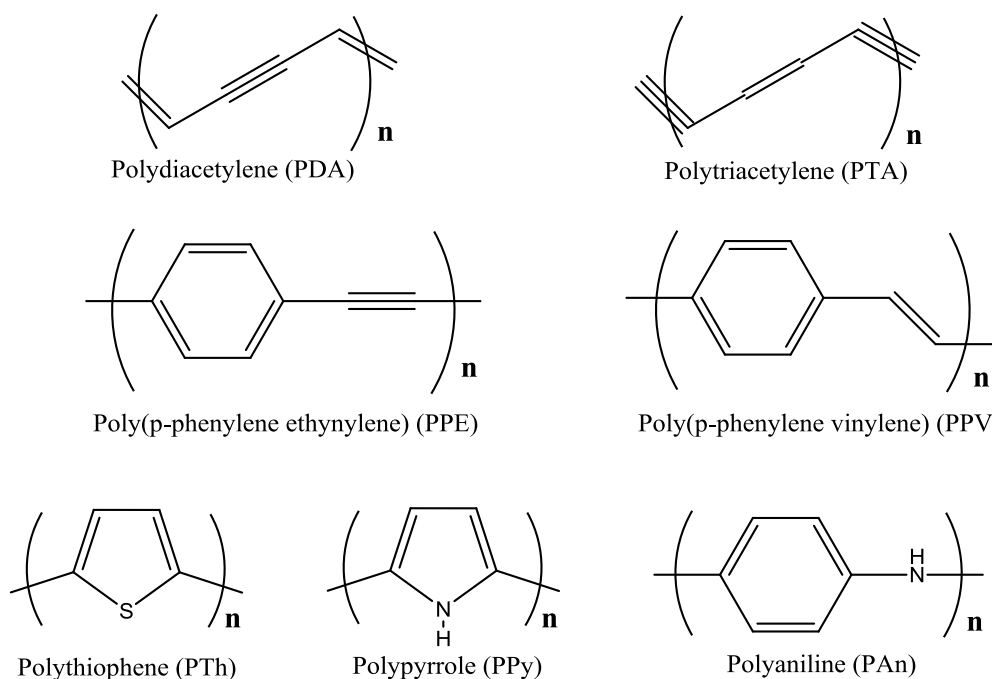


As more and more attention is paid to conjugated polymers (CPs), a variety of new CPs and their derivatives have been synthesized with enhanced properties.

Figure 1-2 demonstrates common types of CPs, including polydiacetylene, the closest relative to polyacetylene, which consists of alternate double and triple bonds. PDAs are a research topic in our group, and are correlated to my project. More details of PDA will be covered in the Chapter Two. Polytriacetylene (PTA) contains one additional acetylene group in the repeat unit. The synthesis of PTAs is the main theme of this thesis. Other π -conjugated polymers, such as the alternating copolymer

poly(para-phenylene vinylene) (PPV), as well as poly(para-phenylene ethynylene) (PPE), or poly(para-phenylene) (PPP), are also widely studied as analogues to PA. The hydrocarbon polymers, containing aromatic rings, such as polypyrrole (PPy), polythiophene (PTh), and polyaniline (PAn), are also of great interest for their electronic or photonic properties.

Figure 1- 2 The structures of organic conjugated π -systems constructed with classic building block



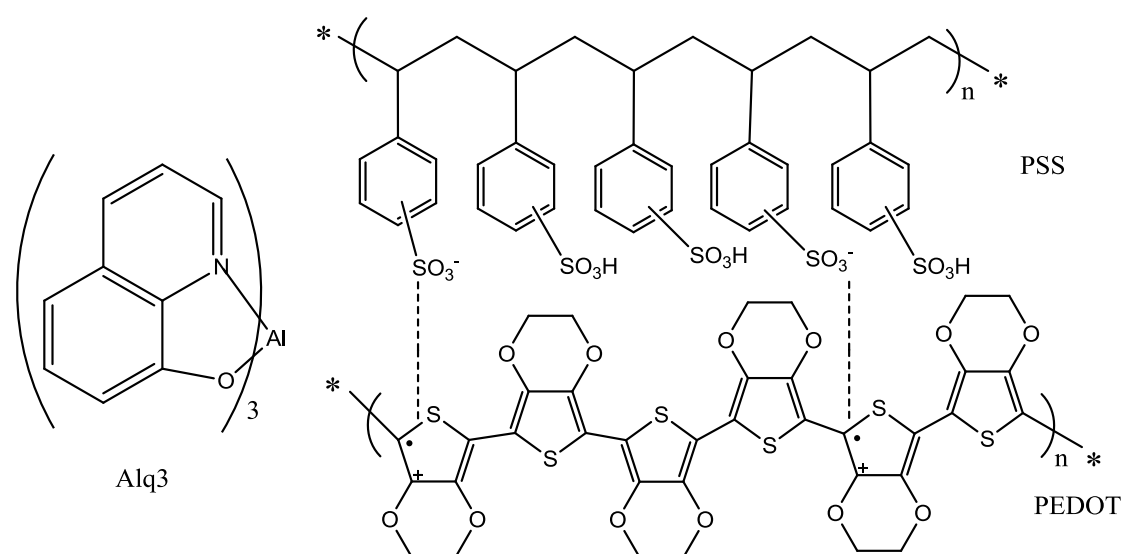
On the molecular level, the crucial characteristic of all conjugated polymers is the quasi-infinite π system extending along the polymer. The great length of the conjugated polymers makes them a material with directional conductivity. The optical and electronic properties of these highly conjugated materials are determined by the band gap between π -bonding orbitals and π -antibonding orbitals.

Any tiny variations of the molecular structure in conjugated polymers will directly influence the absorption, emission and charge transport properties of the polymer³. The various physical properties of polymer materials motivate the research effort by academia and industry to study further such properties as magnetism⁴, photoconductivity⁵, conductivity⁶, electronically stimulated light-emission⁷, photorefractivity⁸, field-effect charge mobility (field-effect transistors)⁹, and nonlinear optical properties. Another promising property of these organic materials is their applications as photodiodes, solar cells, and bio-sensors¹⁰. Compared to inorganic compound, the advantage of organic conducting polymers is the synthetic flexibility. Organic materials are of low cost, and have ease of processing. The traditional ways to process organic polymers are spin coating, inkjet printing, and casting from solution.

With advantages as the photonic and electrical devices, the applications of organic conducting polymers are very widely studied. Until recently, they have combined inorganic conducting materials in some specific applications. Organic light-emitting diodes (OLEDs) have entered into the electrical market as a low-resolution display material produced by Kodak, or Philips. Four or five years ago, the high definition television (HDTV) with high resolution display capacities hit the market. The most significant discovery in the field of organic electronics occurred when Tang and Van Slyke reported the first electroluminescent device in 1987. This kind of device is based on tris(8-hydroxyquinoline) aluminum (Alq₃) (see Figure 1-3) which is a π -

conjugated molecular material. In 1990, Friend and co-workers design the electroluminescent polymer- poly(para-phenylenevinylene)(see Figure 1-2), which laid the foundation for polymer light-emitting diodes (PLED)¹¹. Poly(3,4-ethylenedioxythiophen) -polystyrenesulfonate (PEDOT:PSS) (see Figure 1-3) is another example for CP's application. It was first introduced by Bayer AG Germany in 1990s, and was famous for its electronic and optoelectronic applications such as antistatic coating in photographic films, and the material for capacitor electrodes.

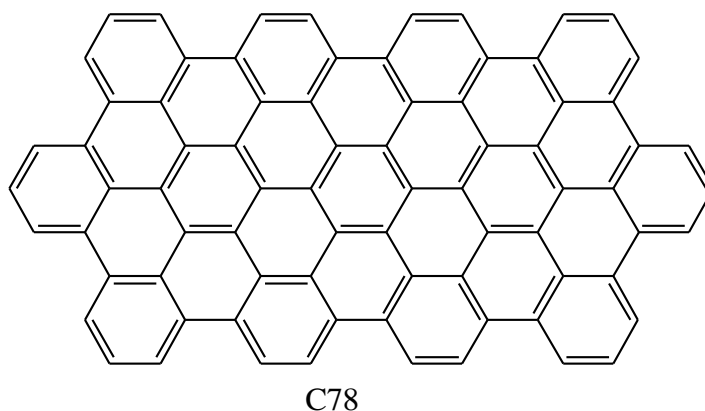
Figure 1- 3 On the left: Tris(8-hydroxyquinoline) aluminum (Alq3); On the right: Poly(3,4-ethylenedioxythiophen)-polystyrenesulfonate (PEDOT: PSS)



The conjugation at a molecular level and the electronic interactions at supramolecular level must both be considered when we discuss dimensionality of organic conjugated polymers. CPs are linear conjugated polymers, or one-dimensional systems, compared with two translational parts such as extended conjugated

molecules that look like a disk are in the category of two-dimensional systems. Some two-dimensional system molecules like ladder or ribbons are of great attraction to scientists¹² (Figure 1-4). Three-dimensional networks contain conjugated fragments which electronically interact with each other to form three-dimensional conjugation.

Figure 1- 4 Linear Homologue of Graphite Ribbon ¹²



Although organic conjugated polymers have promising advantages over inorganic materials, there still exist some difficulties in synthesis. One problem we have to face is concerned about non-linear optical properties of CPs. The weak non-linear optical properties can be overcome by increasing the effective conjugated length, which is the number of the units repeated in the whole polymer¹³. To further optimize the conjugated polymers, comprehensive characterization and analysis of the chemical and physical properties are required. Poor solubility is always the obstacle for us to resolve conjugated polymers in organic solvents. Another challenge we meet is the structural instability during the course of synthesis, workup, and processing. We will

discuss the synthetic strategies that are widely applied to resolve some of these problems.

1.1 Strategies to modify the effective conjugation

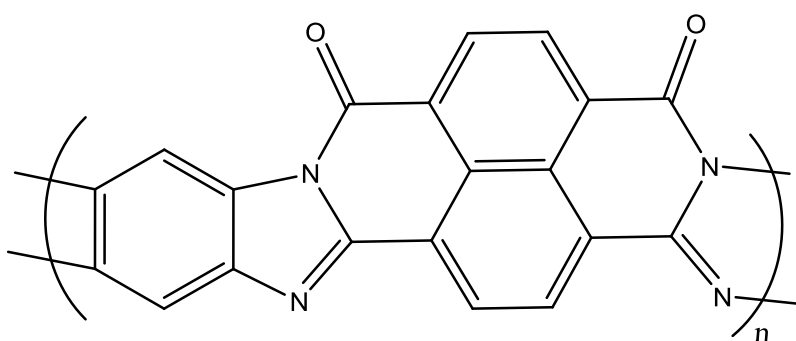
For a conjugated polymer, the charge moves along the chain via π - electron conjugation. This is the source of optical non-linearities, on molecular level. The macroscopic second-order nonlinearity is determined by the centrosymmetry of the crystal structure. Third order nonlinearity, isn't affected by crystal symmetry, but instead, by the macroscopic third-order susceptibility¹⁴. Among various kinds of advanced materials, π - conjugated polymers possess the greatest non-linear optical applications. The investigation on the control of effective conjugation length, packing structures, and the intermolecular interaction are still ongoing.

A large number of attempts have been devoted to modify the conjugation of PA s. For instance, polyphenylacetylene (PPA), with high molecular weights, are stable while heating, and also have good solubility in organic solvents.

When evaluating semiconductors, the efficiency of charge transportation between holes and electrons is important. In 2003, Jenekhe and co-workers reported a kind of double-stranded (ladder) polymer BBL which possesses high electron mobility in a π - conjugated system¹⁵.

Jenekhe also further characterized this material. The glass transition temperature was higher than 500°C, which indicates the excellent thermal stability of BBL, see figure 1-5. Meanwhile, Jenekhe attributed this high efficiency of electron mobility to the rich nitrogen and oxygen heteroatoms in this polymer.

Figure 1- 5 Poly(benzobisimidazobenzophenanthroline) (BBL)¹⁵.



1.2 Synthetic Strategy to Linear π -Conjugated Polymers

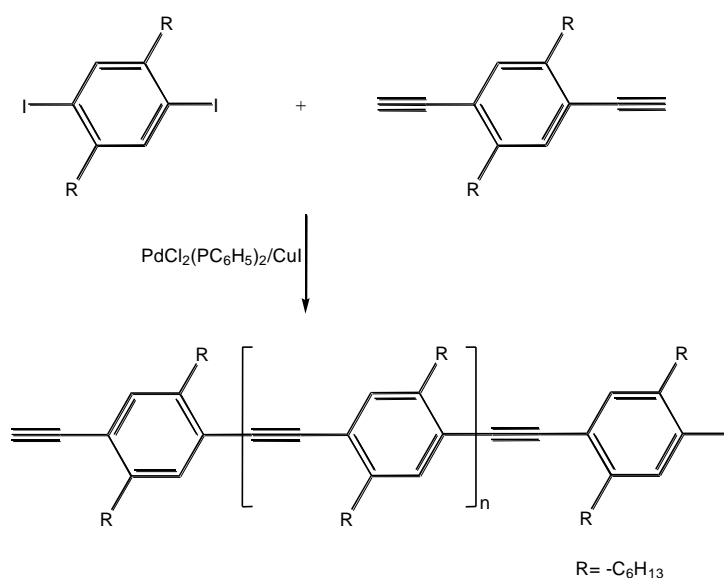
A reliable synthetic strategy, which could provide a perfect formation and processable system is a requirement for the synthesis for π -conjugated polymers. The supramolecular order, in two or three dimension, should be controlled through self-assembly which depends upon the chemical behavior of the synthesized compound. Linear π -conjugated polymers are one-dimension molecules with extended delocalization of electrons along the backbone.

Poly(phenyleneethylene)s (PPEs), for example, possess a π - π conjugated system with perfect uninterrupted charge transportation, which attracts attention in this area.

Swager¹⁶, Mullen¹⁷ and Weder¹⁸ reported the unique property of PPEs which could be applied into the areas such as explosive detection, molecular wires in bridging nanogaps, and LC displays.

The first route for the synthesis of PPEs is Heck-Cassar-Sonogashira- Hagihara reaction (Figure 1-6). It is catalyzed by a palladium catalyst to couple the terminal alkynes to aromatic bromides or iodides.

Figure 1- 6 Using Heck- Hagihara-Sonogashira approach to produce PPEs¹⁹.

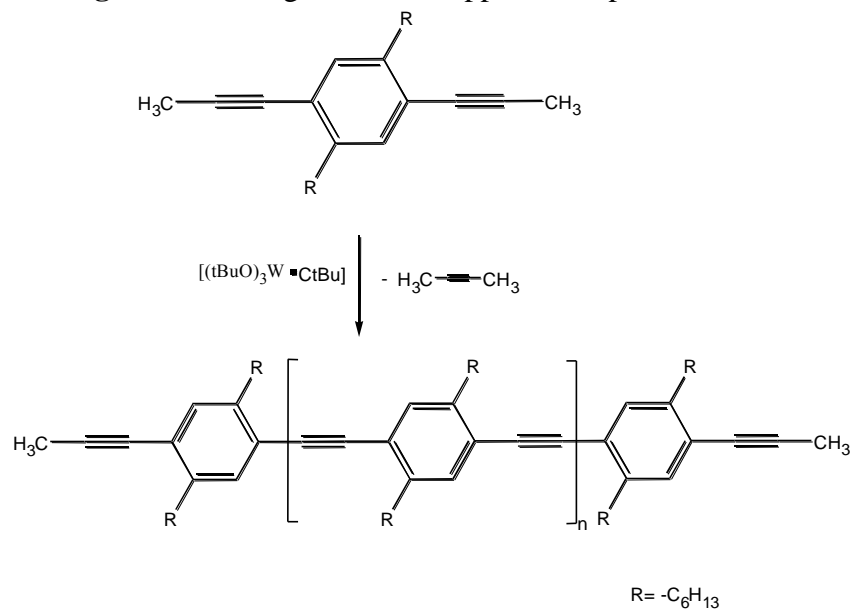


However, there are some drawbacks of this synthesis route for the use of Pd¹⁹. Low molecular weights of side products are obtained even in optimum conditions; the defects are formed; No long π -conjugated compounds are produced; instead, only moderate and low molecular polymers form.

A more efficient synthesis route was studied and further developed by Weiss and Müllen in 1996²⁰. They modified the reaction by using Schrock's tungsten-carbyne to get higher molecular weight polymers (Figure 1-7). Nevertheless, due to the complicated preparation for Schrock's catalyst and its high sensitivity to air and water, this strategy is still unpractical. In 2000, Bunz et. reported the optimized reaction condition of alkyne metathesis by using $\text{Mo}(\text{CO})_6$ ¹⁹.

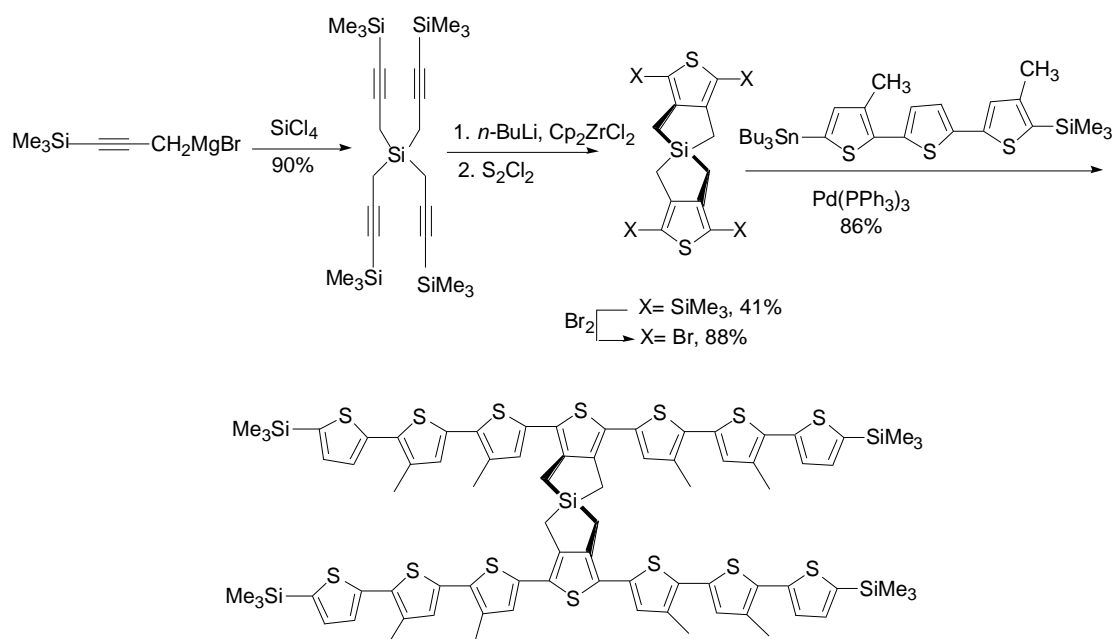
As mentioned in the case of BBL¹⁵, hetero-atoms contained in the repeat unit always affect the electrical and/or thermal dynamical properties. Sulfur, for instance, plays a significant role in improving the thermal stability of thermoplastic materials.

Figure 1- 7 Using metathesis approach to produce PPEs.



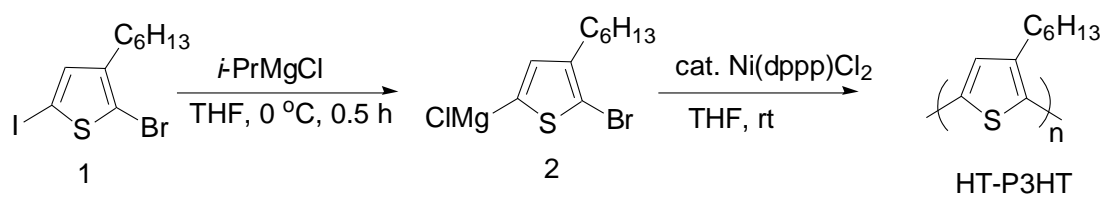
This Pd catalysis method can be also applied to synthesize the spiro compound below²¹.

Figure 1- 8 Using palladium catalyst to synthesize spiro with thiophene-based core²¹.



It is difficult to get the desired polymers with particular molecular weight and low polydispersity by controlled polymerization. The synthesis route shown in Figure 1-9 is a way to minimize the polydispersity and grow the molecular weight by chain propagation²².

Figure 1- 9 Synthesis HT-P3HT²².



1.3 Synthetic Strategy for the Non-linear π -Conjugated Polymer

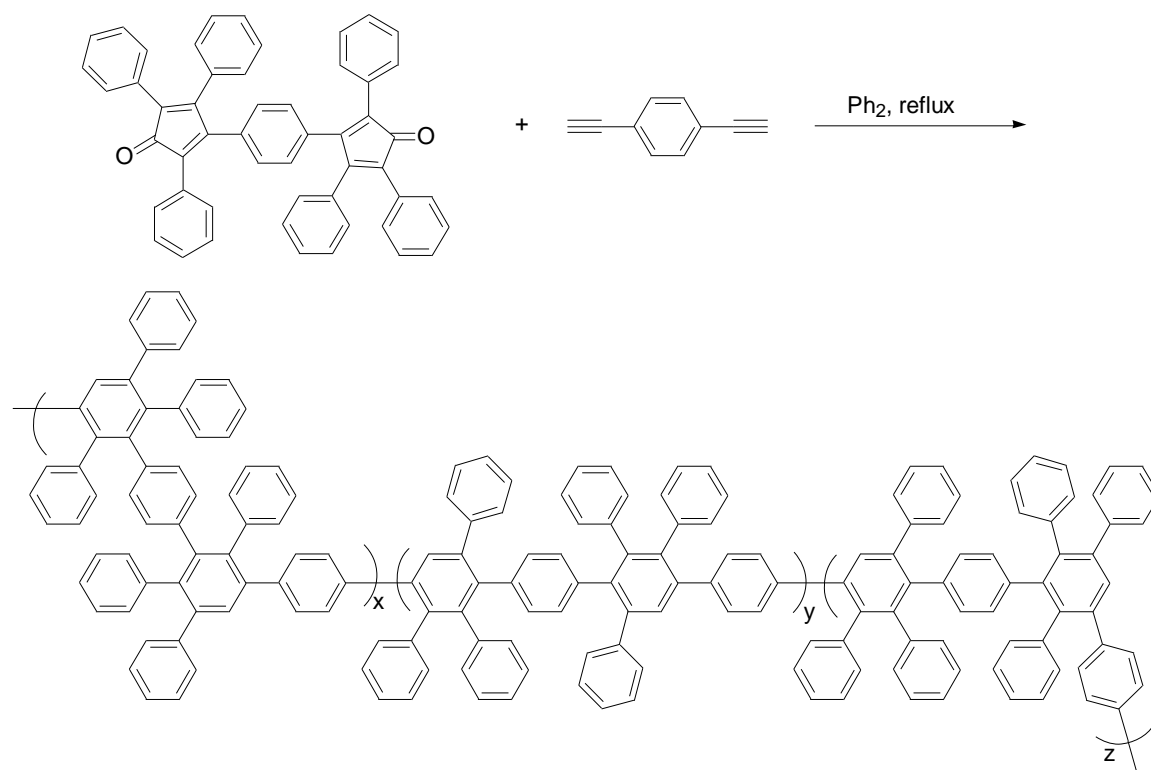
For π -conjugated polymers, the synthesis method and its characterization are both challenges in the field of synthetic chemistry. As far as we know, there are mainly three different routes of synthesis that are widely applied¹².

1. Repeating Diels-Alder cycloaddition of tetraphenylcyclopentadienones with arylolethynyls to obtain three dimensional branched oligophenylenes.
2. cobalt-catalyzed cyclotrimerization of diarylethynyls.
3. Oxidative cyclodehydrogenation the existing three dimensional polyphenylene precursors with FeCl_3 or $\text{Cu}(\text{OTf})_2\text{-AlCl}_3$ to obtain graphite segments of a two-dimensional network.

As shown in figure 1-10, the repetitive Diels-Alder cycloaddition of 1,4-diethynylbenzene and bis(tetraphenylcyclopentadienoneyl)-benzene yields high molecular branched polyphenylenes.

Those two methods have been proved to be practical and effective. One can obtain the two-dimensional conjugated polymers via these reliable synthetic approaches.

Figure 1- 10 The synthetic strategy of Diels-Alder Cycloaddition to get branched polyphenylenes



2. Supramolecular Chemistry

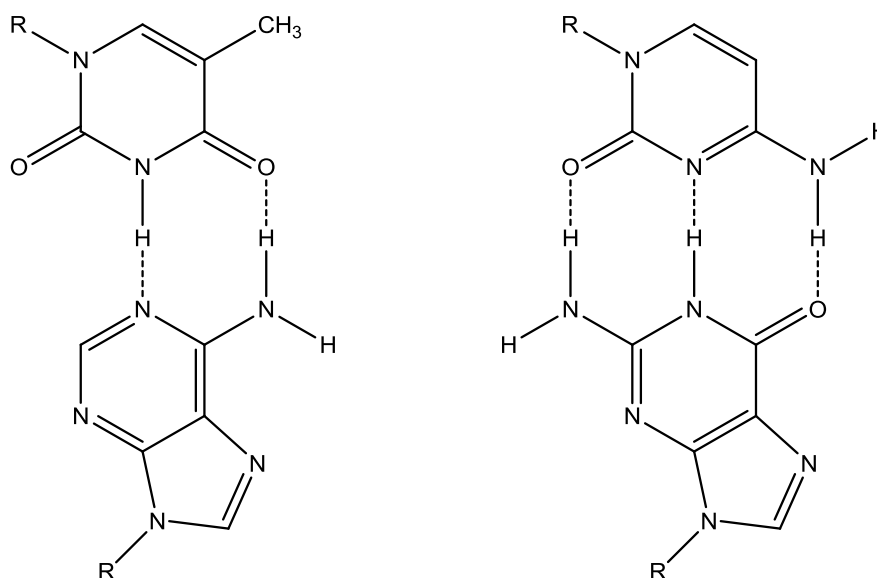
As mentioned in the last section, two or three-dimensional networks can be attained through self-assembly, and therefore leading to varying physical properties of the synthesized conjugated polymers. In this section, we will discuss supramolecular chemistry, and self-assembly.

Jean-Marie Lehn defined supramolecular chemistry as “the chemistry of molecular assemblies and of the intermolecular bond”²³. In supramolecular chemistry,

various intermolecular/intramolecular forces are considered, such as π - π interactions, van der Waals, ion-ion interaction, dipole-dipole, hydrogen bonding and many other forces. Also, supramolecular chemistry involves in the non-covalently connected molecule, the intermolecular interactions between them, and higher ordered complexes beyond covalent bonds.

Compared to other disciplines of chemistry, supramolecular chemistry is young, dating back to the 1970s. However, it has been one of the fastest growing fields of chemistry. This discipline was inspired and originated biological chemistry found in living systems. In nature, there are millions of supramolecular structural models. The most classic supramolecular structure is the DNA double-stranded helical structure²⁴. The effect of four nucleobases pairing and π - π stacking into the double-stranded helical structure is the perfect example for self-assembly. The four nucleobases(adenine(A), thymine(T), cytosine(C), and guanine(G)) form two kinds of complementary hydrogen bond pairs (Watson-crick base pairing), see figure 1-11, which specifically convey the information of molecular recognition and organization²⁵. Effort has been exploited in supramolecular chemistry in order to model biological processes and to discuss more sophisticated abiotic analogues.

Figure 1- 11 Watson-Crick base pairing.



3. Hydrogen Bonding--- A significant intermolecular interactions

Dipole-dipole and ion-ion interactions, Van derwaals forces, π - π stacking, and hydrogen bonding are different types of intermolecular interactions. The intermolecular interactions differentiate from strength, and which thereby determines the crystal structures of supramolecules.

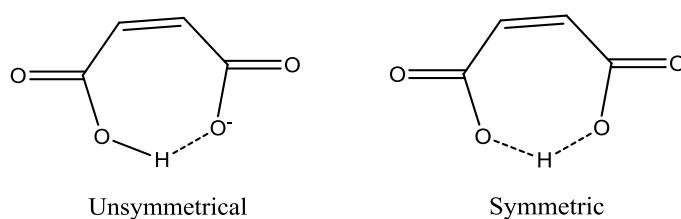
These interactions are also the prerequisite for greater crystal stability. An illustration of medium-range force is the Van der Waals interaction.

Hydrogen bonding is the donor-acceptor interaction involving hydrogen atoms. In Pauling's theory, the hydrogen bond is formed when the more electronegative atom A (compared to the hydrogen atom that in a covalent bond of A-H) withdraws electrons. The loss of electrons leave the proton partially charged. The hydrogen

acceptor B, provides lone-pair electrons or polarizable electrons²⁶. The strength of hydrogen bonds varies from very strong bonds, which are similar to covalent bonds, to weak hydrogen bonds, which are comparable to Van der Waals forces. Bond energy of hydrogen varies from 15 to 40 kcal/mol⁻¹ for a strong bond, 4 to 15kcal/mol⁻¹ for moderate bond and 1 to 4kcal/mol⁻¹ for a weak bond.

Figure 1-12, shown below, is another illustration for strong hydrogen bond. These half protonated carboxylate anions generate either a symmetric or unsymmetrical hydrogen bond.

Figure 1- 12 Unsymmetrical and symmetric carboxylate anions.



In this case of symmetric hydrogen bond, the proton is spaced at the center of the two oxygen atoms, which makes the distance between hydrogen and each oxygen less than 2.56 Å. While in unsymmetrical hydrogen bond, proton is alternating around two hetero atoms, and the distance of O---O is greater than 2.56 Å. In 1995, Zimmerman et al. also reported their research on the symmetric hydrogen bonding. The molecule they discussed about is the crystallization of trimesic acid in two-dimensional network, which finally formed zeolite-like channels inside the crystal²⁷. Usually, the energy assigned to this type of bond ranges from 15 to 40kcal/mol.

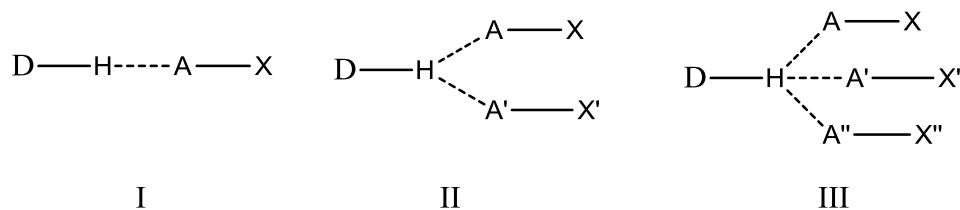
Moderate Hydrogen Bonds are consisted of neutral donor and acceptor groups. P-OH----O=C, R₃-N-H----O=C, OH----N, N-H----P. This sort of hydrogen bonding is common in chemistry and biological system, which is viewed as normal hydrogen bonds. Moderate hydrogen bonds play significant role in determining supramolecular structures, packing style, solvation and conformation especially in biological systems where hydrogen bonding between nitrogen and oxygen atoms are common. Amines, alcohol, carboxylic acids and amides are common functional groups that involve in moderate hydrogen bonding. From the perspective of Etter, the existence of such functional groups always cause the hydrogen bonds in solid state²⁸. The energy of moderate hydrogen bond ranges from 4 to 15kcal/mol and bond distance between donor and acceptor is in the range of 2.5-3.2 Å²⁹. Jeffrey and co-workers reported a series of distances between donors and acceptors, which is based on the survey among the crystal structures of purines, pyrimidines, nucleosides, and nucleotides²⁶ (Table 1-1). The table shown below demonstrates a varying distance of hydrogen bond in different molecules

Table 1- 1 Hydrogen Bond Distance Observed from Purines, Pyrimidines, and Nucleosides²⁶.

Type of Bond (D-H---A) Å	Observed Range of D(H—A) Å
O-H---O=C	1.63-2.65
O-H---N=	1.71-2.62
N-H---O=C	1.69-2.32
N-H---N=	1.73-2.23
N-H---O-H	1.72-2.16

Bonding distances depends on the strength and size of the donor-acceptor molecules. Although hydrogen bond data listed above can be useful when comparing qualitatively donor and acceptor strength, they fail to provide the information on bond energies according to Burgi and Dunitz³⁰. X-ray diffraction is a reliable method for us to determine where the hydrogen bond is spaced because that X-rays scattered by electrons where concentrated around the heavier atom. On the other hand, neutron diffraction avoid the problem for the centers it scatters are atomic nuclei, and the distances calculated from neutron diffraction are close to the interatomic distances.

Figure 1- 13 I, II, III illustrate the geometry of two, three, and four center hydrogen bonds, respectively.



Weak hydrogen bonds are formed when one of the two atoms has low electronegativity such as in C-H, Si-H, or when the lone pairs are absent in the acceptor group, but π -electrons still exist in aromatic rings and carbon-carbon triple bonds. Until Taylor and Kennard's research in the C-H hydrogen bonds, these bonds were generally omitted by crystallographers since their contact radii are close to Van der Waals's³¹. In their report, a number of hydrogen bonds (C-H \cdots X) are demonstrated to be responsible for crystal packing. From the perspective of Dougall and Jeffrey²⁶, the dimethylzolate crystal has a relatively high melting point, and a difference between liquid and solid state was observed in IR spectra. All of which, concluded by Dougall and Jeffrey, are due to the hydrogen bonds C-H \cdots O.

Defined by the degree of translational symmetry, supramolecular structures are categorized by four crystallographic symmetries: discrete assemblies, α -, β -, and γ -networks (Table 1-2). No matter what symmetry the structure is, hydrogen bond is definitely the most important portion that builds up the supramolecular structure.

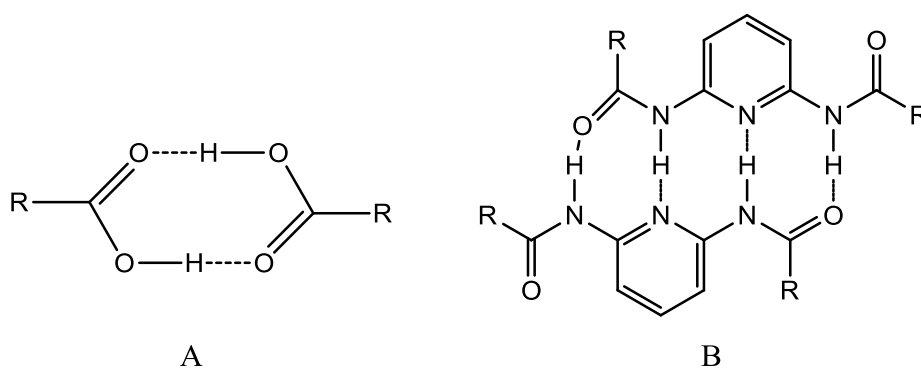
Table 1- 2 The four fundamental supramolecular structures.

Structure Type	Translations	Group Symmetry
Discrete assembly	No translation	Point group symmetry
α -network	One-direction	Rod group symmetry
β -network	Two directions	Layer group symmetry
γ -network	Three dimensions	Space group symmetry

A. Discrete Assembly

Discrete assembly is a kind of supramolecular complex without translational symmetry. It contains small, finite molecules that are alike or unlike, which generate symmetrical or asymmetrical operators. Figure 1-14 **A** shown below, demonstrates the centrosymmetric carboxylic acid dimer which is widely applied in supramolecular engineering, and the other example (**B**) is the diaminopyridine derivative designed and made by Beijer FH³².

Figure 1- 14 A) Carboxylic dimer B) Diaminopyridine³².

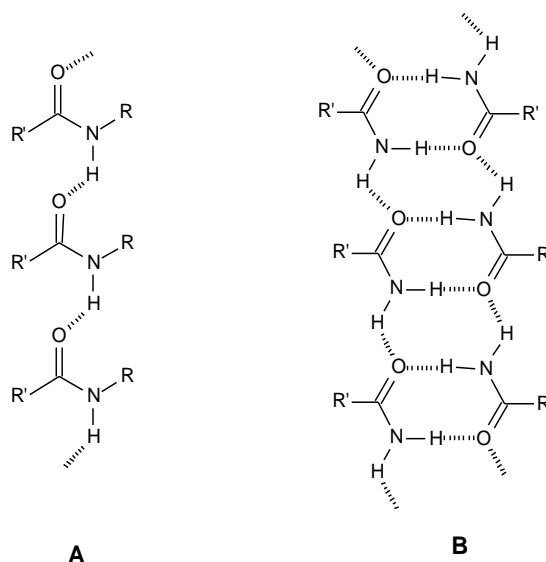


B. One Dimensional α -Networks

The simplest network has one degree of translational symmetry is one dimensional α -network, which defined by its rod group symmetry. Often, it is the interaction of primary and secondary amides that generate one-dimensional networks.

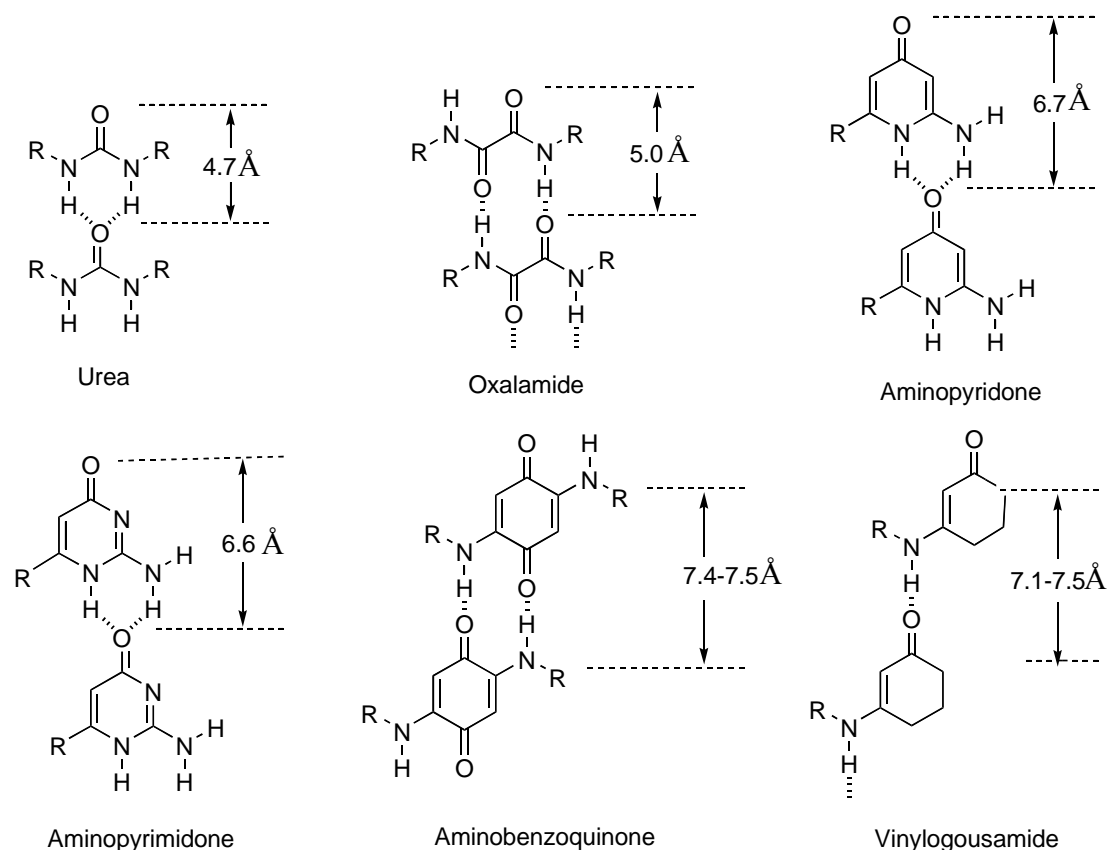
The networks generated have “infinite” number of molecules³³.

Figure 1- 15 Examples of one-dimensional network



In order to study the self-assemblies in one-dimensional networks, Fowler and Lauher set up a library of functionalities (Figure 1-16)³⁴. Different hydrogen bonding groups, each with its own translational repeat distance, determine each of the functionality. A particular spacing of molecules can be designed or engineered by choosing a certain functionality to give corresponding spacing.

Figure 1- 16 The Library of functionalities that self-assemble to one-dimensional π -networks.

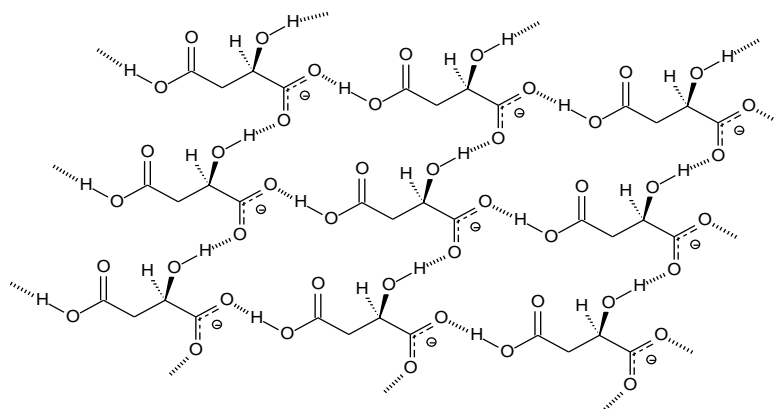


C. Two-Dimensional β -Network

In comparison with one dimensional α -network, a β -network is more complicated. It can be determined by various intermolecular interactions and it has two degrees of translational symmetry. Hydrogen bonding based β -networks require polyvalent planar molecules, which contains three or more hydrogen bonding functionalities³⁵. However, only stronger intermolecular interactions can determine the structure. Aakeroy reported the carboxylic-carboxylate hydrogen bond from malate anions or oxamate, which is a good example of layer by layer β -network made

by hydrogen bonds³⁶. As Figure 1-17 shows, one dimension is determined by carboxylate-carboxylic acid hydrogen bond while the other direction is by the alcohol-carboxylate hydrogen bond.

Figure 1- 17 Malate anion generates β -network through hydrogen bond

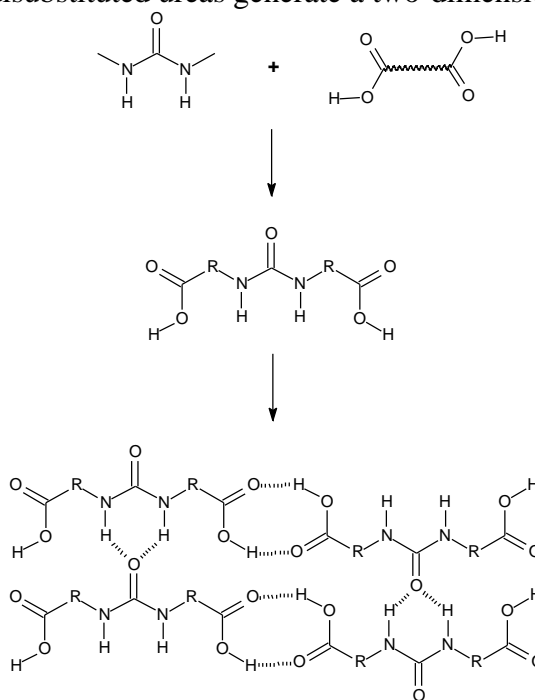


When molecular protrusions from one plane fit into hollow up and down to maximize Van der Waals forces, an assembly of two-dimensional sheets is achieved. β -networks also possess sub-structures that, as well, can be defined as independent α -networks or discrete assemblies. Consequently, a β -network can be only produced whenever a designed molecule have nonparallel and independent hydrogen bond groups or 'sticky ends'. Recently, by employing two orthogonal hydrogen bonding functional groups, Fowler and Lauher successfully developed the designed β -networks.

Previously, ureylenedicarboxylic acid and N, N'-disubstituted ureas are thought to be the functionalities that predictably and reliably construct one-dimensional α -

networks³⁷. Once combined into a single molecule, these two functional groups generate a series of ureylenedicarboxylic acid derivatives (Figure 1-18). The molecule's translation makes the urea α -networks. The carboxylic acid groups can form the centro symmetric dimers about inversion center to attach the urea α -networks to β -networks. P2/c layer group can be obtained by adding an inversion operator to the P2 rod group of the urea network. The ureylene derivative can have either symmetrically or asymmetrically disubstituted product. The ureylene derivatives can be characterized by X-Ray crystallography, which structural analysis reveals the solid-state structure featured the predicted two-dimensional β -network with a molecular repeat distance along the urea α -network of 4.5-4.7 Å.

Figure 1- 18 N, N'-disubstituted ureas generate a two-dimensional β -network.



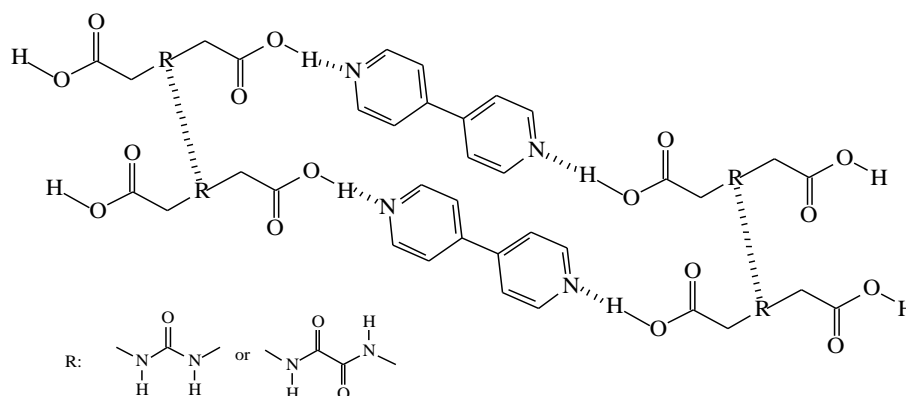
D. Three Dimensional γ -networks

Three-dimensional γ -network possess three degrees of translational symmetry which characterized by space group symmetry. It can be achieved in molecules by forming three nonparallel and independent α -networks. The γ -network structures is not going to be demonstrated by example here.

E. Binary β -Network System

A binary system can be viewed as the combination of two different molecules in a supramolecular fashion. To obtain a binary system, strong and reliable intermolecular contacts are prerequisites. In 1995 and 2000, Fowler and Lauher reported the associated-two-molecule that is interconnected by strong pyridine-carboxylic acid hydrogen bond³⁸. The urea to urea, the oxalamide to oxalamide and the pyridine-carboxylic acid hydrogen bonds are all possible interactions that form β -networks, see figure 1-19.

Figure 1- 19 β -network is formed Pyridine-carboxylic acid hydrogen bonds



Using the binary system is another way to help us constructing a desired supramolecular structure. The functionality that two molecules provide is essential for the design of molecular network and a structure feature of interest. In this way, the desired structure, such as a photochemical chromophore, a magnetic center, or a monomeric unit for a solid- state reaction, can be successfully distributed into two linked molecules. The benefit of this binary system is more efficient and less demanding molecular synthesis process than mono-molecular system.

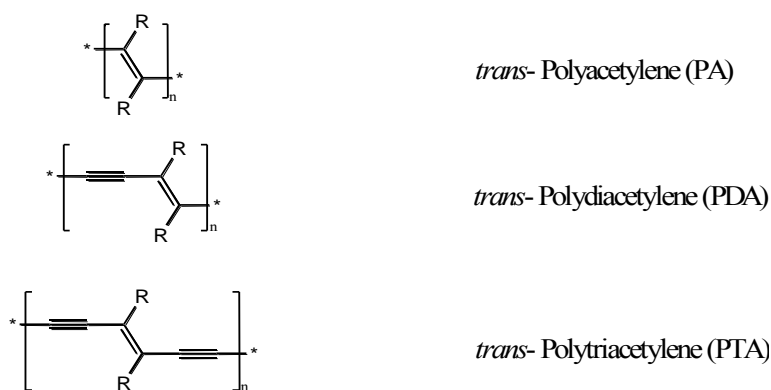
II. Some applications of Supramolecular Chemistry

---- The Host and Guest strategy

As it introduces in the first chapter, the promising perspectives and the difficulties of π -conjugated polymers make them mysterious and attractive to us. In this chapter, we will focus on one particular family of polymers (Figure 2-1)-- polyacetylenes and its monomer, which have great meaning for the future advanced materials. Various synthesis strategies have been applied to produce the target compound.

Among all of them, the Host-Guest strategy demonstrated the most reliable result. Therefore, more details of this strategy will be discussed in the following section.

Figure 2- 1 Poly-acetylene, Poly-diacetylene, and Poly triacetylene



To better apply the supramolecular chemistry knowledge into the strategy of synthesis we need to know some generic terms.

1. Topochemical reaction

This is a chemical reaction that occurs in solid phases. It is usually influenced and controlled by the condensed media. Since 1950's, Cohen and Schmidt did a series of research in the solid-state reactions of organic compounds³⁹. Their research helps us to systematically understand how the geometry of the reactant lattice determines the types of solid-state reactions, particularly in photo-induced reactions. Based on the study of photochemistry of the aminocinnamic acids and the extensive research, they confirmed the topochemical postulate proposed by Kohlschutter in 1918⁴⁰. From the perspective of Kohlschutter, the reactions in crystals proceed with a minimum of atomic and molecular movement.

2. Host-Guest Strategy

There are mainly two approaches to the synthesis in the area of supramolecular chemistry: One is using single molecules; the other is utilizing host-guest/co-crystal strategy. In supramolecular synthesis, knowing the ways in which inter- and intra-molecular forces control packing of molecules is the crucial point designed topochemical reaction. The host-guest strategy could simplify the synthesis route and design. With a proper design, host and guest molecules can self-assemble into hydrogen connected networks. Both host and guest molecules can provide functionality in this system. In the past years, our group focused on the functionality of host molecules in order to make the host-guest strategy work well. A library of

functionalities is shown in Chapter 1, see Figure 1-16.

2.1 Synthesizing Polydiacetylene by using Host-Guest strategy

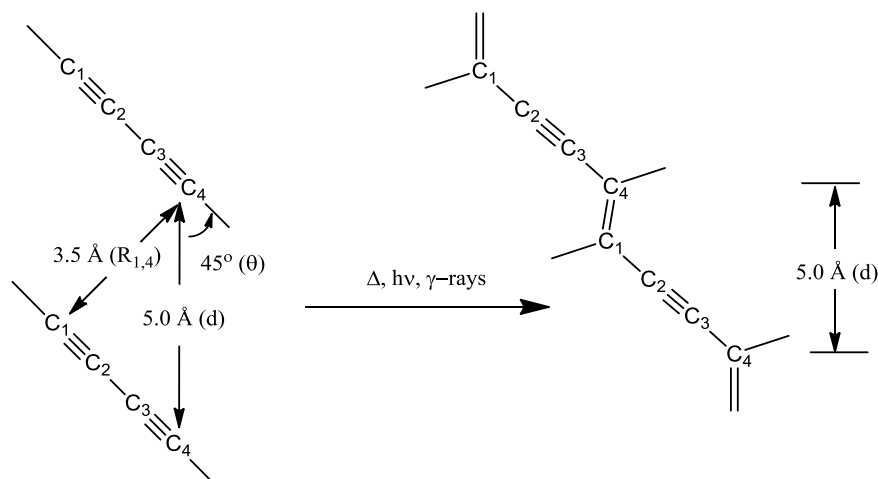
In 1969, Wegner firstly reported the synthesis of Polydiacetylene (PDA)⁴¹. Prior to his research, polyacetylenes(PA s) were mainly made in solution. Although PAs and their derivatives are easier prepared than the polymers (Figure 1-2), the PDA is obviously an exception. Instead of forming in solution, PDA is only accessible through topochemical polymerization. A organized pattern of diynes is needed for 1,4-polymerization. This kind of topochemical polymerization is unique for the reason that the chain polymerization occurs between monomer single crystals to produce the polymer single crystal⁴². This topochemical reaction involves 1,4-addition to form the extended conjugated polymer. This solid-state polymerization of acetylene depends on three parameters as far as we know. And a good control of these parameters will give us a clean single crystal. These three parameters are shown below.

Table 2- 1 Three parameters for 1,4-topochemical polymerization

R	Intermolecular distance between reacting carbons	$< 4\text{\AA}$
d	Distance between neighboring diacetylene	$< 5\text{\AA}$
θ	Inclination angle between stacking axis and diacetylene rod	45°

Enkelmann and Baughman pointed out that in order to maximize the reactivity of center for polymerization of diacetylene monomer, monomers should be organized layer by layer at proper orientations⁴³, see Figure 2-2.

Figure 2-2 The spatial requirements for ideal topochemical polymerization of diacetylene⁴³.



As shown in Figure 2-2, the intermolecular repeat distance is 5.0 Å. This distance is the same to that of its corresponding polymer. Although there is a great difference of the alignment between diacetylene and PDA, the stacking space remains constant. The monomer's tilt angle should be 45° with respect to the axis.

However, the problem of making PDA with 1,4 addition is that the guest molecules (diacetylene monomers) often fail to self-assemble into precursor structures with parameters needed for topochemical polymerization. Unfortunately, a general procedure for organizing diacetylenes to self-assemble is not available.

In previous years, our group has worked on aligning diacetylenes effectively for their topochemical polymerization. We use a Host-Guest Strategy. To attain our goal, we established a library of functional groups that assemble into one-dimensional network, each of these molecules is distinguished by intermolecular spacing

parameter. After that, we designed and synthesized host-guest systems to meet the ideal requirement for topochemical 1,4- polymerization.

The first successful example of self-assembled topochemical polymerization is achieved by co-crystallizing the oxalamide of glycine with a bispyridyl-substituted diacetylene^{38b}.

Figure 2-3 On the left, the repeat distance of the co-crystal (oxalamide of glycine with a bis-pyridyl substituted diacetylene) is 4.97 Å. The tilt angle with respect to the axis is 43°^{38b}.

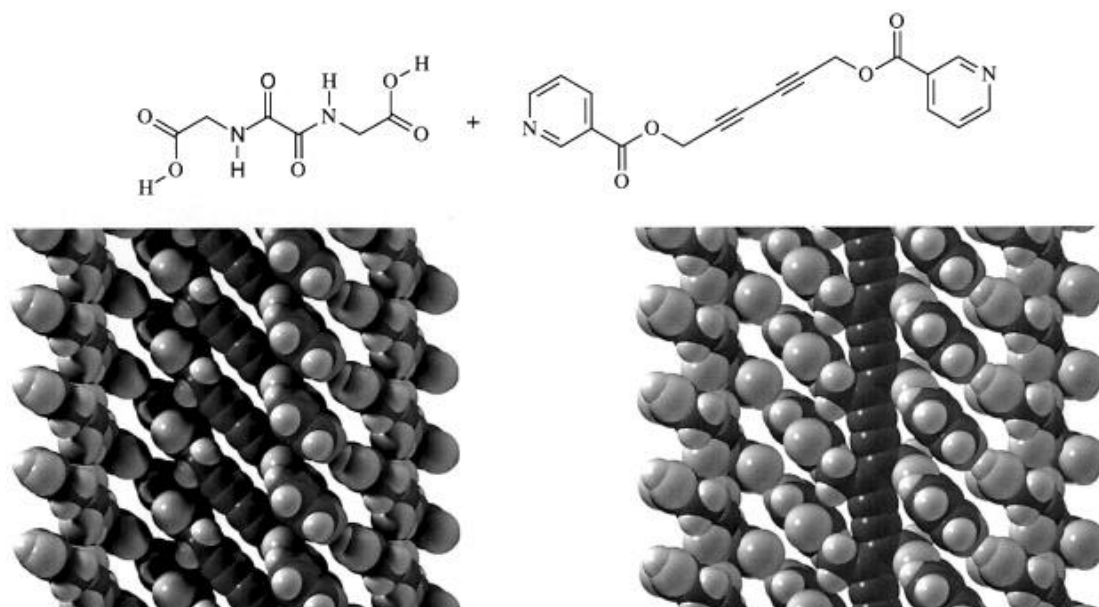


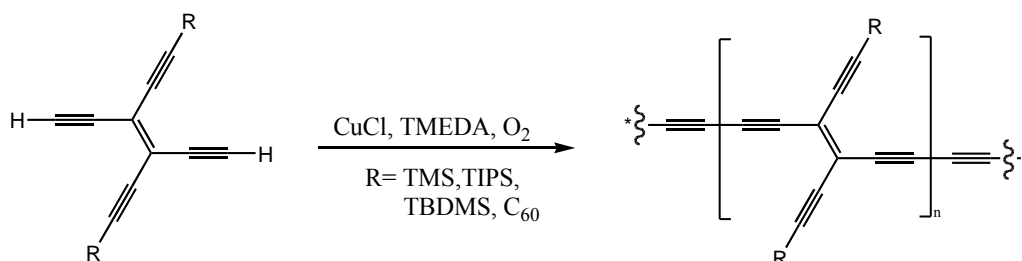
Figure 2-3 shows above. The two spatial parameters in this case almost perfectly meet the ideal value shown in table. Another crucial distance between C4 of diacetylene and C1 of the neighboring one is 3.38 Å, nearly 3.5 Å, which is the value within the region the maximum reactivity can we expected. Significantly, the slow polymerization occurs to the single crystal to single crystal at room temperature. The process of polymerization could be accelerated with slightly increasing temperature.

2.1.1 Pre-organization for Polytriacetylene (PTA)

PA, PDA and PTA are the simplest conjugated linear polymers. However, the synthetic strategy for PDA is not that easy. Similar to the synthesis of PDA, the most direct way to make polytriacetylene is topochemical polymerization. However, prior to the work from our group, PTA was never been successfully prepared through direct polymerization of triacetylene⁴⁴. In 1973, Kiji et. studied a series of triacetylene and examined their topochemical reactivity^{44b}. He reported that 1,4- addition occurs between two neighboring monomers during the polymerization, rather than 1,6- addition. In 1994, Enkelmann⁴³ also drew the similar conclusion, which pointed that 1,2, 1,4 and 1,6- additions are all existed in the polymerization of triacetylene because there are 6 unsaturated carbons between 2 triacetylene monomers. After that, in the following years, Diederich and his workmates tried to use indirect ways, rather than polymerizing triacetylene directly, to produce PTA⁴⁵. Under homocoupling condition, Diederich constructed PTA backbone by oxidatively polymerizing tetraethynylethenes, see Scheme 2-1.

Scheme 2- 1 Synthesis of Polytriacetylene (PTA) by oxidative polymerization

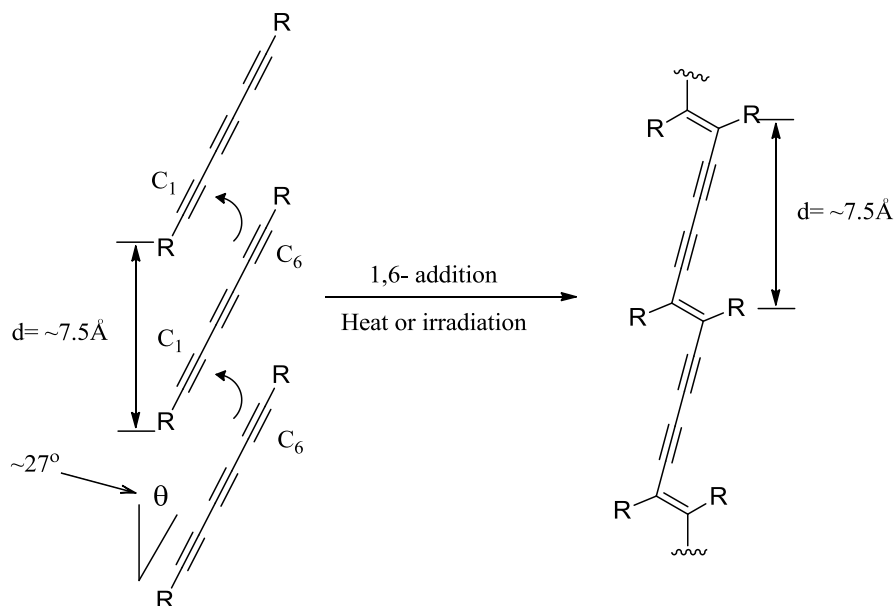
(TMS=trimethylsilyl, TIPS=triisopropylsilyl, TBDMS=tert-butyldimethylsilyl)



To get the triacetylene monomer polymerized directly, a proper preorganized network is required. According to the result of molecular modeling, the ideal repeat distance between two triacetylene monomers is about 7.5 Å, see Figure 2-4. A successful 1,6-addition also requires the tilt angle to be around 27°. Like the case of 1,4-addition in topochemical polymerization of diacetylene, the repeating distance doesn't change during the whole polymerization process.

The distance between reactive carbons, mentioned in the PDA section, should be 3.5 Å, a Van de Waal's contact. As seen in Figure 2-4, the ideal distance for topochemical polymerization of a triacetylene is also 3.5 Å. This alignment ensures the C1 and C6 of neighboring monomers will react with each other reliably. The γ -irradiation, UV or thermal annealing could be the method to induce the polymerization. The last one is preferred for its mildness and safety.

Figure 2-4 Polymerization of triacetylenes(PTA s)

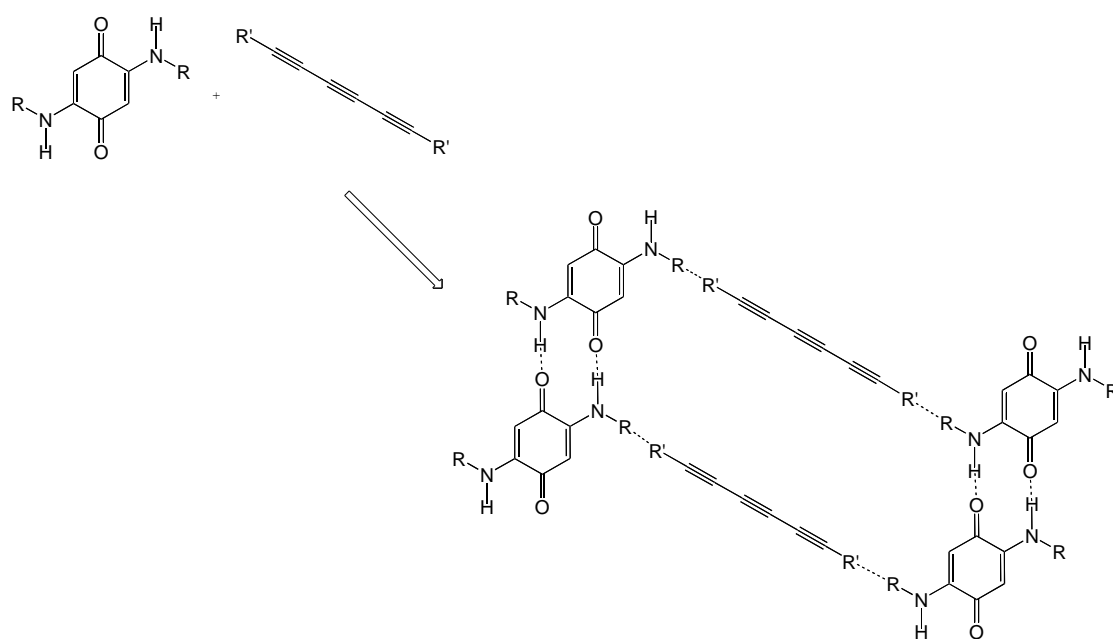


2.1.2 Host-Guest Strategy in preparing PTA.

We learned the significance of intermolecular spacing from the unsuccessful attempts mentioned earlier. Consequently, our goal is to design a desired “Host” and “Guest” system which matches well to meet the ideal requirements for 1,6-polymerization. The host-guest strategy in making PDA requires growing a single crystal of host and guest. But, will this strategy work when it comes to unknown PTA? Can it solve the challenging problem of 1,6- addition? To begin with, a functionality should be provided by host molecules to help it self-assemble into a one dimensional α -network with the suitable repeat spacing. 7.5 \AA is the desired distance between two neighboring monomers, which can be fulfilled by two molecules in our functionalities

library. Aminobenzoquinone (with the RD of 7.4-7.5 Å) and the vinylogous amide (with the RD of 7.1-7.5 Å) are both good candidates for 1,6-polymerization. The other molecule is the guest molecule which either contains pyridyl or carboxylic acid functional groups.

Figure 2-5 Candidate system of aminobenzoquinone host and triacetylene guest



R=pyridyl or carboxylic acid functionality; R'=carboxylic acid or pyridyl functionality

Figure 2-6 Candidate system of vinylogous amide host and triacetylene guest

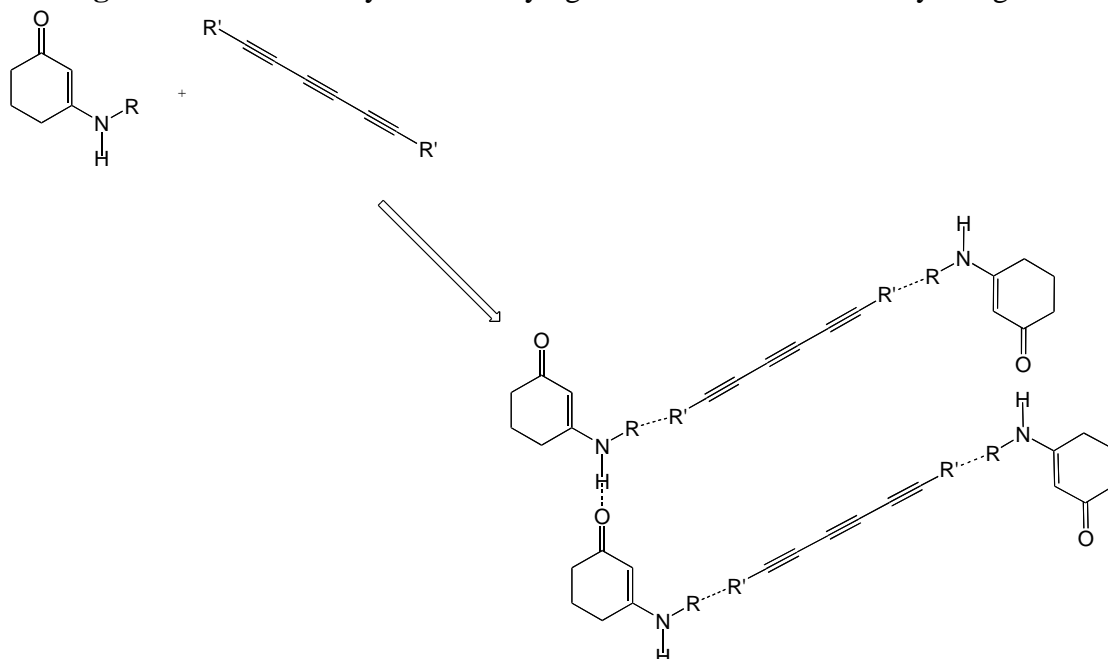
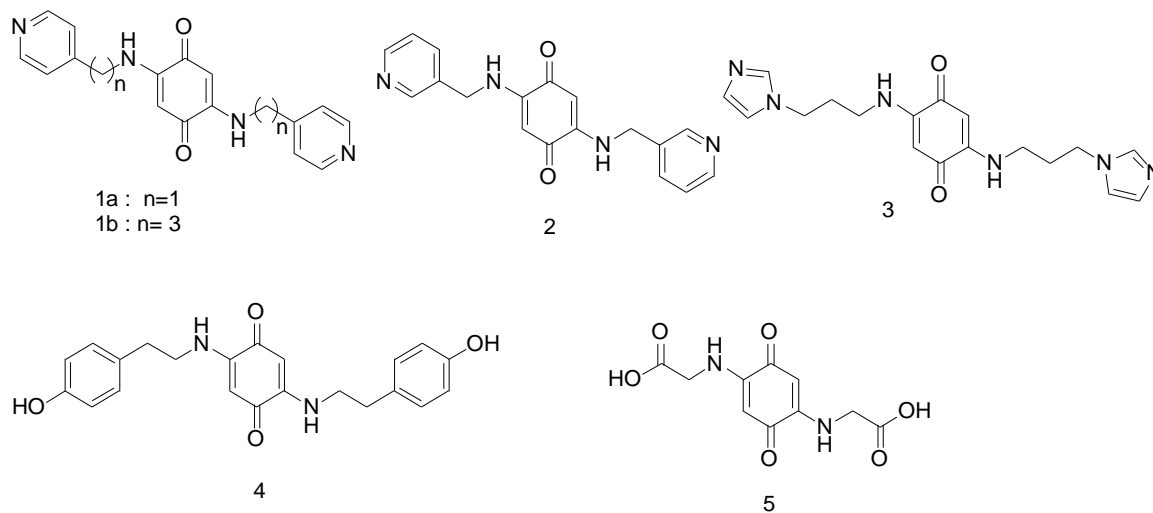


Figure 2-5 and Figure 2-6 shown above are the general design for host and guest molecules, and the host-guest complex is given. The difference between the hosts of aminobenzoquinone and the vinylogous amide is the former ones form two-dimensional β -network, while the latter ones, form an α -network.

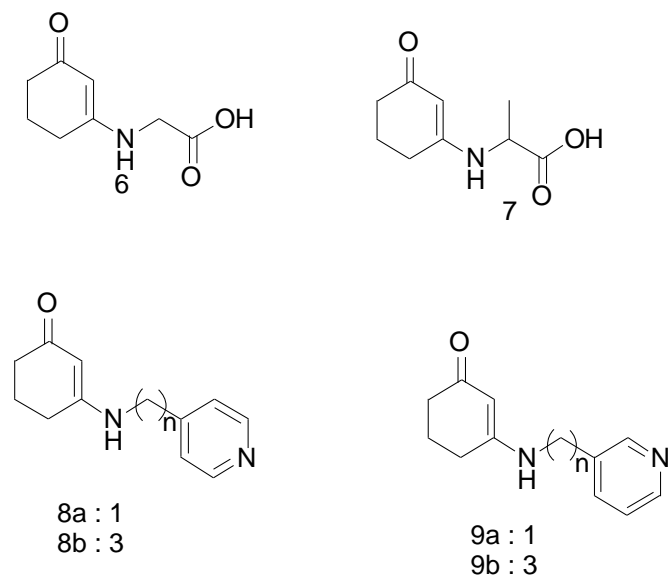
Over the past years, our group has been searching for a good match of “Host” and “Guest” to establish the proper spacing for topochemical polymerization, see Figure 2-7.

Figure 2-7 Host-Guest structure for 1,6- polymerization

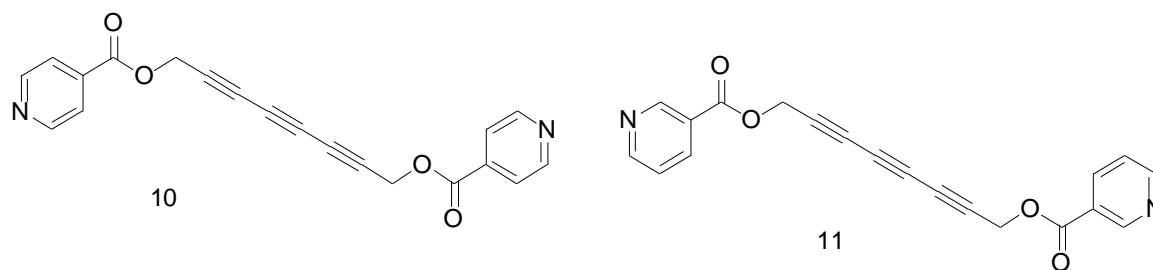
Aminobenzoquinone host



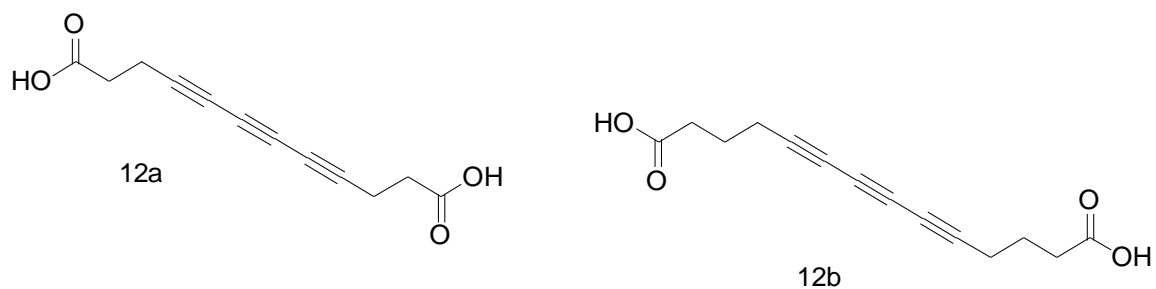
Vinylogous Amide Hosts



Triacetylene Guests with Pyridyl Functionality



Triacetylene Guests with Carboxylic Acid Functionality



At the end of this chapter, several examples of co-crystal made by members in our group would be given⁴⁶.

Figure 2-8 Vinylous amide with succinic acid with repeating distance of 7.233 Å. Below: The observed molecular stacking of the monomer⁴⁶.

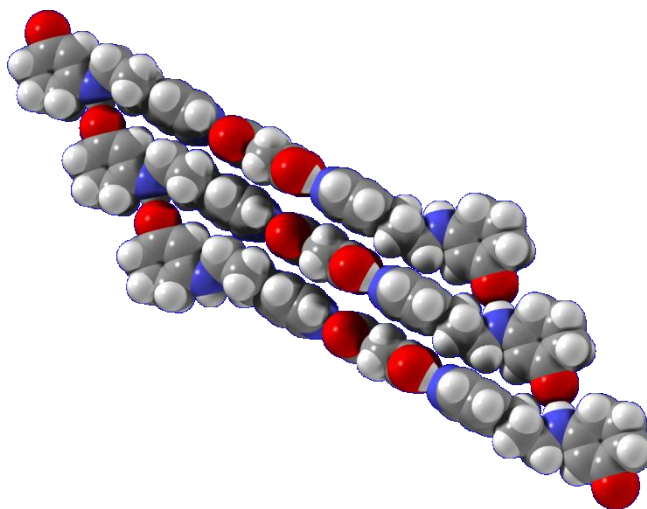
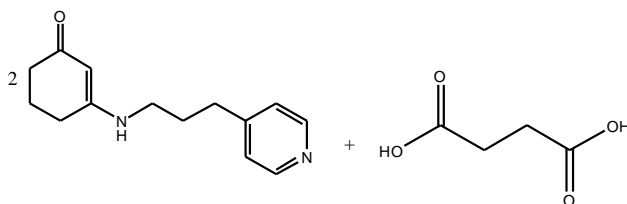


Figure 2-9 Vinylogous amide with adipic acid with packing distance of 7.26 Å.
Below: The observed molecular stacking of the monomer⁴⁶.

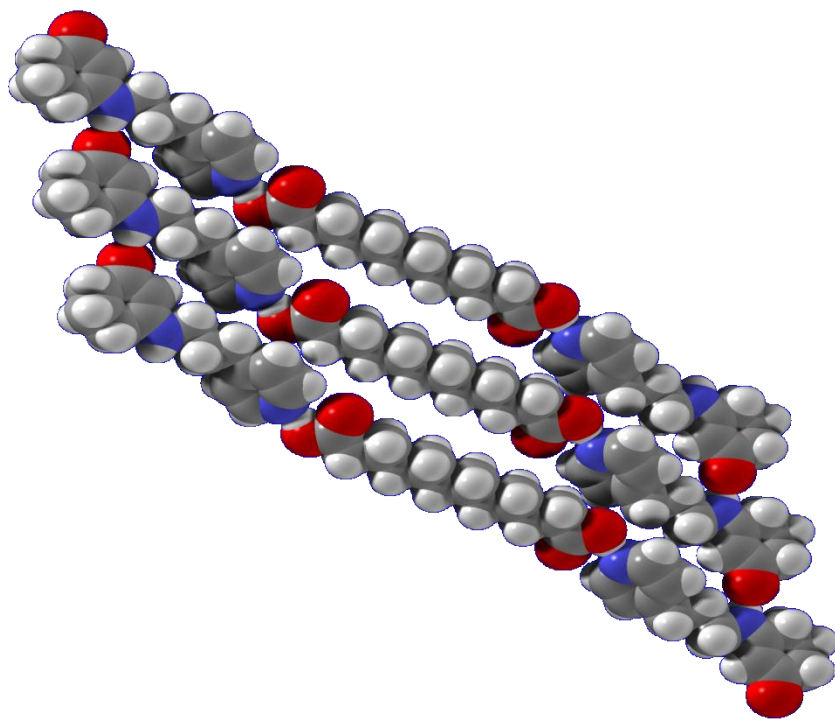
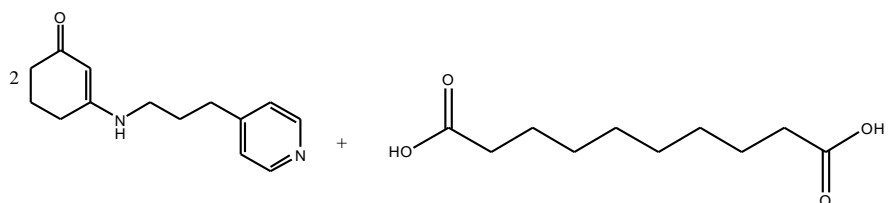
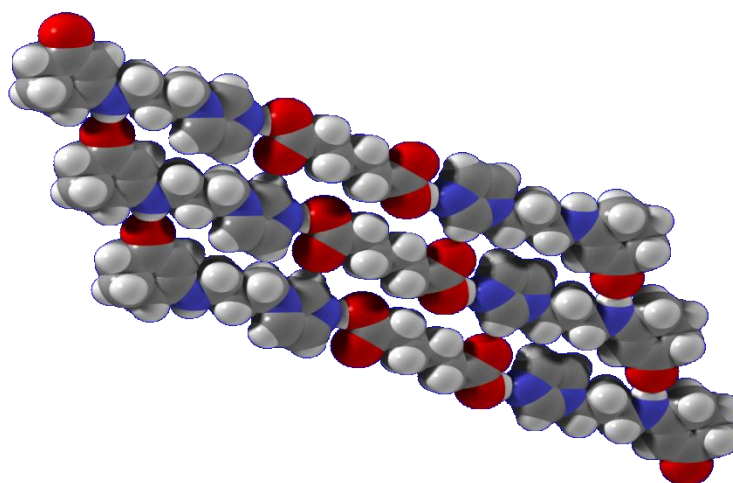
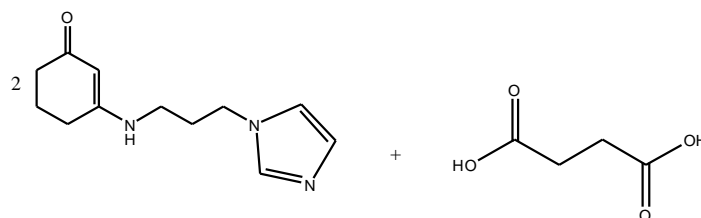


Figure 2-10 Vinylogous amide with succinic acid with a packing distance 7.171Å.
Below: The observed molecular stacking of the monomer⁴⁶.



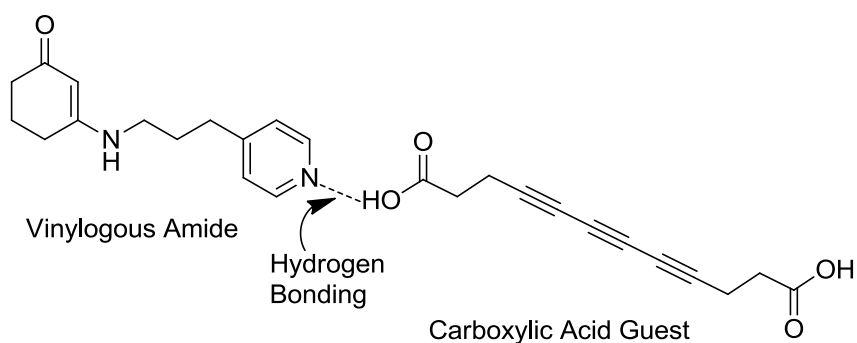
3. Research Goal

First Project: Preparing the Host and Guest for 1,6-Polymerization

For the potential applications in electrical devices, the polytriacetylenes should attract a lot of attention. Since Jun Xiao reported the first successful synthesis of polytriacetylene in 2000⁴⁷, many other attempts in our group have been made to find other matches of “host” and “guest” to explore the 1,6- polymerization. In the first

project, we focused on repeating the work by Xiao, to further confirm the synthesis route and to optimize the reaction condition for a better yield. For better X-Ray data, a lot of effort has been made to grow quality co-crystals of the triacetylene carboxylic acid and pyridyl vinylogous amide, see Figure 2-11.

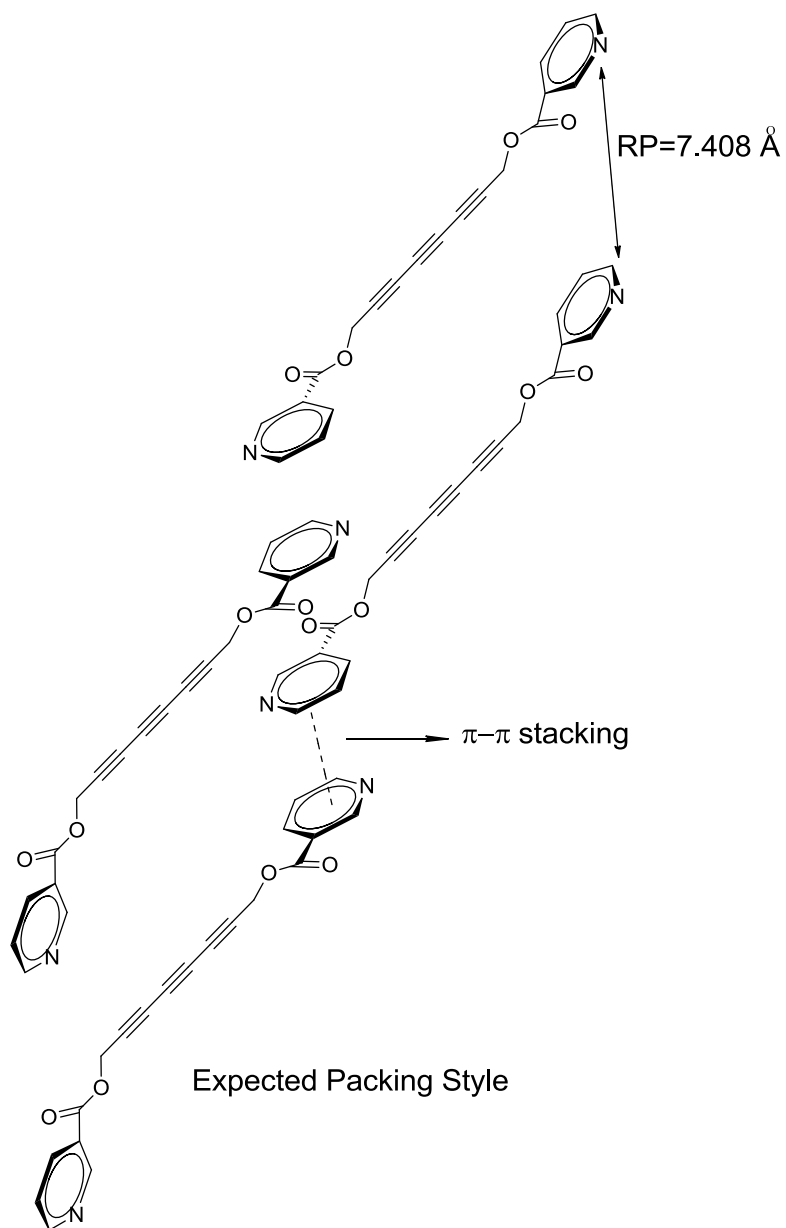
Figure 2-11 Preparing the Host and Guest for 1,6- Polymerization



Second Project: Preparing the π - π stacking Triacetylene for 1,6- polymerization.

In 2002, Hoang reported a successful topochemical 1,6- polymerization of the pyridine substituted triene, with the monomer repeat distance of 7.2 \AA ⁴⁸. Inspired by her work, we are interested in using pyridine group to control the distance between two triacetylene molecules. The crystal structure of pyridyl substituted triacetylene 20b should be studied by X-Ray diffraction to see whether it matches our design, and a 1, 6-polymerization may be carried out, if possible. See Figure 2-12.

Figure 2-12 The pyridyl substituted triacetylenes could be assembled by π - π stacking



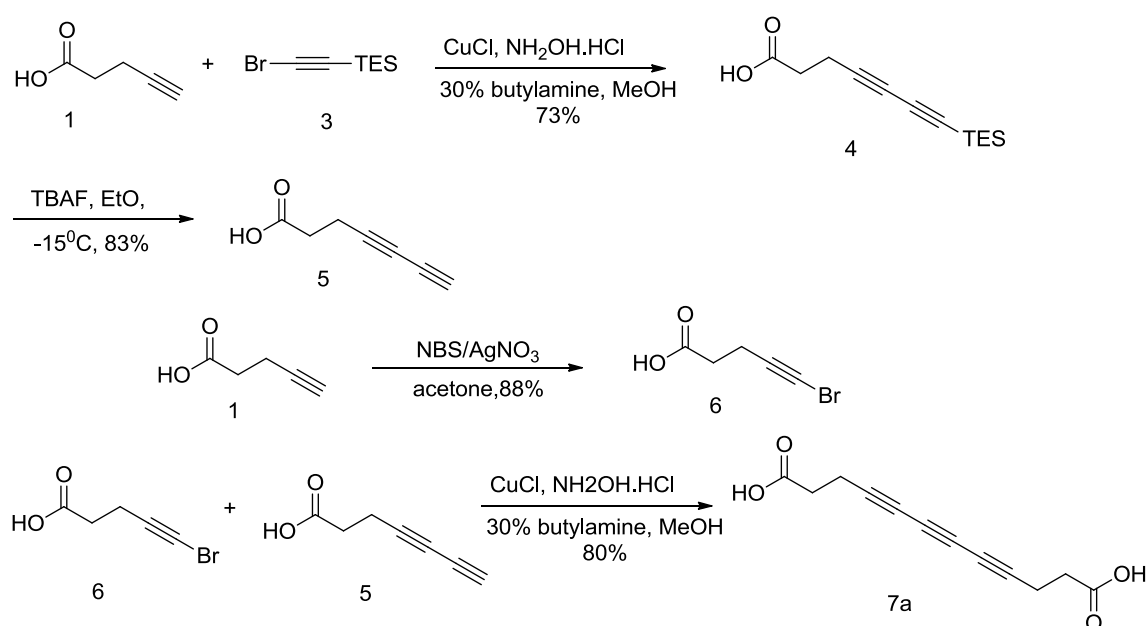
III. Results and Discussion

1. First Project: Preparing the Host and Guest for 1,6-Polymerization

1.1 Synthesis of Triacetylene Guest

The Guest molecules of triacetylene diacids can be prepared through the Cadiot-Chodikiewicz cross-coupling as well⁴⁹. Carboxylic acids were coupled with acetylene bromide **3** followed by deprotection of the TES group to obtain the diacetylene carboxylic acids **5** (Scheme 3-1).

Scheme 3- 1 Synthesis of Triacetylene Carboxylic Acid Guest.



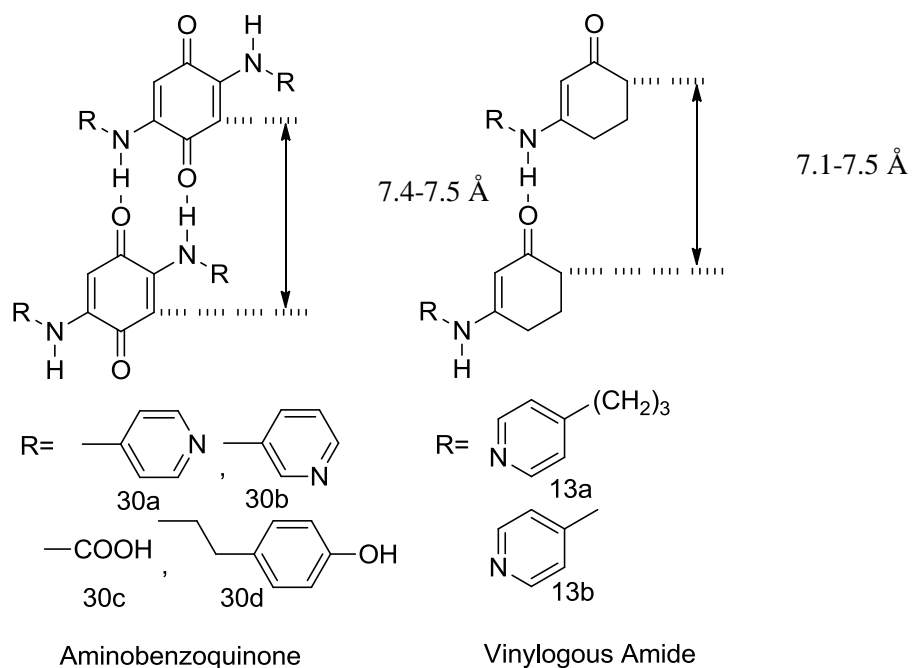
The Copper(I) Iodide catalyzed Cadiot-Chodikiewicz cross-coupling reaction of **6** and **5** in the last step gave a pure product of triacetylene **7a**. As described in the Ahmed's thesis⁴⁶, compound **6** is difficult to prepare. The NMR spectrum did not

exclusively show the expected product. It indicates that the quantity of byproducts (multiple brominated pentynoic acid) is as three times more as the expected product. We think that the excess amount of the NBS may keep reacting with the product newly formed. By reducing the amount of NBS to 1.1 times of acetylene, the 5-bromo-4-pentynoic acid **6** can be obtained in nearly 90% yield. The triacetylene guest **7a** progressively changed to brown color in a few days, which indicated the polymerization occurred slowly.

1.2 Synthesis of Host

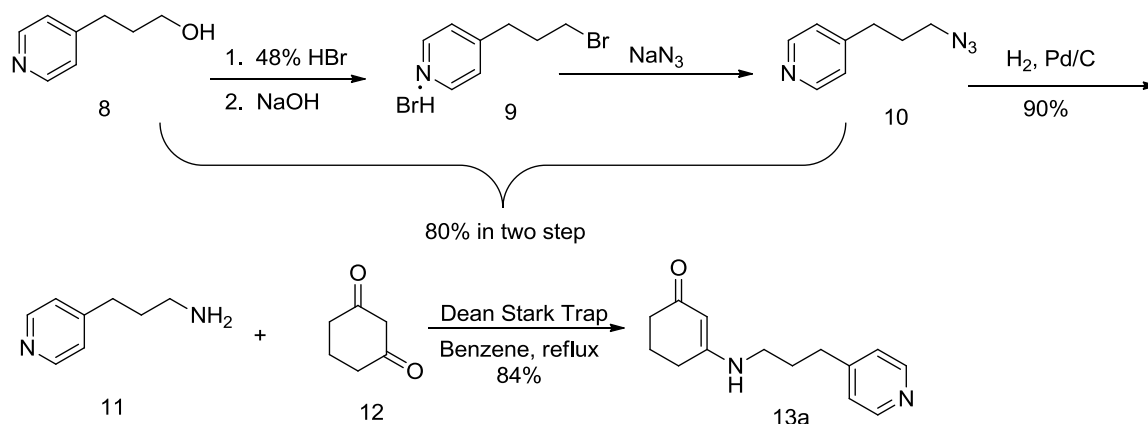
As mentioned in the Chapter 2, aminobenzoquinone (with the RD of 7.4-7.5 Å) and the vinylogous amide (with the RD of 7.1-7.5 Å) are both good candidates for 1,6-polymerization. At the very beginning, aminobenzoquinones were synthesized as a host to pre-organize the triacetylene guest to give a repeat distance of 7.5 Å. The solubility problems were met by our former group member when trying to develop this type of host. Vinylogous amides were therefore introduced and synthesized to overcome this problem. Vinylogous amide compounds (**13a**, **13b**) compared to aminobenzoquinone (**30a**, **30b**, **30c**, **30d**), are easier to dissolve in organic solvents. In addition, the vinylogous amide has only one hydrogen bond donor and two acceptors, which is different from the hydrogen-bonding system of aminobenzoquinone derivatives.

Figure 3- 1 The host molecules of Aminobenzoquinone (**30a**, **30b**, **30c** and **30d**) and Vinylogous Amide (**13a** and **13b**)



Xiao⁵⁰ has successfully designed and synthesized these two generations of vinylogous amide hosts. The second generation of vinylogous amide hosts has been prepared and the synthetic route is shown in Scheme 3-2.

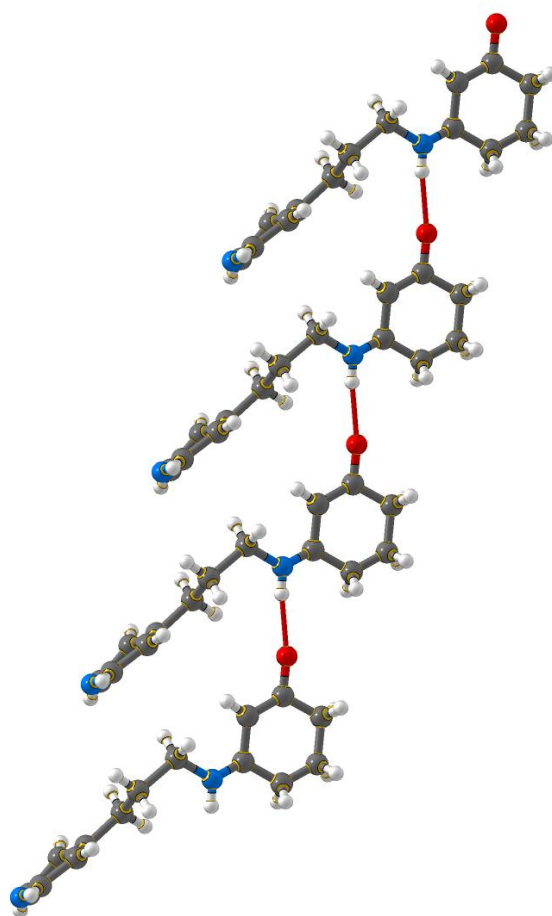
Scheme 3- 2 Synthesis of vinylogous amide host **13a**.



A difficulty was experienced during synthesizing the product 4-(3-bromopropyl)pyridine hydrobromide **9**. In this step, aqueous HBr was used to convert the hydroxyl group to a bromo group. However, we found that the desired product **9** is soluble in water, thus is difficult to be isolated. In consideration of the sodium azide that I used in the second step will appear good nucleophilicity even in water, I chose to start the following step directly without further purification of the compound **9**. The result shows that NaN_3 did exclusively react with the terminal bromide group in compound **9**, and give the expected product **10** in 80 percent yield.

Light yellow crystal of vinylogous amide **13a** was obtained from slow evaporation of ethyl acetate. The crystal structure revealed the repeat distance of 7.21 Å with a space group of P-1, shown in Figure 3-2. As mentioned in the last chapter, this repeat distance (7.21 Å) is close to the ideal value (7.5 Å). Therefore this vinylogous amide is suitable for organizing the guest molecules pack into the desired network. The photograph of single crystal is shown below.

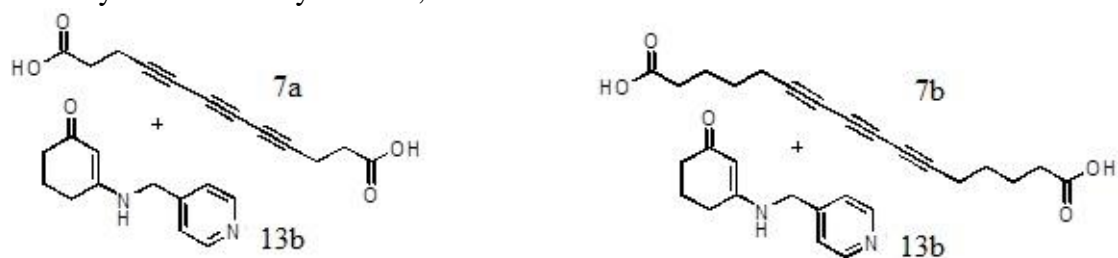
Figure 3- 2 (Photo) The light yellow crystal obtained from solvent (EA), evaporated very slowly. Crystal structure of vinylogous amide **13a**.



1.3 1,6-polymerization of triacetylene.

Xiao and Liu successfully polymerized two types of triacetylenes by using the first generation of vinylogous amide host⁵⁰⁻⁵¹. As shown in Figure 3-3, each had a repeat distance of 7.1 Å, which is a little shorter than the ideal value for 1,6-polymerization of triacetylenes.

Figure 3- 3 1,6-polymerization using first generation host **13b** with two types of carboxylic acid triacetylenes **7a**, **7b**.



7a-13b

RD=7.143Å

$\theta=29.2^\circ$

C₁-C₆=3.485 Å

Space Group: P-1

a=7.143 Å (2) $\alpha=77.28^\circ$ (3)

b=10.695 Å (3) $\beta=90.42^\circ$ (2)

c=11.2825 Å (3) $\gamma=80.15^\circ$ (2)

70% polymerization by γ -irradiation

7b-13b

RD=7.1069Å

$\theta=31.04^\circ$

C₁-C₆=3.665 Å

Space Group: P-1

a=7.1069 Å (15) $\alpha=106.291^\circ$ (4)

b=11.502 Å (3) $\beta=88.849^\circ$ (4)

c=12.418 Å (3) $\gamma=78.749^\circ$ (4)

50% polymerization by γ -irradiation

Under γ -irradiation, both of triacetylenes can be partially polymerized. However, for the preparation of the conjugated polymers, γ -irradiation is not an ideal choice for inducing the topochemical polymerization. In contrast, thermal annealing is a

convenient and desirable way to drive polymerization forward. In Xiao and Liu's work, there was no crystal-to-crystal thermal annealing polymerization observed and γ -irradiation induced only 70% and 50% polymerization of triacetylene respectively. The first-generation host (vinylogous amide) and guest (triacetylene diacids) can only produce a co-crystal with a short repeat distance of 7.1 Å, which is less than ideal distance. Perhaps this shorter repeat distance causes the lack of thermal polymerization in those two co-crystals. Increasing the repeat distance and therefore resulting in a much more completed polymerization is the goal for us. We also wanted to use thermal annealing instead of γ -irradiation to induce the 1,6-polymerization.

To explore the successful 1,6-polymerization of triacetylene, Juan Qian⁵² designed and synthesized the second generation of vinylogous amide host **13a**. As we can see in Figure 3-4, the second generation of vinylogous amide host has two more methylene groups between amide and pyridine. These functionalities were added to reduce the steric repulsion of pyridine ring and vinylogous hydrogen and thus may increase the repeat distance as well as allow a more facile polymerization in keeping the suitable packing style for triacetylene carboxylic acid guest. Fortunately, the co-crystal of host **13a** and triacetylene guest **7a** can undergo a thermal induced 1,6-polymerization to give the desired polytriacetylenes. Qian reported this first 1,6-polymerization of triacetylene and also provided the differences in the crystal lattice from the monomers to the polymers, as the table shown below⁵².

Figure 3- 4 Polymerization of triacetylene **7a**, and vinylogous amide host **13a**.

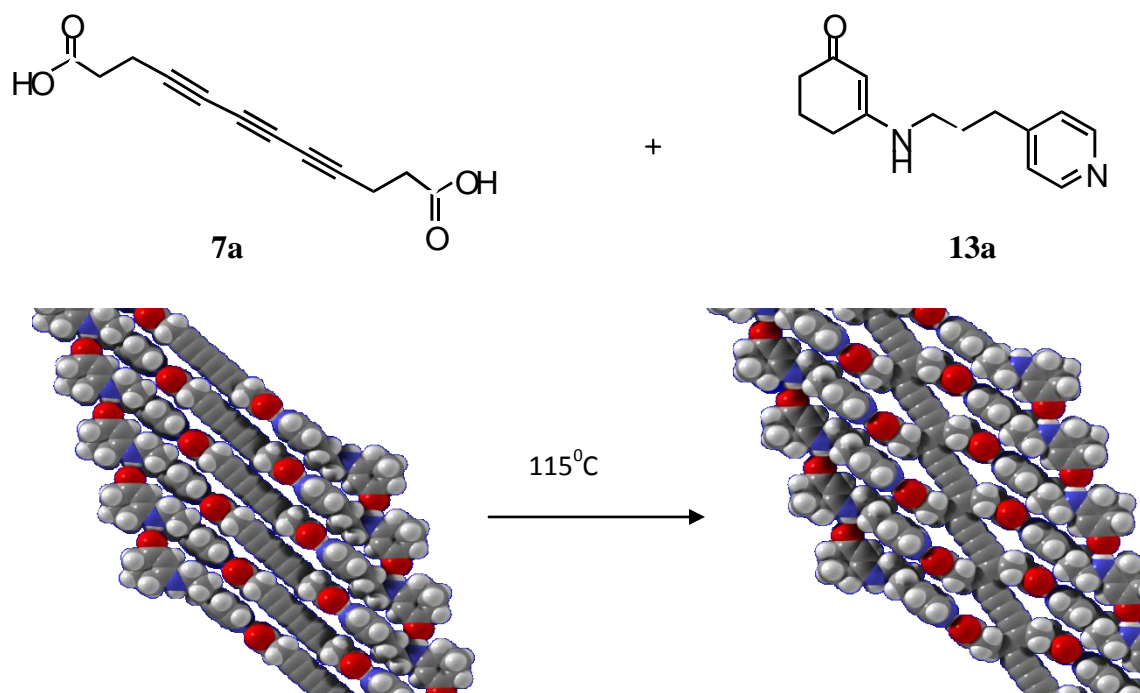
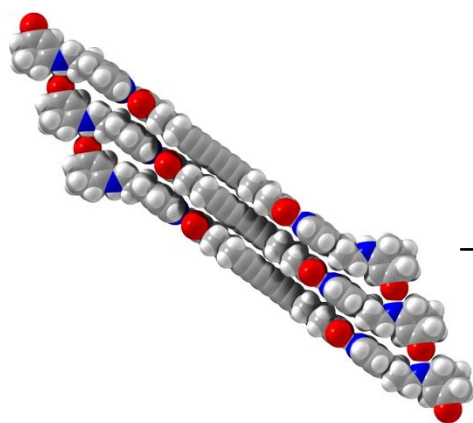
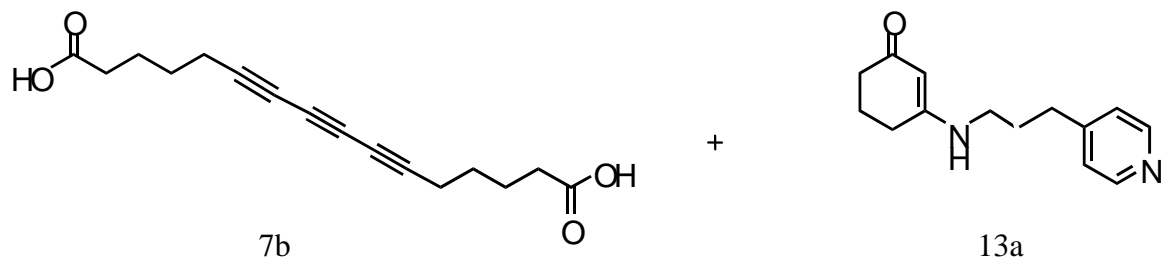


Table 3- 1 Crystal Lattice Data Change for the polymerization of co-crystal **7a-13a**.

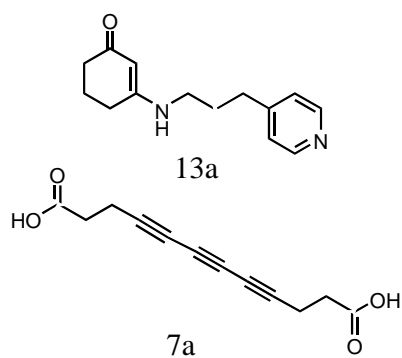
	A	B	C	α	β	γ
monomer	7.259(2)	11.167(3)	11.563(4)	102.357(7)	91.860(5)	94.698(5)
Polymer	7.261(7)	11.007(10)	11.610(11)	102.008(17)	91.310(16)	96.715(16)

On the contrary, the co-crystal of host **13a** and triacetylene guest **7b** did not give any polymerization via UV irradiation or heating, see Figure 3-5.

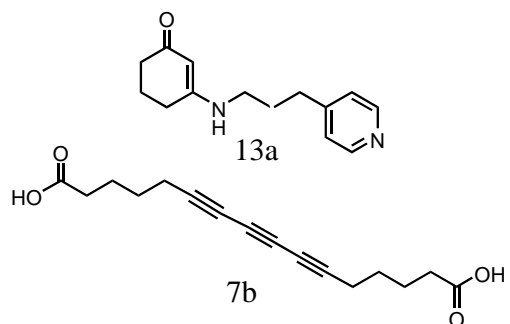
Figure 3- 5 No polymerization observed in the co-crystal of host **13a** and triacetylene guest **7b**.



No polymerization
under UV light and
heating



RD= 7.259Å
 $\theta=29.2^\circ$
 Cl-C6=3.544 Å
 Space group: P-1
 a= 7.259 (2) $\alpha= 102.357 (7)$;
 b= 11.167 (3) $\beta= 91.86 (5)$;
 c= 11.563(4) $\gamma= 94.698 (5)$;
 Percentage of polymerization=100%



RD= 7.178Å
 $\theta=31.0^\circ$
 Cl-C6=3.706 Å
 Space group: P1
 a= 7.178 (7) $\alpha= 107.531 (19)$;
 b= 12.450 (12) $\beta= 93.941 (17)$;
 c= 12.883 (12) $\gamma= 105.802 (16)$;
 No polymerization under heating and UV light

The difference of repeat distance between co-crystal of **7a-13a** and **7b-13a** may explain the difference in reactivity of their monomers.

Among these 4 triacetylenes-vinylogous amide co-crystals above, the best combination of guest and host is **7a** and **13a**, which turns to be an optimum hydrogen-bonding system for triacetylene polymerization. Under topochemical control, 1,6-polymerization of this co-crystal by thermal annealing is the first practical synthesis of a polytriacetylene⁵².

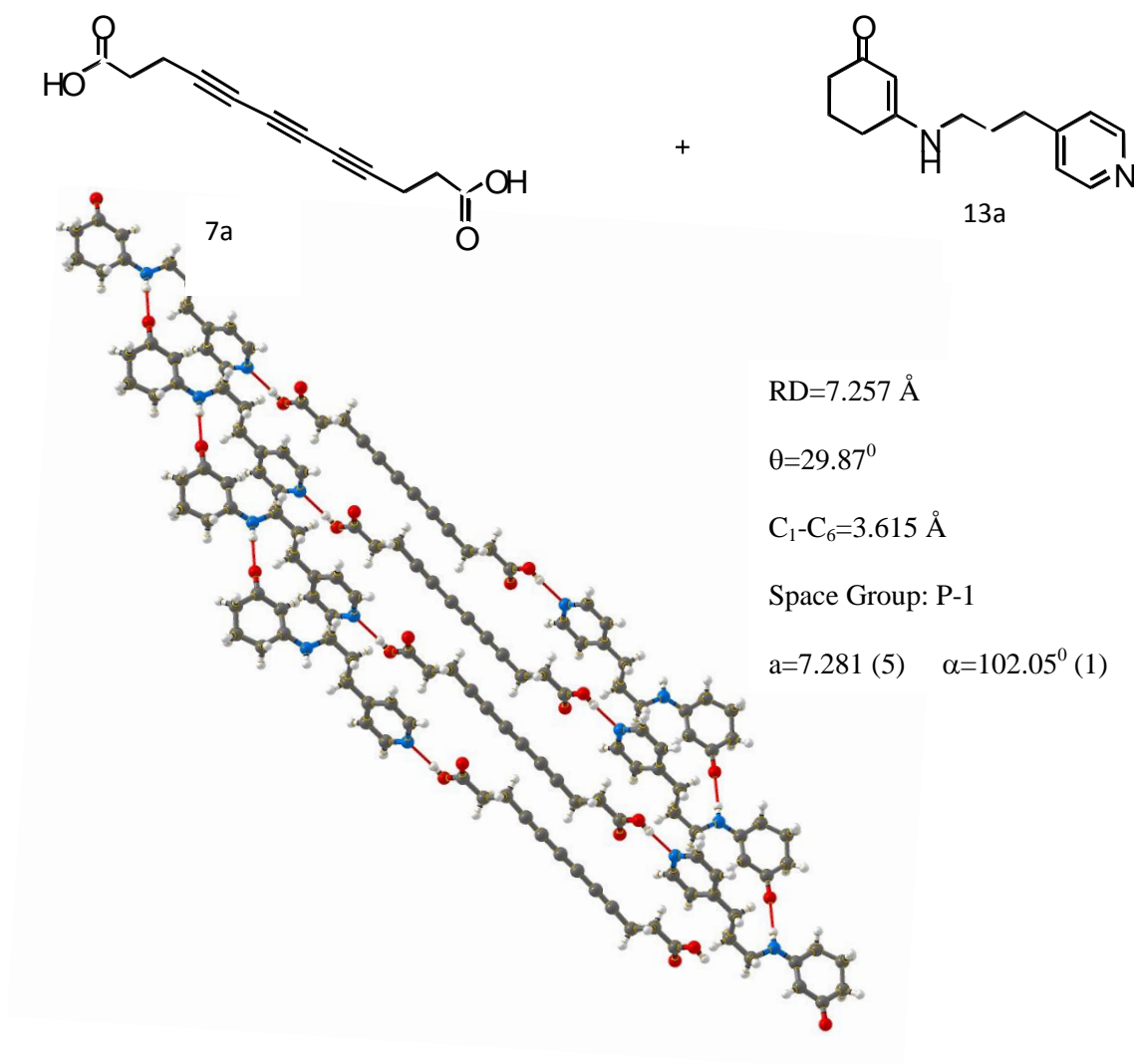
A lot of efforts have been taken to explore the advanced ways for the preparation of polytriacetylenes, which can be utilized for further chemical and physical studies. It was reported previously that triacetylene monomers were of poor stability and became darker color immediately if being exposed to air. To maintain the guest's stability, the compound was stored in methanol constantly. Another problem of growing co-crystal is the quality of the first batch crystal is often unsuitable for X-Ray analysis. Xi Ouyang reported a new method to grow co-crystals. She modified the solvent system by changing ethyl acetate and methanol ratio to 10:1⁵³. However, according to Xi Ouyang, the first batch co-crystals are still not suitable for X-ray diffraction. They should be dissolved in hot ethyl acetate, additional MeOH added to increase the solubility.

After preparing a homogenous solution via filtration, the solution was evaporated slowly over few days. This procedure of growing co-crystals should be repeated until pink crystals were formed which was suitable for XRD analysis⁵³. The three

parameters for triacetylene functionality are within the range of ideal 1,6-polymerization: The repeat distance is 7.26 Å, C1-C6 distance is 3.615 Å, and tilt angle is 29.87°, see Figure 3-6.

The previous study carried out by Xi Ouyang indicated that 115°C was the effective temperature to carry out the triacetylene polymerization. After heating for 72 hours, a completed polymerization was obtained⁵³.

Figure 3- 6 Co-crystal of **7a** and **13a** with crystal lattice data.



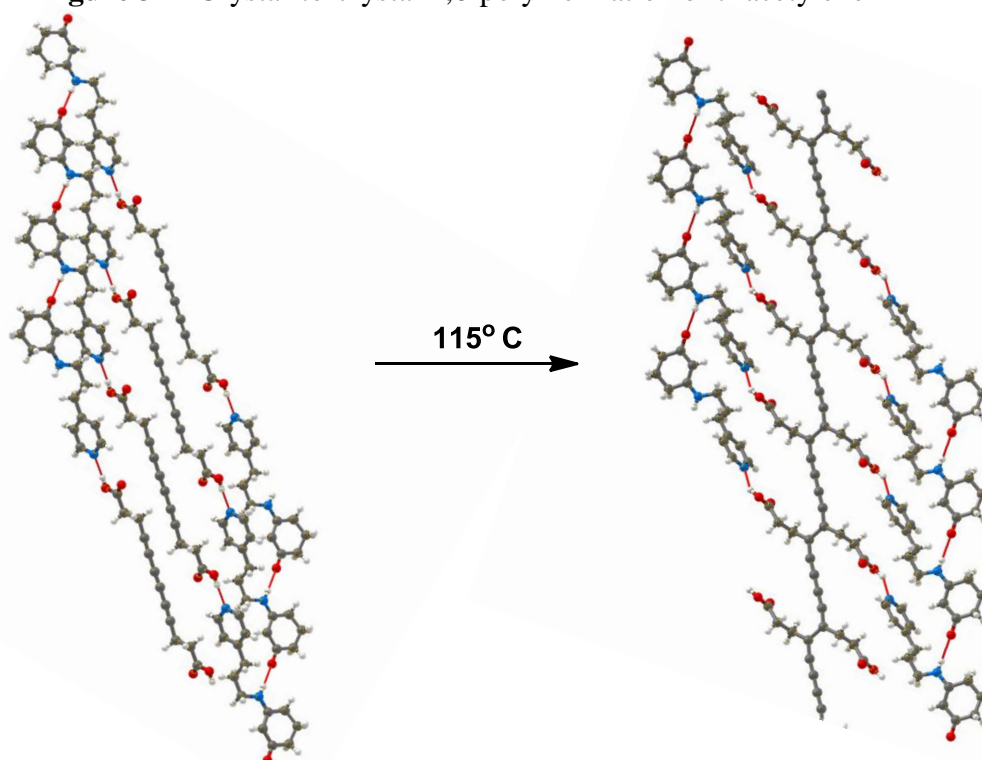
Ahmed⁴⁶ extended the work by heating an additional 24-hour to monitor lattice changes. The X-ray data of this crystal heated for total of 96 hours was collected every 24 hours, and the results are listed and summarized in the table below.

Table 3- 2 Crystal Lattice Data Change for Co-crystal of **7a-13a** as Polymerization proceeds⁴⁶

Time (hr)	Temp (°C)	a	b	c	alpha	beta	gamma
0	115	7.2815	11.1592	11.583	102.05	92.17	94.83
24	115	7.2785	11.1331	11.5878	102.09	91.27	95.56
48	115						
72	115	7.3515	11.1491	11.7081	101.95	91.52	97.03
96	115	7.3147	11.052	11.6909	101.78	91.52	96.85

After 72 hours simple heating of the triacetylene monomer, crystal-to-crystal polymerization occurred to give polytriacetylene, see Figure3-7.

Figure 3- 7 Crystal-to-crystal 1,6-polymerization of triacetylene



Ahmed's work was repeated to get a fresh prepared crystal. The total heating hours is significant longer than 72 hours. It took over 19 days to have a nearly 100% polymerization. X-Ray data was collected as shown in Table 3-3. Until 456 hours of heating, the apparent distance of C1-C6 is nearly 1.36 Å, and the additional 48 hours heating did not change the distance obviously. The X-Ray data of this co-crystal **7a-13a** is listed in the table below.

Table 3- 3 The change of crystal lattice data over 456 hours heating under 115°C.

Hours of Heating	Volume	a	b	c	α	β	γ
no	907.19	7.249	11.1567	11.5393	102.357	91.924	94.771
40h	905.15	7.2664	11.0909	11.5578	102.154	91.646	95.556
80h	905	7.2704	11.0508	11.5989	102.078	91.438	96.095
120h	903.95	7.2712	11.0306	11.6095	101.953	91.434	96.511
156h	904.54	7.2723	11.0245	11.6273	101.92	91.446	96.785
196h	904.44	7.2733	11.0087	11.6437	101.856	91.401	97.001
240h	905.2	7.2756	11.0063	11.6561	101.842	91.386	97.165
288h	905.84	7.2764	11.0017	11.6721	101.866	91.368	97.283
312h	906.06	7.2785	11.0028	11.6719	101.875	91.384	97.319
360h	906.44	7.2791	11.0006	11.6788	101.841	91.396	97.383
408h	907.56	7.2805	11.0074	11.6843	101.818	91.375	97.446
456h	907.12	7.2794	11.0008	11.687	101.804	91.356	97.459
504h	905.83	7.2780	10.9943	11.6812	101.805	91.388	97.505

To determine the extent of polymerization, we investigated the distance between C1 to C6 and C1* to C6*, which indicated the quantity of new bonds formation (C1*, C6*- newly formed atom which will take the place of C1 and C6 in polymers, respectively). The distance of C1-C6 is 3.602 Å in the co-crystal of **7a-13a**, see figure 3-8. The value of 3.602 Å, as discussed in the last chapter, is suitable for 1,6-polymerization. With heating proceeding, the original C1 and C6 faded away

gradually. Instead, the newly formed C1* and C6* appeared and the apparent distance between them is getting smaller and smaller. Figure 3-9 illustrated the molecular structure for the co-crystal which had been heating for 108 hours under 115°C. After heating for nearly 19 days, the C1 and C6 completely disappeared, and the observed length of C1*-C6* was shortened to 1.363 Å, which is very close to the length of carbon-carbon double bond, see Figure 3-10.

Figure 3- 8 Molecular structure for co-crystal **7a-13a**, before heating.

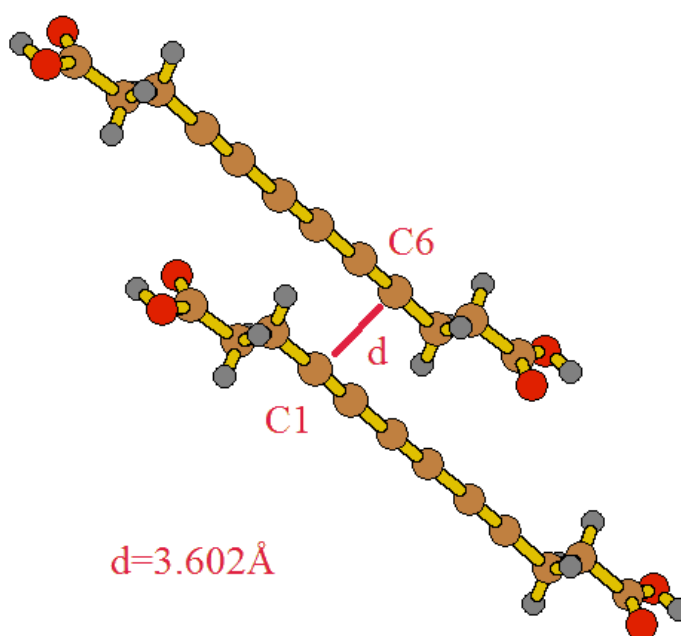


Figure 3- 9 Molecular structure for co-crystal **7a-13a**, after heating 108 hours under the temperature of 115°C.

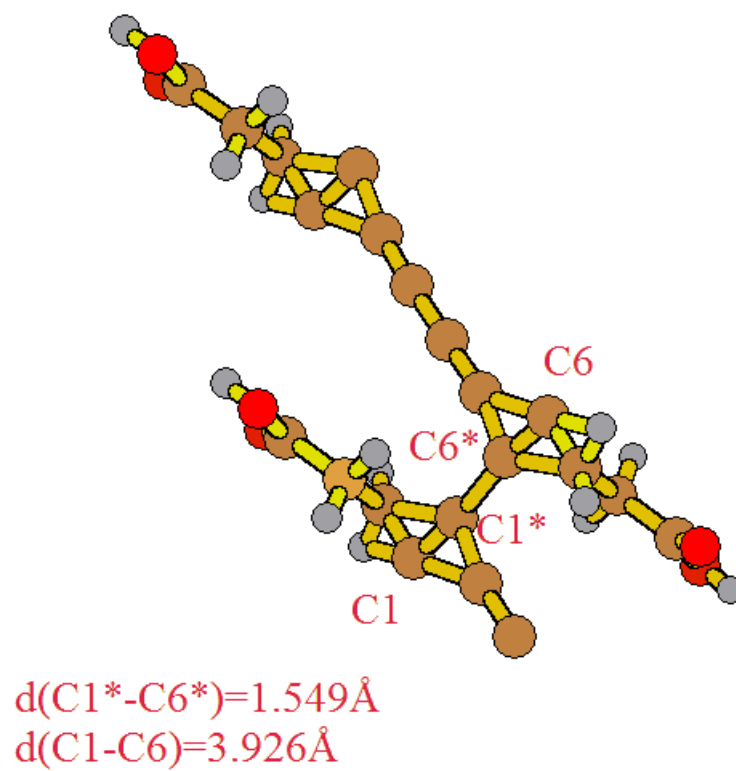
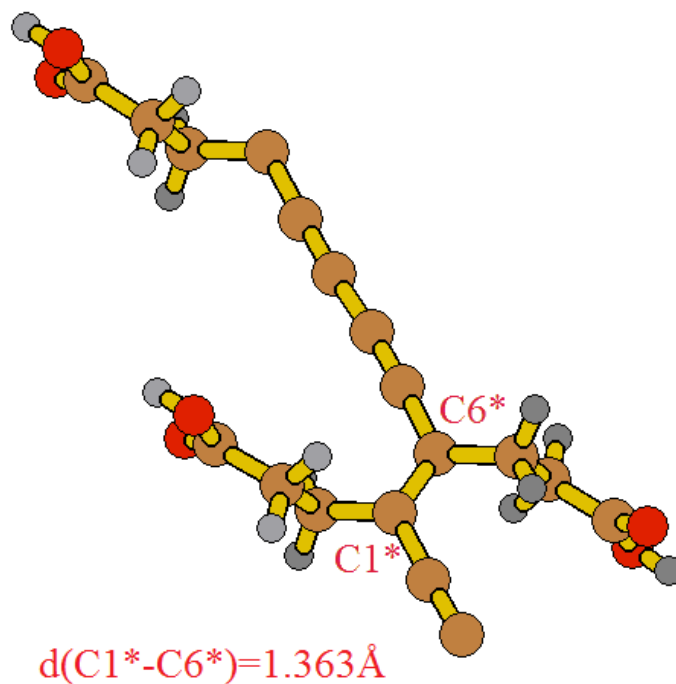
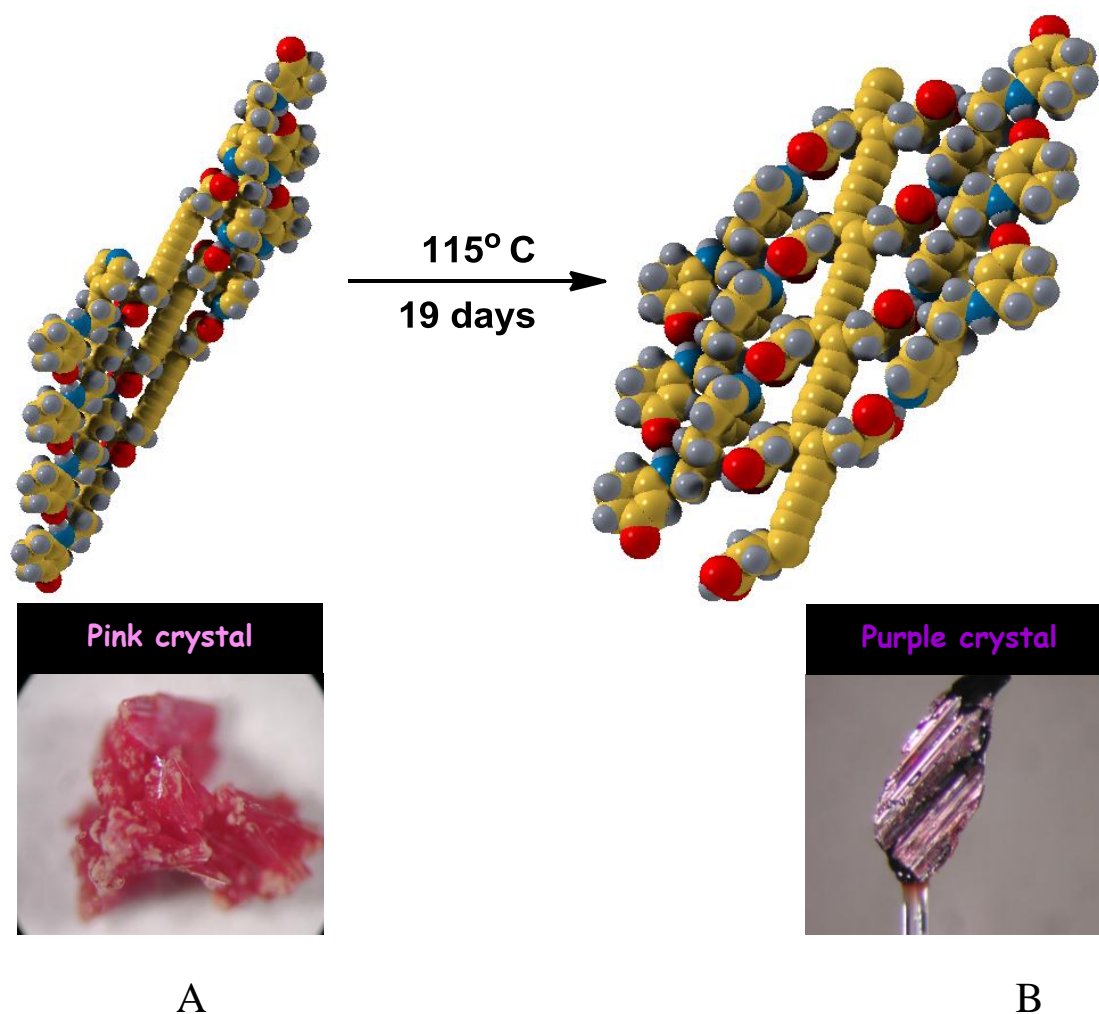


Figure 3-10 Molecular structure for co-crystal **7a-13a**, after heating 456 hours under the temperature of 115°C



Over 456 hours of heating, the pink crystal changed to purple gradually. The color change no longer proceeded with additional heating time. The transition of molecular stacking pattern and color of the crystal are illustrated below, Figure 3-11.

Figure 3- 11 (A) Molecular stacking pattern in the monomer. The repeat distance of 7.250 Å is shorter than the ideal polymerization value of 7.5 Å. (Photo) Freshly formed pink crystals of the monomer grown at room temperature (B) The repeat distance of 7.250 Å is close to the ideal distance, that allows the successful 1,6-topochemical polymerization. (Photo) Freshly formed crystals of the polymer formed through slowly annealing at 115° C.

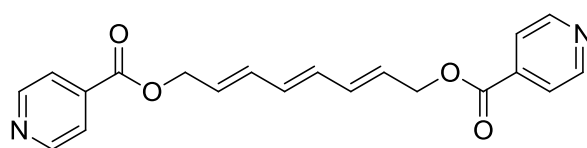


2. Second Project: Preparing the π - π stacking Triacetylene for 1,6-polymerization.

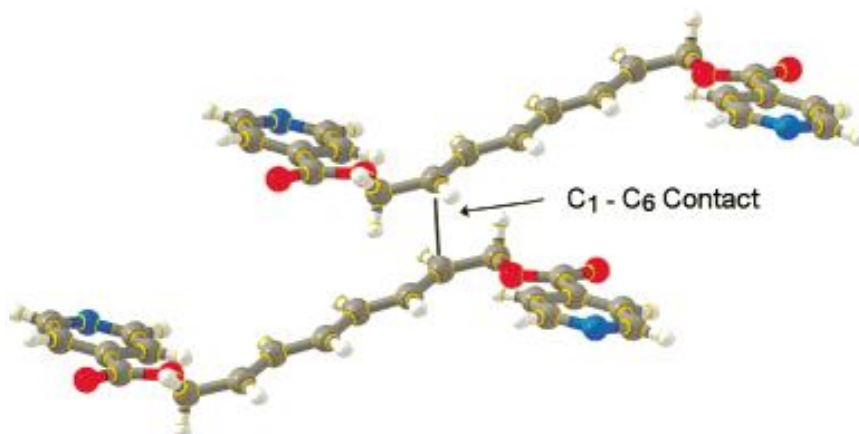
In our research group, the first bipyridine substituted triacetylene guests, **20a** and **20b**, were proposed to co-crystal with a vinylogous amide. These bipyridine substituted triacetylene was originally designed and synthesized by Jun Xiao⁵⁰. Due to

the significant difference in solubility between host and guest, co-crystalization of the two molecules was difficult. Inspired by Tram Hoang's work on 1,6-polymerization of triene, we hypothesized that π - π stacking of pyridine rings could help triene monomers pack into supramolecular structure with repeat distance of 7.2\AA ⁴⁸.

Figure 3- 12 The X-ray crystal structure of **1**. The observed repeat distance is 7.252\AA , the tilt angle θ is 34° , the orientation angle ϕ is 68° , and a C1-to-C6 contact is 4.09\AA ⁴⁸.



Compound 1 Bipyridine substituted triene



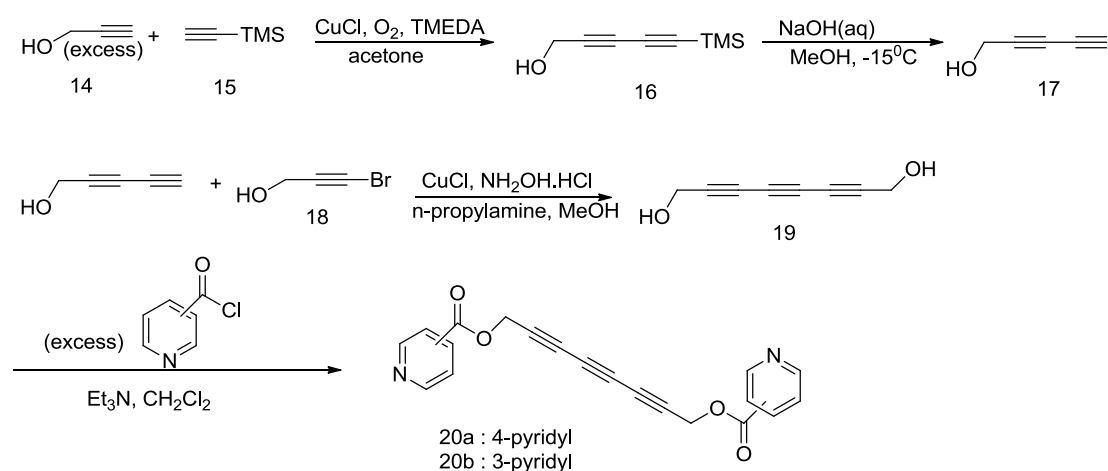
In Tranm Hoang's work, this repeat distance of 7.2\AA was the key value that directly determined the success of 1,6-polymerization of the triene⁴⁸. As mentioned above, Enkelmann, in 1994, indicated that the repeat distance of 7.5\AA is ideal for 1,6-addition⁴³.

We wonder if the pyridines rings in the triacetylene compound would also organize the monomers into preferred supramolecular structure for topochemical 1,6-polymerization. Hoang's work motivates our interest in studying the single crystal

structure of **20a** and **20b**. Our previous student Eilaf Ahmed have obtained the single crystals of **20a** which were grown from CH₂Cl₂/ EtOH (1/1) solvent by slow diffusion. Unfortunately, a suitable single crystal for X-Ray diffraction (XRD) could not be obtained after several attempts⁵⁰. To explore the crystal structure of 3-pyridyl substituted triacetylene, my work focused on the synthesis and crystal analysis of compound **20b**.

The scheme below demonstrates Xiao's synthetic route to the triacetylene **20a** and **20b**.

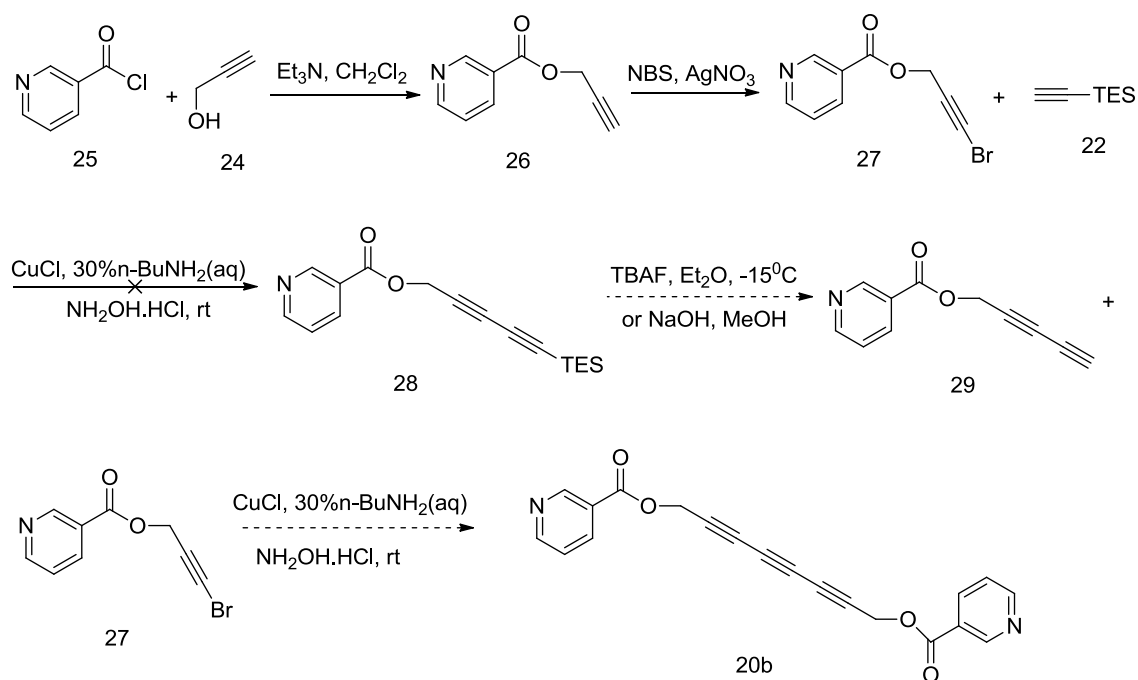
Scheme 3- 3 Synthetic route for Triacetylene **20a**, and **20b**⁵⁰.



In Xiao's synthesis, the reaction of getting TMS diyne alcohol **16** had an extraordinary low yield due to the undesired self-coupled byproduct in the first step.

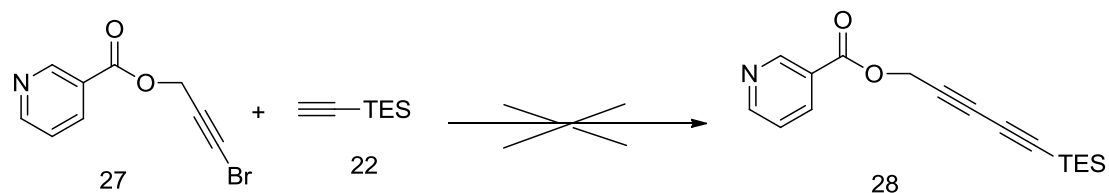
To overcome this problem, a new scheme was introduced for the synthesis of **20b**, Scheme 3-4.

Scheme 3- 4 An unsuccessful attempt to optimize 3-pyridyl triacetylene **20b**



Initially, the starting materials go through a $\text{S}_{\text{N}}2$ reaction. The oxygen anion in compound **24** attacks carbonyl group with kicking out the chloride to give prop-2-yn-1-yl nicotinate **26**. Following by a simple NBS bromination step, we got to the key step—cross-coupling.

Scheme 3- 5 The key step that cannot work out.

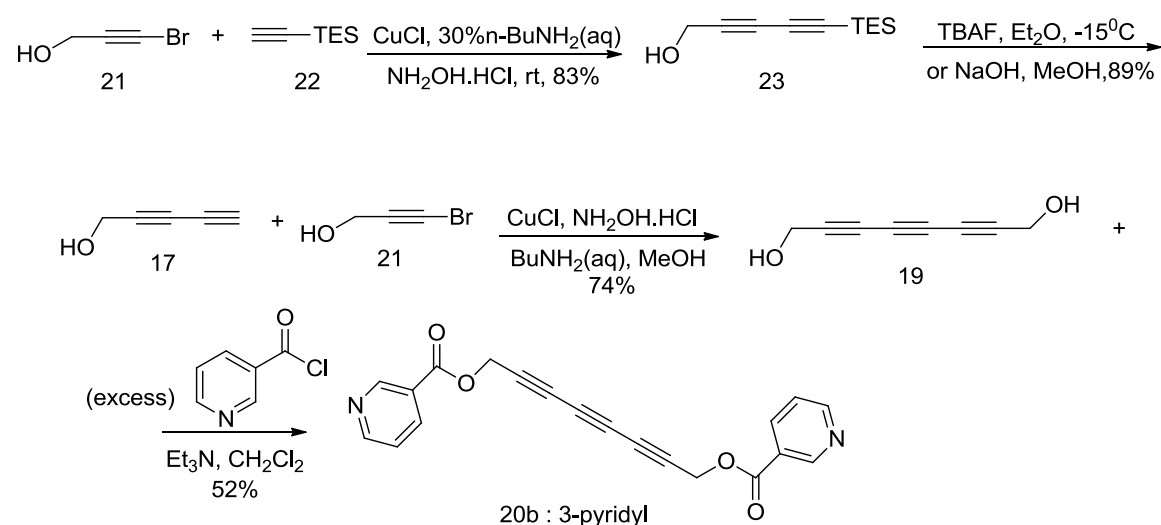


As the Scheme 3-5 shown above, the cross-coupling reaction did not happen between **27** and **22**. The Cadiot-Chodkiewicz cross-coupling that occurs between terminal alkyne and a haloalkyne, driven by copper catalyst, needs an amine base to deprotonate the acetylenic proton at the very beginning⁴⁹. The ester functional group

may hydrolyze under basic condition. The amine acted as a nucleophile, and destroyed the structure of ester. The optimization of the synthesis route requires additional work.

Failing to find out the new synthesis route for **20b**, I turned to repeat the existing approach developed by the previous students^{50, 53}. Based on Xiao's synthesis, Xi Ouyang modified the synthesis by running the Cadiot-Chodikiewicz cross-coupling reaction at the very beginning (Scheme 3-6)⁴⁹. Through this procedure, the diyne alcohol could be made in a relatively high yield.

Scheme 3- 6 An alternative route for bipyridine substituted triacetylene **20b** synthesis⁵³



In the final step, nicotinoyl chloride was added more than double amount to prevent the mono-substituted product. After chromatography purification, a pink solid was obtained. The single crystal of **20b** could be crystallized from the solvent CH_2Cl_2 /Hexane (1/1) by slow evaporation. Like the single crystal of **20a**, the crystal of **20b**

got darker in days. To date, only the preliminary single crystal data could be obtained, as shown in Table 3-4.

Table 3- 4 The preliminary crystal data for compound **20b**

Volume	a	b	c	α	β	γ
1731.36	7.408	12.558	19.0345	90	90	102.108

Figure 3- 13 Two forms of 3-pyridyl triacetylene **20b**. On the left: **20b** aggregated as a pink powder stick to the round flask. On the right: pink thin single crystal was obtained from the solvent ($\text{CH}_2\text{Cl}_2/\text{Hex}=1/1$).



3. Conclusion

The first successful polytriacetylene was obtained by thermal annealing via host-guest strategy. The second generation host molecule vinylogous amide and guest molecule carboxylic acid triacetylene were synthesized in good quality and quantity.

With host and guest in hand, we can prepare polytriacetylenes in a large scale that allows us for further chemical and physical studies.

The triacetylene molecule octa-2,4,6-triyn-1,8-diyl dinicotinate 20b can be synthesized successfully through a five-step route. The single crystal of this triacetylene could be grown but was still not suitable for XRD analysis. Efforts have been taken to optimize the existing synthesis route, but the Cadiot-Chodkiewicz cross-coupling could not be achieved due to the presence of the ester group.

IV. Future Work

1. Removal of the Host from Polytriacetylene

For the good solubility of vinylgous amides in water, it was proposed that washing the PTA with water could be a good method to remove the host from PTA. In Eilaf Ahmed's work⁴⁶, the polymers were washed with slightly heated water. And the IR spectra showed that there are still some traces of the host remained. The pure PTA could be obtained with HCl to eliminate the pyridine host and extracting the solid residue with methanol to clean up any unreacted triacetylene. After then, a red amorphous solid was obtained and there is no melting point observed up to 300°C. In addition, this pure polytriacetylene is insoluble in common organic, such as ethyl acetate, hexane, methanol, and ether.

2. Growing suitable single crystal of octa-2,4,6-triyn-1,8-diyl dinicotinate 20b

The previous experiment showed that we could get the clean crystal of triacetylene compound 20b, but they are not suitable for XRD analysis. The solvents system was used as CH₂Cl₂/Hexane (1/1), which can be evaporated slowly under room temperature. For the reason that 20b have a good solubility in CH₂Cl₂, CH₂Cl₂ was included in all of the solvent systems have been tried, such as CH₂Cl₂/Ether, CH₂Cl₂/Ethyl acetate, CH₂Cl₂/Methanol, CH₂Cl₂/Acetone and pure CH₂Cl₂. More

methods should be utilized to grow a crystal, for example, under the low temperature conditions (Figure 4-1).

Figure 4- 1 Low temperature condition for growing crystal



It would be very exciting to get the supramolecular structure of 20b through XRD data, which would provide us the chance to see the repeat distance, tilt angle and C1-C6 distance. All of these parameter could tell us whether it is good for 1,6-polymerization by thermal annealing.

V. Experimental Section

General Methods: NMR data were recorded with a Varian Gemini-300 MHz instrument using the solvent as an internal standard. The chemical shifts were reported in parts per million (ppm). Coupling constants were reported in hertz (Hz) and were recorded as being either singlet (s), doublet (d), doublet of doublet (dd), triplet (t), quartet (q), quintet (qt) or multiplet (m). Melting points were measured and recorded on Fisher-Johns melting point apparatus.

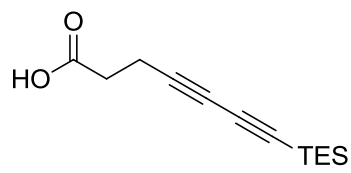
Crystals were obtained as described below, selected and mounted on glass fibers using epoxy cement. The crystals were optically centered on Bruker AXS diffractometer and X-ray data were collected using graphite-monochromated Mo and Cu radiation. Data were collected and structures were solved and refined using the Shelx crystallographic program package. Figures and structure analysis was done using Chem-Ray.

1. The synthesis of the Guest molecule

TES— \equiv —Br **1-Bromo-2-(triethylsilyl)ethyne (3)**⁵⁴. To the solution of triethyl-(ethynyl)silane (30mmol, 4.21g) in 150ml acetone, 1.1 NBS (33mmol, 5.9g) and 0.1 silver nitrite (3mmol, 0.51g) were added. This mixture was stirred at room temperature for 2 hours. The reaction mixture was diluted with hexane, and vacuum filtrate. The filtrate was concentrated and then passed through a column (hexane) to give a colorless oil 5.59g (85%). ¹HNMR (300m Hz, CDCl₃) δ 0.62 (dd, $J = 7.8$,

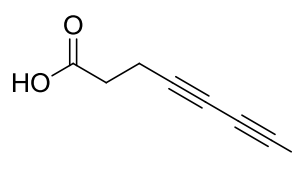
15.9 Hz, 6H, CH₂ in TES), 0.99 (t, *J* = 7.8 Hz, 9H, CH₃ in TES); ¹³C NMR (300 MHz, CDCl₃): δ 4.5 (CH₃), 7.6 (CH₂), 61.9, 84.9 (triple bond carbons).

General Procedure A for the preparation of the triacetylene acid by Cadiot-Chodkiewicz reaction⁴⁹: 0.1 equiv of the CuCl was added to the 10 equiv of 30% n-BuNH₂ aqueous solution. Keep adding in the hydroxylamine hydrochloride to discharge the blue color the mixture turns to. The mixture was cooled in the ice bath. 1 equiv of 4-Pentynoic acid **1** was added into the colorless reaction mixture. The additional hydroxylamine hydrochloride was added into the solution to prevent the mixture from turning blue. Then, 1.1 equiv of bromoalkyne which was diluted in the 10ml diethyl ether was added drop wise into the flask. After 15-30min, the ice bath was removed and the reaction was continued for another 2h. The reaction was quenched by adding the 2N HCl to adjust the solution to pH=2. Ethyl ether was used to extract the reaction mixture four times. The organic layer was dried by MgSO₄ and the solvent was removed to get the crude product.

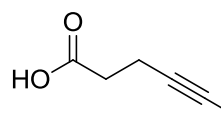


Hepta-7-triethylsilyl-4, 6-diynoic acid (4)⁵⁵. Following general procedure A, 1-Bromo-2-(triethylsilyl)ethyne (25.5mmol,5.59g) was allowed to react with 4-pentynoic acid (21.25mmol, 2.08g) yielding 3.67g of product (73%).

Hepta-7-triethylsilyl-4, 6-diynoic acid (**4**) is yellow oil: ^1H NMR (300 MHz, CDCl_3): δ 0.61 (dd, $J = 7.8, 15.9$ Hz, 6H, CH_2 in TES), 0.98 (t, $J = 7.8$ Hz, 9H, CH_3), 2.61 (s, 4H, CH_2). ^{13}C NMR (300 MHz, CDCl_3): δ 4.1 (CH_3), 7.3 (CH_2), δ 14.8 (CH_2), 32.4 (CH_2) 66.5, 76.3, 82.2, 88.8 (triple bond carbons), 176.8 ($\text{C}=\text{O}$).

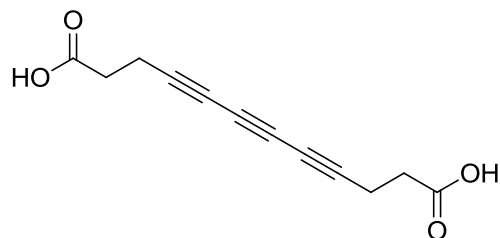


Hepta-4,6-diynoic acid (5)⁵⁵. To 3.67g Hepta-7-triethylsilyl-4,6-diynoic acid (**4**) (15.51mmol), 120ml diethyl ether was added as a solvent. 1M THF TBAF (15.5ml) was added into the reaction mixture at -15°C . Water was used to quench the reaction after 1h. Sodium hydride (6.25 N) was added to the flask to adjust the pH to 10. Then, the aqueous layer was acidified with hydrochloric (12N) acid to pH=2. The reaction mixture was extracted by ethyl ether 4 times. The combined organic layer was dried with magnesium sulfate and the solvent was removed to yield crude product. The crude product was further purified by chromatography (EA/Hexane=1/3) yielding 1.57g product (83%) as light yellow oil. ^1H NMR (300 MHz, CDCl_3): δ 2.00 (s, 1H, H in triple bond), 2.57-2.65 (m, 4H, CH_2 - CH_2); ^{13}C NMR (300 MHz, CDCl_3): δ 14.6 (CH_2), 32.5 (CH_2); 65.5, 68.0, 75.5, 80.5 (triple bond carbons), 177.7 ($\text{C}=\text{O}$).



Br **5-Bromo-4-pentynoic acid (6)**⁵⁶. To 1.57g 4-pentynoic acid (**1**)

(16mmol) in 40 ml acetone were added 3.13g *N*-bromosuccinimide and 0.27g silver nitrate. The reaction mixture was stirred at room temperature for 2 hours. 20ml water was added to the flask and the organic layer was extracted by dichloromethane 3 times. The combined organic layer was dried with magnesium sulfate. The combined organic solution was concentrated in vacuum to give the crude product. The residue was purified by chromatography (EA/Hexane= 1/2) to afford pure product 2.49g. ¹H NMR (300MHz, CDCl₃): δ 2.53-2.61 (m, CH₂) ¹³C NMR (300 MHz, CDCl₃): δ 15.24 (CH₂), 32.79 (CH₂), 69.24, 77.9 (triple bond carbons), 177.23(C=O).

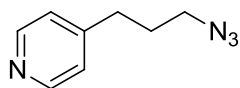


Dodeca-4,6,8-triynoic acid (7a)⁵².

Following the general procedure A, the hepta-4,6-diyynoic acid (**5**) (12.8mmol, 1.56g) and 5-bromo-4-pentynoic acid (**6**) (14.1mmol, 2.49g) reacted to afford the crude product. The crude product was purified by recrystallization to give a beige solid 2.23g (80%). This carboxylic acid is sensitive to the light and heat. It turns to dark if exposed to the air without protection. The dark color may be because of the polymerization process. ¹H NMR (400MHz, CD₃OD): δ 2.50-2.60 (dd, *J* = 4.8, 12.6

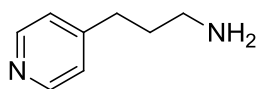
Hz, 4H in CH₂). ¹³CNMR (400 MHz, CD₃OD): δ 14.68 (CH₂), δ 32.25 (CH₂), 61.1, 66.3, 77.8 (triple bond carbons), δ175.1 (CO₂H).

2. The synthesis of the Host molecule



4-(3-Azidopropyl)-pyridine (10)^{46, 57}. Pyridyl propanol (**8**)

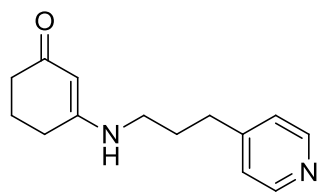
(20mmol, 2.74g) was refluxed 8h with 48% hydrobromic acid (27.3ml). The reaction mixture was concentrated in vacuum to give a brownish oil. After adding 5ml 25% sodium hydride, the viscous oil was dissolved in 70 mL of DMF. Then, sodium azide (1.3g) in 8ml water was added to the flask. The reaction was stirred around 95°C for 4h. Once cooled down, the 200ml water was added and extracted them with ethyl ether 5 times. The combined organic layer was collected and washed by sodium chloride solution. The solvent was reduced in vacuum to give a yellow oil (2.60g). ¹HNMR (300 MHz, CDCl₃) δ 1.87-1.96 (m, 2H, CH₂), 2.71 (t, *J* = 7.7 Hz, 2H, CH₂), 3.31 (t, *J* = 6.8 Hz, 2H, CH₂), 7.12 (d, *J* = 5.7 Hz, 2H, pyridyl hydrogen), 8.52 (d, *J* = 3.9 Hz, 2H, pyridyl hydrogen).



3-(4-Pyridyl)-propylamine (11)⁵⁸. To the solution of **10**

(16.0mmol, 2.60g) in 95% ethanol (100ml), Palladium-on-charcoal was used as the

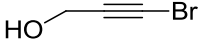
catalyst (5%, 200mg). The mixture was hydrogenated under 30 psi of hydrogen at room temperature. TLC was used to follow the reaction. The reaction was stopped when TLC showed only one spot. The residue was filtered through celite, and the filtrate was concentrated to get a yellow oil 1.96g (90%). ¹HNMR (300 MHz, CDCl₃) δ 1.597 (s, 2H, NH₂ coupled with OH), 1.73-1.83 (m, 2H, CH₂), 2.65 (t, *J* = 7.8 Hz, 2H, CH₂), 2.74 (t, *J* = 7.2 Hz, 2H, CH₂), 7.11 (d, *J* = 6.0 Hz, 2H, pyridyl hydrogen), 8.48 (d, *J* = 6.0 Hz, 2H, pyridyl hydrogen).



4-(3-Oxo-cyclohex-1-enylamino) propyl pyridine (13a)⁴⁶.

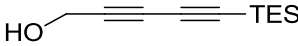
3-(4-pyridyl) –propylamine (**11**) (14.4mmol, 1.96g) and cyclohexanedione (**12**) (29mmol, 3.25g) in 35ml of benzene were refluxed for 8h with a Dean-Stark trap to remove the water. Benzene was removed under reduced pressure. The residue was purified by chromatography (CH₂Cl₂/MeOH= 8/1) to afford pure yellow crystal 2.79g (84%). Mp: 113-114°C; ¹HNMR (300 MHz, CDCl₃) δ 1.89-1.99 (m, 4H, CH₂), 2.27-2.33 (m, 4H, CH₂), 2.67 (t, *J* = 5.9 Hz, 2H, CH₂), 3.09-3.16 (m, 2H, CH₂), 4.76 (s, 1H, NH), 5.11 (s, 1H, C=CH), 7.11 (d, *J* = 6 Hz, 2H, d, pyridyl hydrogen), 8.50 (d, *J* = 6 Hz, 2H, pyridyl hydrogen). ¹³CNMR (300MHz, CDCl₃): δ 21.89 (CH₂), 28.82 (CH₂), 29.63 (CH₂), 32.56 (CH₂), 35.55 (CH₂), 42.26 (CH₂), 96.86 (=C-H), 123.71, 149.75, 149.97 (pyridyl carbons), 164.28 (=C-NH), 197.14 (C=O). X-ray qualified crystal was obtained by slow evaporation from EtOAc.

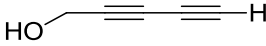
3. The synthesis of octa-2,4,6-triyn-1,8-diyl dinicotinate

 **3-bromoprop-2-yn-1-ol (21)**. A mixture of NBS (33mmol, 5.87g), propargyl alcohol (30mmol, 1.68g) and silver nitrate (3mmol, 0.51g) was stirred for 2h at room temperature. The solvent was removed in vacuum and the residue was dissolved in icy water (100ml) and ethyl ether (150ml). The aqueous layer was extracted with ethyl ether 5 times. The combined organic layer was collected and dried over with brine and sodium sulfate. The filtrate was concentrated to yield 3.36g of bromopropargyl alcohol (83%). ¹H NMR (300 MHz, CDCl₃) δ 1.88 (s, 1H in OH), 4.29 (s, 2H, CH₂); ¹³C NMR (300MHz, CDCl₃): δ 51.89 (CH₂), 45.94, 78.14 (C in triple bond).

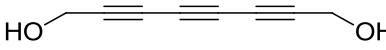
General Procedure B for the preparation of the triacetylene propargyl alcohol by Cadiot-Chodkiewicz reaction⁴⁹: At room temperature, CuCl (0.2 equiv.) was added into 30% butyl amine aqueous solution, which led to the formation of a blue solution fast. Crystals of hydroxylamine hydrochloride were added slowly until the blue color of the mixture was discharged. The color of the resulting colorless solution indicated the existence of Cu (I) cation. A yellow acetylide suspension was formed when triethylsilyl acetylene (1.2equiv.) was added into the colorless solution at room

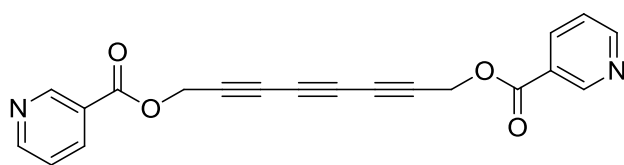
temperature. A ice-water bath to cool down the reaction mixture immediately. Once the bromopropargyl alcohol (1 equiv.) was added, the ice-water bath was removed. Additional crystals of hydroxylamine hydrochloride were occasionally added to prevent the solution from turning blue or green. 10 minutes later, the reaction mixture appeared to be rusty color. TLC showed one spot (EA/Hex= 1/9) which indicated the completeness of this reaction. The reaction mixture was repeatedly extracted with ether 5 times. And the crude product can be purified by flash chromatography (EA/Hex= 1/10) to give the pure compound.


5-(triethylsilyl)penta-2,4-diyne-1-ol (23). Following the general procedure A, 3-bromoprop-2-yn-1-ol (**21**) (24.9mmol, 3.36g) and triethyl(ethynyl)silane (**22**) (29.9mmol, 4.19g) reacted to give 3.05g product(83%). 5-(triethylsilyl)penta -2,4-diyne-1-ol as a yellow oil. ¹HNMR (300 MHz, CDCl₃) δ 0.58 (q, *J*=8.0Hz, 6H, CH₂ in TES), 0.94 (t, *J*=8.0Hz, 9H, CH₃ in TES), 4.28 (s, 2H, CH₂); ¹³CNMR (300MHz, CDCl₃): δ 4.42, 7.38 (C in TES) 51.44 (C in CH₂), 88.10, 86.23, 71.20, 75.30 (C in triple bond)


penta-2,4-diyne-1-ol (17)⁵⁹. To 3.05g 5-(triethylsilyl)penta -2,4-diyne-1-ol (**23**) (15.69mmol), 80ml diethyl ether was added as a solvent. 1M THF TBAF (15.7ml) and Sodium Hydride(6.25 N) were added into the reaction mixture at -15°C. After 2 hours, extract the reaction mixture by ethyl ether 4 times. The

combined organic layer was dried with magnesium sulfate and the solvent was removed to yield crude product. The crude product was further purified by chromatography (EA/Hexane=1/3) yielding 1.12g product as light yellow oil (89%). ¹HNMR (300 MHz, CDCl₃) δ 2.18 (s, 1H, terminal H), 2.33 (s, 1H in OH), 4.31 (s, 2H, CH₂); ¹³CNMR (300MHz, CDCl₃): δ 51.22 (C in CH₂), 67.29, 68.47, 69.94, 74.31 (C in triple bond)

 **octa-2,4,6-triyn-1,8-diol (19)**⁶⁰. Following the general procedure A, penta-2,4-diyne-1-ol (**17**) (13.96mmol, 1.12g) and 3-bromoprop-2-yn-1-ol (**18**) (11.63mmol, 1.57g) reacted to give 1.15g product (74%). octa-2,4,6-triyn-1,8-diol is pink solid. ¹HNMR (300 MHz, CDCl₃) δ 1.85 (s, 2H in OH), 2.70 (s, 2H, CH₂)



octa-2,4,6-triyn-1,8-diyl

dinicotinate (20b)⁵³. Excess of nicotinoyl chloride hydrochloride (21.53mmol, 3.04g) was added methylene chloride 20ml while the solution was stirred, dry Et₃N (3.2ml, 22.2mmol) was added as well. This reaction mixture was stirred at room temperature for a half hour. The octa-2,4,6-triyn-1,8-diol (**19**) (8.61mmol, 1.15g) dissolved in small amount of methylene chloride was added dropwisely to the reaction via pipette.

The reaction mixture was stirred overnight and quenched with water. Extract the reaction mixture by methylene chloride 4 times. The combined organic layer was dried with magnesium sulfate and removed the solvent under vacuum to yield crude product. The crude product could be purified by flash chromatography (EA/ Hex =1/2) to give octa-2,4,6-triyn-1,8-diyl dinicotinate pink solid 1.54g (52%). ¹HNMR (300 MHz, CDCl₃) δ 5.03 (s, 2H, CH₂), 7.42 (dd, *J*=5.1Hz, *J*=2.7Hz, 2H), 8.31(dt, *J*=7.8Hz, 2H), 8.81 (d, *J*=3.9Hz, 2H), 9.24 (s, 2H); ¹³CNMR (300MHz, CDCl₃): δ 53.06 (C in CH₂), 63.01, 71.62, 72.18 (C in triple bond), 123.41, 125.06, 137.30, 151.06, 153.94 (pyridyl carbons); 164.29 (C=O).

4. Growing crystals

Co-crystal **7a-13a**⁴⁶:

13.09 mg of compound **7a** and 13.82mg of **13a** (in a vial) were dissolved in EA by heating and stirring. A tiny amount of methanol was added to increase the solubility. The solvents were allowed to evaporate very slowly in a covered vial. After 4 days, there were some pink rock like crystals on the bottom of the vial. X-ray crystallography verified the structure of co-crystal 7a-13a with 2:1 ratio of host and guest respectively. Mp: 161-165°C

Single crystal **13a**⁴⁶:

15mg of compound **13a** was dissolved in ethyl acetate. The light yellow solvent

was added to a vial via an additional funnel. The resulting solvent was allowed to evaporate at room temperature in a covered vial. 2 days later, there were some light yellow crystals on the wall of vial. X-ray crystallography verified the structure of the host 13a. Mp 113-114°C.

Single crystal **20b**:

15mg of compound **20b** was dissolved in methylene chloride. The light yellow solvent was added to a vial via an additional funnel. Additional hexane was added slowly into the vial (CH₂Cl₂/Hexane=1/1). The resulting solvent was allowed to evaporate at room temperature in a covered vial. 2 days later, there were some pink crystals on the bottom of vial. X-ray crystallography verified the structure of this 3-pyridyl substituted triacetylene, 20b. This pink crystal turned to black when heated up to 158°C and showed no melting point up to 300°C.

Reference

1. (a) Miller, J. S., *Molecular Materials* .7. .B. Conducting Polymers - Materials of Commerce. *Adv Mater* **1993**, 5 (9), 671-676; (b) *Handbook of Conducting Polymers*. Dekker: New York, 1986; Vol. 1,2; (c) The Interconnection of Chemical and Electronic Structure. In *Conjugated Polymers and Related Materials*, W. R. Salaneck, I. L., B. Ranby, Ed. Oxford University Press: Oxford, 1993; (d) Liphardt, M.; Goonesekera, A.; Jones, B. E.; Ducharme, S.; Takacs, J. M.; Zhang, L., High-performance photorefractive polymers. *Science* **1994**, 263 (5145), 367-9; (e) Greenham, N. C.; Moratti, S. C.; Bradley, D. D. C.; Friend, R. H.; Holmes, A. B., Efficient Light-Emitting-Diodes Based on Polymers with High Electron-Affinities. *Nature* **1993**, 365 (6447), 628-630.
2. Chiang, C. K.; Fincher, C. R.; Park, Y. W.; Heeger, A. J.; Shirakawa, H.; Louis, E. J.; Gau, S. C.; Macdiarmid, A. G., Electrical-Conductivity in Doped Polyacetylene. *Phys. Rev. Lett.* **1977**, 39 (17), 1098-1101.
3. Bredas, J. L.; Beljonne, D.; Coropceanu, V.; Cornil, J., Charge-transfer and energy-transfer processes in pi-conjugated oligomers and polymers: A molecular picture. *Chem Rev* **2004**, 104 (11), 4971-5003.

4. Groenendaal, L.; Meijer, E.; Vekemans, J.; Müllen, K.; Wegner, G., *Electronic Materials: The Oligomer Approach*. Weinheim: Wiley: 1997.
5. Martin, R. E.; Diederich, F., Linear monodisperse pi-conjugated oligomers: Model compounds for polymers and more. *Angew. Chem.-Int. Edit.* **1999**, *38* (10), 1350-1377.
6. Roncali, J., Synthetic principles for bandgap control in linear pi-conjugated systems. *Chem Rev* **1997**, *97* (1), 173-205.
7. Tour, J. M., Conjugated macromolecules of precise length and constitution. Organic synthesis for the construction of nanoarchitectures. *Chem Rev* **1996**, *96* (1), 537-553.
8. Scherf, U.; Mullen, K., Design and Synthesis of Extended Pi-Systems - Monomers, Oligomers, Polymers. *Synthesis-Stuttgart* **1992**, (1-2), 23-38.
9. Mullen, K., Extended Pi-Systems in Conjugated Oligomers and Polymers - the Longer, the Better. *Pure Appl Chem* **1993**, *65* (1), 89-96.
10. (a) Horowitz, G., Organic field-effect transistors. *Adv Mater* **1998**, *10* (5), 365-377; (b) Huitema, H. E. A.; Gelinck, G. H.; van der Putten, J.; Kuijk, K. E.; Hart, K. M.; Cantatore, E.; de Leeuw, D. M., Active-matrix displays driven by solution processed polymeric transistors. *Adv Mater* **2002**, *14* (17), 1201-+; (c) Halls, J. J. M.; Walsh, C. A.; Greenham, N. C.; Marseglia, E. A.; Friend, R. H.; Moratti, S. C.; Holmes, A. B., Efficient Photodiodes from Interpenetrating Polymer Networks. *Nature* **1995**, *376* (6540), 498-500; (d) Brabec, C. J.; Sariciftci, N. S.; Hummelen, J.

- C., Plastic solar cells. *Advanced Functional Materials* **2001**, *11* (1), 15-26; (e) Zhou, Q.; Swager, T. M., Fluorescent chemosensors based on energy migration in conjugated polymers: The molecular wire approach to increased sensitivity. *Journal of the American Chemical Society* **1995**, *117* (50), 12593-12602; (f) McQuade, D. T.; Pullen, A. E.; Swager, T. M., Conjugated polymer-based chemical sensors. *Chem Rev* **2000**, *100* (7), 2537-2574; (g) McQuade, D. T.; Hegedus, A. H.; Swager, T. M., Signal amplification of a "turn-on" sensor: Harvesting the light captured by a conjugated polymer. *Journal of the American Chemical Society* **2000**, *122* (49), 12389-12390.
11. Burroughes, J. H.; Bradley, D. D. C.; Brown, A. R.; Marks, R. N.; Mackay, K.; Friend, R. H.; Burns, P. L.; Holmes, A. B., Light-Emitting-Diodes Based on Conjugated Polymers. *Nature* **1990**, *347* (6293), 539-541.
12. Wu, J. S.; Gherghel, L.; Watson, M. D.; Li, J. X.; Wang, Z. H.; Simpson, C. D.; Kolb, U.; Mullen, K., From branched polyphenylenes to graphite ribbons. *Macromolecules* **2003**, *36* (19), 7082-7089.
13. Baumann, H.; Martin, R. E.; Diederich, F., PM3 geometry optimization and CNDO/S-CI computation of UV/Vis spectra of large organic structures: Program description and application to poly(triacetylene) hexamer and taxotere. *Journal of Computational Chemistry* **1999**, *20* (4), 396-411.

14. Brédas, J. L., *Conjugated oligomers, polymers, and dendrimers: from polyacetylene to DNA: proceedings of the fourth Francqui Colloquium, 21-23 October 1998, Brussels*. De Boeck Supérieur: 1999; Vol. 4.
15. Babel, A.; Jenekhe, S. A., High electron mobility in ladder polymer field-effect transistors. *Journal of the American Chemical Society* **2003**, *125* (45), 13656-13657.
16. Yang, J. S.; Swager, T. M., Fluorescent porous polymer films as TNT chemosensors: Electronic and structural effects. *Journal of the American Chemical Society* **1998**, *120* (46), 11864-11873.
17. Mangel, T.; Eberhardt, A.; Scherf, U.; Bunz, U. H. F.; Mullen, K., Synthesis and Optical-Properties of Some Novel Arylene-Alkynylene Polymers. *Macromol Rapid Comm* **1995**, *16* (8), 571-580.
18. Weder, C.; Sarwa, C.; Montali, A.; Bastiaansen, C.; Smith, P., Incorporation of Photoluminescent Polarizers into Liquid Crystal Displays. *Science* **1998**, *279* (5352), 835-837.
19. Bunz, U. H. F., Poly(aryleneethynylene)s: Syntheses, properties, structures, and applications. *Chem Rev* **2000**, *100* (4), 1605-1644.
20. Bumm, L. A.; Arnold, J. J.; Cygan, M. T.; Dunbar, T. D.; Burgin, T. P.; Jones, L.; Allara, D. L.; Tour, J. M.; Weiss, P. S., Are single molecular wires conducting? *Science* **1996**, *271* (5256), 1705-1707.

21. Tour, J. M.; Wu, R.; Schumm, J. S., Extended orthogonally fused conducting oligomers for molecular electronic devices. *Journal of the American Chemical Society* **1991**, *113* (18), 7064-7066.
22. Yokoyama, A.; Miyakoshi, R.; Yokozawa, T., Chain-growth polymerization for poly(3-hexylthiophene) with a defined molecular weight and a low polydispersity. *Macromolecules* **2004**, *37* (4), 1169-1171.
23. Atwood, J. L. S., Jonathan W., *Supramolecular Chemistry*. John Wiley & Sons, Ltd: West Sussex PO19 1UD, England, 2000.
24. Rawn, D. J., *Biochemistry*. Paterson: Burlington, 1989.
25. Conn, M. M.; Rebek, J., Self-assembling capsules. *Chem Rev* **1997**, *97* (5), 1647-1668.
26. Jeffrey, G. A., *An Introduction to Hydrogen Bonding*. Oxford University Press: Oxford, 1997.
27. Kolotuchin, S. V.; Fenlon, E. E.; Wilson, S. R.; Loweth, C. J.; Zimmerman, S. C., Self-assembly of 1,3,5-benzenetricarboxylic acids (trimesic acids) and several analogues in the solid state. *Angew. Chem.-Int. Edit.* **1995**, *34* (23-24), 2654-2657.
28. Etter, M. C., Hydrogen-Bonds as Design Elements in Organic-Chemistry. *J Phys Chem-US* **1991**, *95* (12), 4601-4610.
29. Desiraju, G. R. S., T., *The Weak Hydrogen Bond In Structural Chemistry and Biology*. Oxford University Press Inc.: New York, 1999.

30. Burgi, H. B.; Dunitz, J. D., Can statistical analysis of structural parameters from different crystal environments lead to quantitative energy relationships? *Acta Crystallographica Section B* **1988**, *44* (4), 445-448.
31. Taylor, R.; Kennard, O., Crystallographic evidence for the existence of CH.cntdot..cntdot..cntdot.O, CH.cntdot..cntdot..cntdot.N and CH.cntdot..cntdot..cntdot.Cl hydrogen bonds. *Journal of the American Chemical Society* **1982**, *104* (19), 5063-5070.
32. Beijer, F. H.; Kooijman, H.; Spek, A. L.; Sijbesma, R. P.; Meijer, E. W., Self-complementarity achieved through quadruple hydrogen bonding. *Angew. Chem.-Int. Edit.* **1998**, *37* (1-2), 75-78.
33. Macdonald, J. C.; Whitesides, G. M., Solid-State Structures of Hydrogen-Bonded Tapes Based on Cyclic Secondary Diamides. *Chem Rev* **1994**, *94* (8), 2383-2420.
34. (a) Chang, Y. L.; West, M. A.; Fowler, F. W.; Lauher, J. W., An Approach to the Design of Molecular-Solids - Strategies for Controlling the Assembly of Molecules into 2-Dimensional Layered Structures. *Journal of the American Chemical Society* **1993**, *115* (14), 5991-6000; (b) Toledo, L. M.; Lauher, J. W.; Fowler, F. W., Design of Molecular-Solids - Application of 2-Amini-4(1h)-Pyridones to the Preparation of Hydrogen-Bonded Alpha-Networks and Beta-Networks. *Chem Mater* **1994**, *6* (8), 1222-1226; (c) Toledo, L. M.; Musa, K. M.; Lauher, J. W.; Fowler, F. W., Development of Strategies for the Preparation of Designed Solids - an Investigation of

the 2-Amino-4(1h)-Pyrimidone Ring-System for the Molecular Self-Assembly of Hydrogen-Bonded Alpha-Networks and Beta-Networks. *Chem Mater* **1995**, 7 (9), 1639-1647; (d) Coe, S.; Kane, J. J.; Nguyen, T. L.; Toledo, L. M.; Wininger, E.; Fowler, F. W.; Lauher, J. W., Molecular symmetry and the design of molecular solids: The oxalamide functionality as a persistent hydrogen bonding unit. *Journal of the American Chemical Society* **1997**, 119 (1), 86-93.

35. Russell, V. A.; Ward, M. D., Molecular Crystals with Dimensionally Controlled Hydrogen-Bonded Nanostructures. *Chem Mater* **1996**, 8 (8), 1654-1666.

36. (a) Aakeroy, C. B.; Nieuwenhuyzen, M., Hydrogen-Bonded Layers of Hydrogen Malate Anions - a Framework for Crystal Engineering. *Journal of the American Chemical Society* **1994**, 116 (24), 10983-10991; (b) Aakeroy, C. B.; Nieuwenhuyzen, M., Hydrogen bonding and structural motifs in organic L-malate(2-) salts. *Chem Mater* **1996**, 8 (6), 1229-1235.

37. Leiserowitz, L., Molecular Packing Modes - Carboxylic-Acids. *Acta Crystallogr B* **1976**, 32 (Mar15), 775-802.

38. (a) Kane, J. J.; Liao, R. F.; Lauher, J. W.; Fowler, F. W., Preparation of Layered Diacetylenes as a Demonstration of Strategies for Supramolecular Synthesis. *Journal of the American Chemical Society* **1995**, 117 (48), 12003-12004; (b) Fowler, F. W.; Lauher, J. W., A rational design of molecular materials. *Journal of Physical Organic Chemistry* **2000**, 13 (12), 850-857.

39. (a) Cohen, M. D.; Schmidt, G. M. J., 383. Topochemistry. Part I. A survey. *Journal of the Chemical Society (Resumed)* **1964**, 1996-2000; (b) Cohen, M. D.; Schmidt, G. M. J.; Sonntag, F. I., 384. Topochemistry. Part II. The photochemistry of trans-cinnamic acids. *Journal of the Chemical Society (Resumed)* **1964**, 2000-2013; (c) Schmidt, G. M. J., 385. Topochemistry. Part III. The crystal chemistry of some trans-cinnamic acids. *Journal of the Chemical Society (Resumed)* **1964**, 2014-2021.
40. Kohlschütter, V.; Haenni, P., Zur Kenntnis des Graphitischen Kohlenstoffs und der Graphitsäure. *Zeitschrift für anorganische und allgemeine Chemie* **1919**, *105* (1), 121-144.
41. Wegner, G., Topochemical Reactions of Monomers with Conjugated Triple Bonds .I. Polymerization of 2.4-Hexadiyn-1.6-Diols Deivatives in Crystalline State. *Z Naturforsch Pt B* **1969**, *B 24* (7), 824-&.
42. (a) Takahashi, S.; Miura, H.; Kasai, H.; Okada, S.; Oikawa, H.; Nakanishi, H., Single-crystal-to-single-crystal transformation of diolefin derivatives in nanocrystals. *Journal of the American Chemical Society* **2002**, *124* (37), 10944-10945; (b) Baughman, R. H., Solid-State Synthesis of Large Polymer Single-Crystals. *J Polym Sci Pol Phys* **1974**, *12* (8), 1511-1535.
43. Enkelmann, V., Solid-State Reactivity of Triacetylenes. *Chem Mater* **1994**, *6* (8), 1337-1340.
44. (a) Bunz, U. H. F., Polyynes-Fascinating Monomers for the Construction of Carbon Networks. *Angew Chem Int Edit* **1994**, *33* (10), 1073-1076; (b) Kiji, J.; Kaiser,

J.; Wegner, G.; Schulz, R. C., Solid-State Polymerization of Derivatives of 2,4,6-Octatriyne - .9. Topochemical Reactions of Monomers with Conjugated Triple Bonds. *Polymer* **1973**, *14* (9), 433-439.

45. (a) Anthony, J.; Boudon, C.; Diederich, F.; Gisselbrecht, J. P.; Gramlich, V.; Gross, M.; Hobi, M.; Seiler, P., Stable Soluble Conjugated Carbon Rods with a Persilylethynylated Polytriacetylene Backbone. *Angew Chem Int Edit* **1994**, *33* (7), 763-766; (b) Boldi, A. M.; Anthony, J.; Gramlich, V.; Knobler, C. B.; Boudon, C.; Gisselbrecht, J. P.; Gross, M.; Diederich, F., Acyclic Tetraethynylethene Molecular Scaffolding - Multinanometer-Sized Linearly Conjugated Rods with the Poly(Triacetylene) Backbone and Cross-Conjugated Expanded Dendralenes. *Helv. Chim. Acta* **1995**, *78* (4), 779-796; (c) Martin, R. E.; Mader, T.; Diederich, F., Monodisperse poly(triacetylene) rods: Synthesis of a 11.9 nm long molecular wire and direct determination of the effective conjugation length by UV/Vis and Raman spectroscopies. *Angew. Chem.-Int. Edit.* **1999**, *38* (6), 817-821; (d) Anthony, J.; Boldi, A. M.; Rubin, Y.; Hobi, M.; Gramlich, V.; Knobler, C. B.; Seiler, P.; Diederich, F., Tetraethynylethenes - Fully Cross-Conjugated Pi-Electron Chromophores and Molecular Scaffolds for All-Carbon Networks and Carbon-Rich Nanomaterials. *Helv. Chim. Acta* **1995**, *78* (1), 13-45.

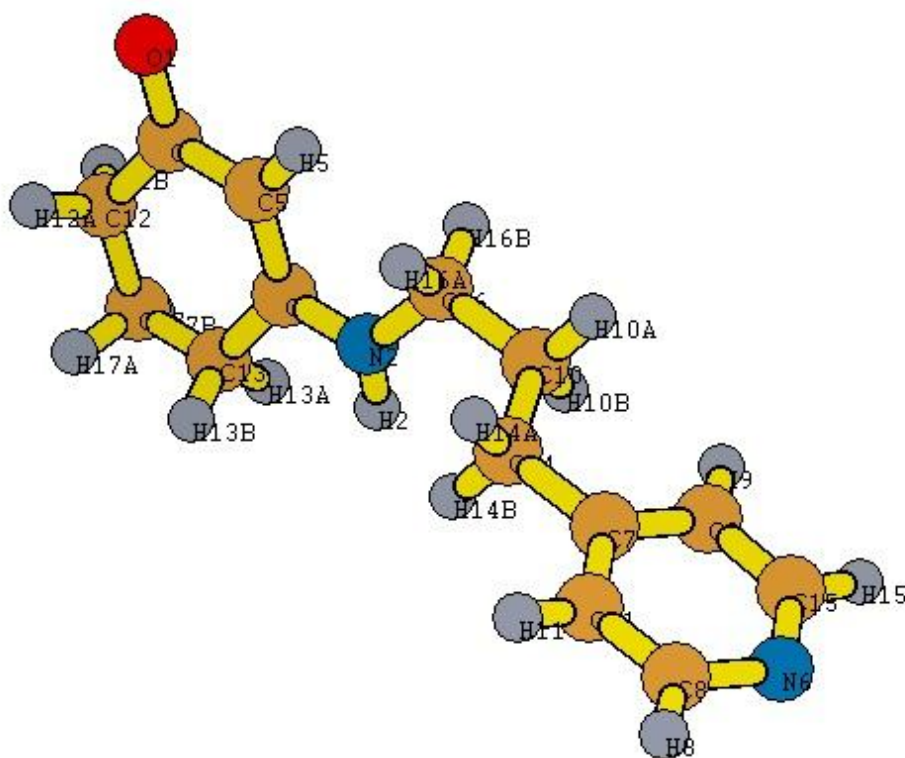
46. Ahmed, E., M.S. Thesis: Supramolecular design for a 1,6-topochemical polymerization of a triacetylene. **2005**.

47. Xiao, J.; Yang, M.; Lauher, J. W.; Fowler, F. W., A supramolecular solution to a long-standing problem: The 1,6-polymerization of a triacetylene. *Angew. Chem.-Int. Edit.* **2000**, *39* (12), 2132-+.
48. Hoang, T.; Lauher, J. W.; Fowler, F. W., The topochemical 1,16-polymerization of a triene. *Journal of the American Chemical Society* **2002**, *124* (36), 10656-10657.
49. Chodkiewicz, W.; Cadiot, P., Nouvelle Synthèse De Composés Polyacetyleniques Conjugués Symétriques Et Dissymétriques. *Cr Hebd Acad Sci* **1955**, *241* (16), 1055-1057.
50. Xiao, J., M.S. Thesis: The preparation of a polytriacetylene through a convergent host guest strategy. **1999**.
51. Liu, Y., M.S. Thesis: Supramolecular synthesis of ppolydiacetylenes and polytriacetylenes. **2001**.
52. Qian, J., M.S. Thesis: Supramolecular synthesis of polytriacetylenes using host-guest strategy. **2002**.
53. Ouyang, X., M.S. Thesis: Supramolecular synthesis of conjugated acetylene polymers using the host-guest strategy. **2003**.
54. Nie, X.; Wang, G., Synthesis and Self-Assembling Properties of Diacetylene-Containing Glycolipids. *The Journal of Organic Chemistry* **2006**, *71* (13), 4734-4741.
55. Ushakova, T. M., *Journal of Organic Chemistry USSR (English Translation)* **1968**, *4*, 242-244.

56. Krafft, G. A.; Katzenellenbogen, J. A., Synthesis of Halo Enol Lactones - Mechanism-Based Inactivators of Serine Proteases. *Journal of the American Chemical Society* **1981**, *103* (18), 5459-5466.
57. Hawes, E. M.; Davis, H. L., Intramolecular Nucleophilic Cyclization of 3-Substituted Pyridylalkylamines onto 2-Position of Pyridine Ring. *J. Heterocycl. Chem.* **1973**, *10* (1), 39-42.
58. Mayer, J. M.; Testa, B., Structural Factors Affecting the Basicity of Omega-Pyridylalkanols, Omega-Pyridylalkanamides and Omega-Pyridylalkylamines. *Helv. Chim. Acta* **1982**, *65* (6), 1868-1884.
59. Jones, E. R. H.; Thompson, J. M.; Whiting, M. C., Researches on Acetylenic Compounds .55. The Preparation and Properties of Some Polyacetylenic Acids and Their Derivatives. *Journal of the Chemical Society* **1957**, (May), 2012-2017.
60. Armitage, J. B.; Cook, C. L.; Jones, E. R. H.; Whiting, M. C., Researches on Acetylenic Compounds .36. The Synthesis of Symmetrical Conjugated Triacetylenic Compounds. *Journal of the Chemical Society* **1952**, (Jun), 2010-2014.

Appendix 1: Crystal Graphic Data

Molecular Structure and Crystallography Data for single crystal 13a



Crystal data and structure refinement for single crystal 13a

Empirical formula	C ₁₄ H ₁₈ N ₂ O
Formula weight	230.30
Temperature	293(2) K
Wavelength	0.71073 Å
Crystal system	Orthorhombic
Space group	P2(1)2(1)2
Unit cell dimensions	a = 9.1521(10) Å α = 90° b = 19.5172(14) Å β = 90° c = 7.2120(5) Å γ = 90°
Volume	1288.23(19) Å ³
Z	4
Density (calculated)	1.187 Mg/m ³
Absorption coefficient	0.076 mm ⁻¹
F(000)	496
Theta range for data collection	3.51 to 29.22°.
Index ranges	-11 ≤ h ≤ 9, -23 ≤ k ≤ 26, -5 ≤ l ≤ 9
Reflections collected	4178
Independent reflections	2816 [R(int) = 0.0222]
Completeness to theta = 29.22°	86.2 %
Absorption correction	None
Refinement method	Full-matrix least-squares on F ²
Data / restraints / parameters	2816 / 0 / 154
Goodness-of-fit on F ²	1.042
Final R indices [I > 2σ(I)]	R1 = 0.0692, wR2 = 0.1790
R indices (all data)	R1 = 0.1118, wR2 = 0.2192

Atomic coordinates (x 10⁴) and equivalent isotropic displacement parameters**(Å²x 10³)**

	x	y	z	U(eq)
O(1)	7852(3)	3794(1)	11026(3)	68(1)
N(2)	8115(4)	3239(1)	4682(4)	61(1)
C(3)	7762(4)	3960(2)	9371(4)	49(1)
C(4)	7893(4)	3671(2)	6074(4)	47(1)
C(5)	7974(4)	3494(2)	7905(4)	51(1)
N(6)	8071(5)	898(2)	-3095(5)	75(1)
C(7)	7726(4)	1633(2)	232(5)	52(1)
C(8)	6752(5)	1064(2)	-2407(6)	77(1)
C(9)	9064(4)	1461(2)	-470(5)	62(1)
C(10)	8821(5)	2159(2)	3164(5)	65(1)
C(11)	6548(5)	1427(2)	-781(5)	62(1)
C(12)	7416(6)	4689(2)	8886(4)	74(1)
C(13)	7571(6)	4401(2)	5552(4)	73(1)
C(14)	7490(5)	2028(2)	2035(6)	68(1)
C(15)	9184(5)	1103(2)	-2097(6)	71(1)
C(16)	8510(5)	2527(2)	4981(5)	70(1)
C(17)	7379(11)	4856(2)	6989(6)	168(4)

Anisotropic displacement parameters ($\text{\AA}^2 \times 10^3$)

	U ₁₁	U ₂₂	U ₃₃	U ₂₃	U ₁₃	U ₁₂
O(1)	99(2)	82(2)	24(1)	3(1)	0(1)	15(2)
N(2)	109(3)	49(1)	26(1)	-1(1)	-2(2)	3(2)
C(3)	63(2)	57(2)	26(1)	-2(1)	-1(1)	3(2)
C(4)	73(2)	44(2)	26(1)	-1(1)	0(2)	-4(2)
C(5)	76(2)	46(2)	30(1)	4(1)	0(2)	8(2)
N(6)	118(3)	64(2)	44(2)	-7(2)	-2(2)	-2(2)
C(7)	68(2)	44(2)	44(2)	-5(1)	2(2)	-2(2)
C(8)	106(4)	63(2)	61(3)	5(2)	-35(2)	-15(2)
C(9)	69(3)	64(2)	53(2)	-14(2)	0(2)	3(2)
C(10)	94(3)	60(2)	42(2)	-10(2)	-7(2)	14(2)
C(11)	69(3)	59(2)	59(2)	2(2)	-3(2)	-1(2)
C(12)	137(4)	50(2)	35(2)	-9(1)	-2(2)	13(2)
C(13)	146(4)	45(2)	29(1)	3(1)	-6(2)	9(2)
C(14)	84(3)	62(2)	58(2)	-15(2)	11(2)	0(2)
C(15)	88(3)	72(2)	54(2)	-9(2)	6(2)	10(2)
C(16)	119(3)	52(2)	39(2)	-5(2)	-5(2)	20(2)
C(17)	397(12)	67(3)	40(2)	6(2)	2(5)	78(5)

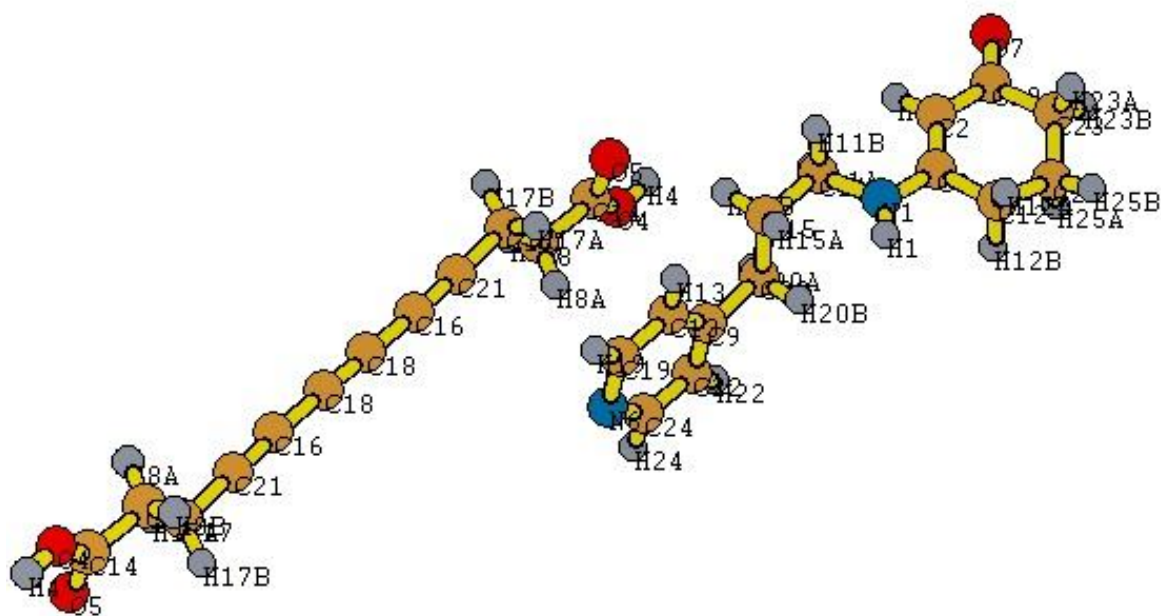
Bond lengths [Å]

O(1)-C(3)	1.240(3)
N(2)-C(4)	1.327(4)
N(2)-C(16)	1.452(4)
C(3)-C(5)	1.409(4)
C(3)-C(12)	1.498(4)
C(4)-C(5)	1.367(4)
C(4)-C(13)	1.503(4)
N(6)-C(15)	1.309(5)
N(6)-C(8)	1.345(6)
C(7)-C(11)	1.363(5)
C(7)-C(9)	1.366(5)
C(7)-C(14)	1.527(5)
C(8)-C(11)	1.383(6)
C(9)-C(15)	1.371(5)
C(10)-C(14)	1.487(6)
C(10)-C(16)	1.522(5)
C(12)-C(17)	1.407(5)
C(13)-C(17)	1.376(5)

Bond angles[°]

C(4)-N(2)-C(16)	122.3(3)
O(1)-C(3)-C(5)	123.0(3)
O(1)-C(3)-C(12)	119.2(3)
C(5)-C(3)-C(12)	117.8(3)
N(2)-C(4)-C(5)	124.2(3)
N(2)-C(4)-C(13)	116.3(2)
C(5)-C(4)-C(13)	119.5(3)
C(4)-C(5)-C(3)	123.7(3)
C(15)-N(6)-C(8)	115.0(3)
C(11)-C(7)-C(9)	116.0(3)
C(11)-C(7)-C(14)	119.6(3)
C(9)-C(7)-C(14)	124.5(3)
N(6)-C(8)-C(11)	123.9(4)
C(7)-C(9)-C(15)	120.9(4)
C(14)-C(10)-C(16)	113.5(3)
C(7)-C(11)-C(8)	119.9(4)
C(17)-C(12)-C(3)	116.9(3)
C(17)-C(13)-C(4)	116.6(3)
C(10)-C(14)-C(7)	115.9(3)
N(6)-C(15)-C(9)	124.3(4)
N(2)-C(16)-C(10)	111.8(3)
C(13)-C(17)-C(12)	125.4(4)

Molecular Structure and Crystallography Data for 7a-13a Co-crystal



Crystal data and structure refinement for Co-crystal 7a-13a

Empirical formula	C ₄₀ H ₄₆ N ₄ O ₆	
Formula weight	678.81	
Temperature	293(2) K	
Wavelength	0.71073 Å	
Crystal system	Triclinic	
Space group	P-1	
Unit cell dimensions	a = 7.2490(3) Å	α = 102.357(4) °
	b = 11.1567(5) Å	β = 91.924(4) °
	c = 11.5393(5) Å	γ = 94.771(4) °
Volume	907.19(7) Å ³	
Z	1	
Density (calculated)	1.242 Mg/m ³	
Absorption coefficient	0.084 mm ⁻¹	
F(000)	362	
Theta range for data collection	3.24 to 32.97°.	
Index ranges	-11 ≤ h ≤ 11, -16 ≤ k ≤ 16, -17 ≤ l ≤ 17	
Reflections collected	25620	
Independent reflections	6336 [R(int) = 0.0648]	
Completeness to theta = 32.97°	93.0 %	
Refinement method	Full-matrix least-squares on F ²	
Data / restraints / parameters	6336 / 0 / 226	
Goodness-of-fit on F ²	1.010	
Final R indices [I > 2σ(I)]	R1 = 0.0829, wR2 = 0.2015	
R indices (all data)	R1 = 0.1932, wR2 = 0.2759	

Atomic coordinates (x 10⁴) and equivalent isotropic displacement parameters**(Å²x 10³)**

	x	y	z	U(eq)
N(1)	4575(2)	7776(2)	2728(2)	52(1)
C(2)	7785(3)	7920(2)	2370(2)	46(1)
C(3)	5984(3)	8069(2)	2098(2)	43(1)
O(4)	4173(3)	7645(2)	7970(2)	75(1)
O(5)	3547(3)	5762(2)	6863(2)	71(1)
N(6)	-2811(3)	7793(2)	6755(2)	60(1)
O(7)	10887(2)	8062(2)	1910(2)	78(1)
C(8)	1514(3)	6517(2)	8382(2)	52(1)
C(9)	444(3)	7969(2)	5540(2)	50(1)
C(10)	9252(3)	8202(2)	1674(2)	52(1)
C(11)	4810(3)	7197(3)	3736(2)	58(1)
C(12)	5475(3)	8565(3)	1039(2)	63(1)
C(13)	-615(4)	6860(2)	5438(2)	58(1)
C(14)	3182(3)	6585(2)	7664(2)	50(1)
C(15)	2976(4)	6965(2)	4284(2)	58(1)
C(16)	-2686(3)	5127(2)	9167(2)	59(1)
C(17)	472(3)	5256(3)	8095(2)	61(1)
C(18)	-4313(3)	5041(2)	9740(2)	58(1)
C(19)	-2225(3)	6813(2)	6053(2)	58(1)
C(20)	2217(4)	8119(2)	4911(2)	62(1)
C(21)	-1259(4)	5189(2)	8689(2)	59(1)
C(22)	-196(4)	8978(3)	6258(2)	67(1)
C(23)	8779(4)	8654(3)	585(3)	74(1)

C(24)	-1794(4)	8847(3)	6849(3)	72(1)
C(25)	7019(4)	9162(4)	550(3)	97(1)

Anisotropic displacement parameters ($\text{\AA}^2 \times 10^3$)

	U11	U22	U33	U23	U13	U12
N(1)	30(1)	78(1)	54(1)	29(1)	9(1)	11(1)
C(2)	35(1)	55(1)	53(1)	18(1)	5(1)	10(1)
C(3)	30(1)	57(1)	43(1)	14(1)	6(1)	6(1)
O(4)	60(1)	77(1)	80(1)	2(1)	33(1)	-10(1)
O(5)	69(1)	69(1)	74(1)	9(1)	34(1)	5(1)
N(6)	47(1)	71(1)	61(1)	15(1)	17(1)	-1(1)
O(7)	29(1)	107(2)	108(2)	41(1)	10(1)	15(1)
C(8)	42(1)	63(2)	52(1)	14(1)	14(1)	6(1)
C(9)	42(1)	63(2)	48(1)	16(1)	9(1)	3(1)
C(10)	32(1)	53(1)	72(2)	16(1)	10(1)	8(1)
C(11)	45(1)	76(2)	60(1)	29(1)	14(1)	15(1)
C(12)	37(1)	101(2)	65(2)	42(2)	10(1)	19(1)
C(13)	59(2)	57(1)	61(1)	17(1)	18(1)	11(1)
C(14)	43(1)	61(2)	48(1)	18(1)	10(1)	7(1)
C(15)	55(2)	64(2)	61(1)	23(1)	21(1)	5(1)
C(16)	45(1)	60(2)	71(2)	18(1)	7(1)	-5(1)
C(17)	49(1)	70(2)	61(2)	11(1)	17(1)	2(1)
C(18)	41(1)	59(2)	74(2)	20(1)	9(1)	-4(1)
C(19)	49(1)	59(2)	69(2)	21(1)	11(1)	-1(1)
C(20)	54(2)	69(2)	65(2)	17(1)	23(1)	2(1)
C(21)	48(1)	64(2)	65(2)	14(1)	9(1)	-3(1)
C(22)	63(2)	61(2)	72(2)	1(1)	27(1)	-7(1)
C(23)	48(2)	101(2)	93(2)	54(2)	30(1)	22(1)
C(24)	64(2)	68(2)	78(2)	1(1)	30(1)	-1(1)

C(25) 56(2) 157(3) 113(3) 97(3) 21(2) 24(2)

Bond lengths [Å]

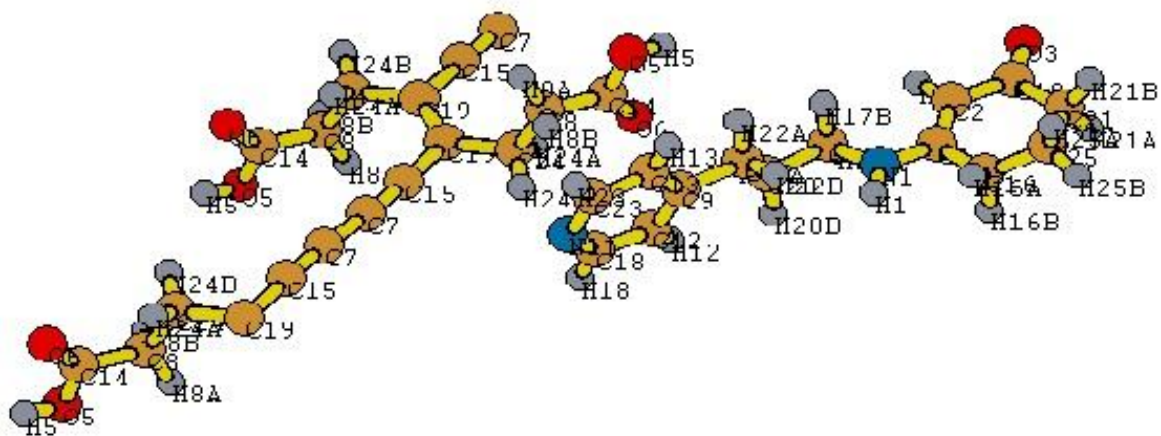
N(1)-C(3)	1.333(3)
N(1)-C(11)	1.457(3)
C(2)-C(3)	1.364(3)
C(2)-C(10)	1.408(3)
C(3)-C(12)	1.493(3)
O(4)-C(14)	1.305(3)
O(5)-C(14)	1.209(3)
N(6)-C(24)	1.316(3)
N(6)-C(19)	1.325(3)
O(7)-C(10)	1.237(3)
C(8)-C(14)	1.494(3)
C(8)-C(17)	1.506(3)
C(9)-C(22)	1.372(4)
C(9)-C(13)	1.382(3)
C(9)-C(20)	1.511(3)
C(10)-C(23)	1.491(4)
C(11)-C(15)	1.518(3)
C(12)-C(25)	1.447(4)
C(13)-C(19)	1.389(3)
C(15)-C(20)	1.493(4)
C(16)-C(21)	1.192(3)
C(16)-C(18)	1.378(3)
C(17)-C(21)	1.454(3)
C(18)-C(18)#1	1.187(4)
C(22)-C(24)	1.377(3)
C(23)-C(25)	1.442(4)

Bond angles[°]

C(3)-N(1)-C(11)	122.72(19)
C(3)-C(2)-C(10)	122.7(2)
N(1)-C(3)-C(2)	123.5(2)
N(1)-C(3)-C(12)	115.60(18)
C(2)-C(3)-C(12)	120.92(19)
C(24)-N(6)-C(19)	116.9(2)
C(14)-C(8)-C(17)	112.2(2)
C(22)-C(9)-C(13)	116.4(2)
C(22)-C(9)-C(20)	119.6(2)
C(13)-C(9)-C(20)	124.0(2)
O(7)-C(10)-C(2)	123.2(2)
O(7)-C(10)-C(23)	119.2(2)
C(2)-C(10)-C(23)	117.6(2)
N(1)-C(11)-C(15)	111.5(2)
C(25)-C(12)-C(3)	114.4(2)
C(9)-C(13)-C(19)	119.9(2)
O(5)-C(14)-O(4)	123.5(2)
O(5)-C(14)-C(8)	123.8(2)
O(4)-C(14)-C(8)	112.7(2)
C(20)-C(15)-C(11)	113.3(2)
C(21)-C(16)-C(18)	178.5(3)
C(21)-C(17)-C(8)	113.7(2)
C(18)#1-C(18)-C(16)	178.1(4)
N(6)-C(19)-C(13)	123.0(2)
C(15)-C(20)-C(9)	116.8(2)
C(16)-C(21)-C(17)	179.4(3)
C(9)-C(22)-C(24)	120.0(2)
C(25)-C(23)-C(10)	116.1(2)

N(6)-C(24)-C(22)	123.9(3)
C(23)-C(25)-C(12)	117.4(3)

Molecular Structure and Crystallography Data for 7a-13a polymer



Crystal data and structure refinement for polymer7a-13a

Empirical formula	C ₄₀ H ₄₆ N ₄ O ₆	
Formula weight	678.81	
Temperature	293(2) K	
Wavelength	0.71073 Å	
Crystal system	Triclinic	
Space group	P-1	
Unit cell dimensions	a = 7.2764(5) Å	α = 101.866(6)?
	b = 11.0017(8) Å	β = 91.368(5)?
	c = 11.6721(7) Å	γ = 97.283(6)?
Volume	905.84(11) Å ³	
Z	1	
Density (calculated)	1.244 Mg/m ³	
Absorption coefficient	0.084 mm ⁻¹	
F(000)	362	
Theta range for data collection	3.26 to 29.56°.	
Index ranges	-10 ≤ h ≤ 9, -15 ≤ k ≤ 14, -15 ≤ l ≤ 16	
Reflections collected	19796	
Independent reflections	4566 [R(int) = 0.0983]	
Completeness to theta = 29.56	90.0 %	
Absorption correction	None	
Refinement method	Full-matrix least-squares on F ²	
Data / restraints / parameters	4566 / 0 / 226	
Goodness-of-fit on F ²	1.014	
Final R indices [I > 2σ(I)]	R1 = 0.0915, wR2 = 0.2334	
R indices (all data)	R1 = 0.2041, wR2 = 0.3087	

Atomic coordinates ($\times 10^4$) and equivalent isotropic displacement parameters ($\text{\AA}^2 \times 10^3$)

	x	y	z	U(eq)
N(1)	599(4)	2259(3)	7259(2)	63(1)
C(2)	-2618(4)	2111(3)	7611(3)	55(1)
O(3)	-5734(3)	1952(3)	8054(3)	83(1)
C(4)	-842(4)	1938(3)	7883(3)	53(1)
O(5)	1071(4)	2326(3)	2103(2)	87(1)
O(6)	1863(4)	4267(3)	3096(3)	87(1)
C(7)	9098(5)	4977(3)	123(3)	65(1)
C(8)	3691(5)	3423(3)	1536(3)	60(1)
C(9)	4729(5)	2071(3)	4490(3)	58(1)
C(10)	-4117(4)	1801(3)	8296(3)	58(1)
N(11)	8010(4)	2250(3)	3296(3)	69(1)
C(12)	5878(5)	3185(4)	4615(3)	67(1)
C(13)	5301(5)	1045(4)	3763(4)	75(1)
C(14)	2129(5)	3408(3)	2329(3)	58(1)
C(15)	7476(5)	4943(3)	312(4)	67(1)
C(16)	-390(5)	1415(4)	8906(4)	73(1)
C(17)	424(5)	2844(4)	6270(4)	75(1)
C(18)	7502(5)	3227(4)	4005(3)	68(1)
C(19)	5545(4)	4927(3)	457(3)	64(1)
C(20)	2252(5)	3072(4)	5700(3)	70(1)
C(21)	-3693(5)	1299(5)	9349(4)	87(1)
C(22)	2935(6)	1912(4)	5103(3)	74(1)
C(23)	6919(6)	1176(4)	3196(4)	83(1)
C(24)	4778(5)	4714(4)	1605(3)	69(1)
C(25)	-1947(6)	944(7)	9479(5)	135(3)

Anisotropic displacement parameters ($\text{\AA}^2 \times 10^3$)

	U11	U22	U33	U23	U13	U12
N(1)	36(2)	100(2)	63(2)	32(2)	12(1)	19(1)
C(2)	35(2)	76(2)	59(2)	22(2)	8(1)	14(2)
O(3)	31(1)	113(2)	112(2)	35(2)	8(1)	19(1)
C(4)	32(2)	76(2)	54(2)	16(2)	10(1)	11(2)
O(5)	68(2)	85(2)	100(2)	5(2)	43(2)	-6(2)
O(6)	89(2)	82(2)	87(2)	9(2)	38(2)	6(2)
C(7)	31(2)	67(2)	99(3)	20(2)	8(2)	2(2)
C(8)	46(2)	70(2)	64(2)	17(2)	14(2)	8(2)
C(9)	46(2)	71(2)	60(2)	23(2)	12(2)	7(2)
C(10)	34(2)	66(2)	78(2)	20(2)	9(2)	10(2)
N(11)	54(2)	79(2)	77(2)	21(2)	19(2)	5(2)
C(12)	57(2)	73(2)	73(2)	17(2)	20(2)	17(2)
C(13)	60(2)	71(2)	86(3)	4(2)	28(2)	-5(2)
C(14)	52(2)	60(2)	64(2)	17(2)	13(2)	9(2)
C(15)	29(2)	72(2)	100(3)	18(2)	11(2)	0(2)
C(16)	41(2)	109(3)	84(3)	45(2)	12(2)	24(2)
C(17)	50(2)	108(3)	79(3)	35(2)	19(2)	22(2)
C(18)	48(2)	73(3)	86(3)	29(2)	12(2)	5(2)
C(19)	35(2)	71(2)	86(3)	17(2)	15(2)	6(2)
C(20)	59(2)	82(3)	73(2)	22(2)	24(2)	10(2)
C(21)	53(2)	118(3)	113(3)	62(3)	38(2)	26(2)
C(22)	62(2)	90(3)	72(2)	18(2)	26(2)	9(2)
C(23)	64(3)	84(3)	93(3)	2(2)	37(2)	5(2)
C(24)	50(2)	76(2)	74(2)	13(2)	8(2)	-6(2)
C(25)	53(3)	248(7)	154(5)	144(5)	30(3)	36(4)

Bond lengths [Å]

N(1)-C(4)	1.343(4)
N(1)-C(17)	1.442(5)
C(2)-C(4)	1.370(4)
C(2)-C(10)	1.417(5)
O(3)-C(10)	1.243(4)
C(4)-C(16)	1.475(5)
O(5)-C(14)	1.308(4)
O(6)-C(14)	1.199(4)
C(7)-C(15)	1.203(5)
C(7)-C(7)#1	1.347(7)
C(8)-C(14)	1.484(5)
C(8)-C(24)	1.521(5)
C(9)-C(12)	1.372(5)
C(9)-C(13)	1.382(5)
C(9)-C(22)	1.512(5)
C(10)-C(21)	1.487(5)
N(11)-C(18)	1.315(5)
N(11)-C(23)	1.319(5)
C(12)-C(18)	1.395(5)
C(13)-C(23)	1.371(5)
C(15)-C(19)	1.417(5)
C(16)-C(25)	1.424(6)
C(17)-C(20)	1.517(5)
C(19)-C(19)#2	1.363(7)
C(19)-C(24)	1.514(5)
C(20)-C(22)	1.474(5)
C(21)-C(25)	1.390(6)

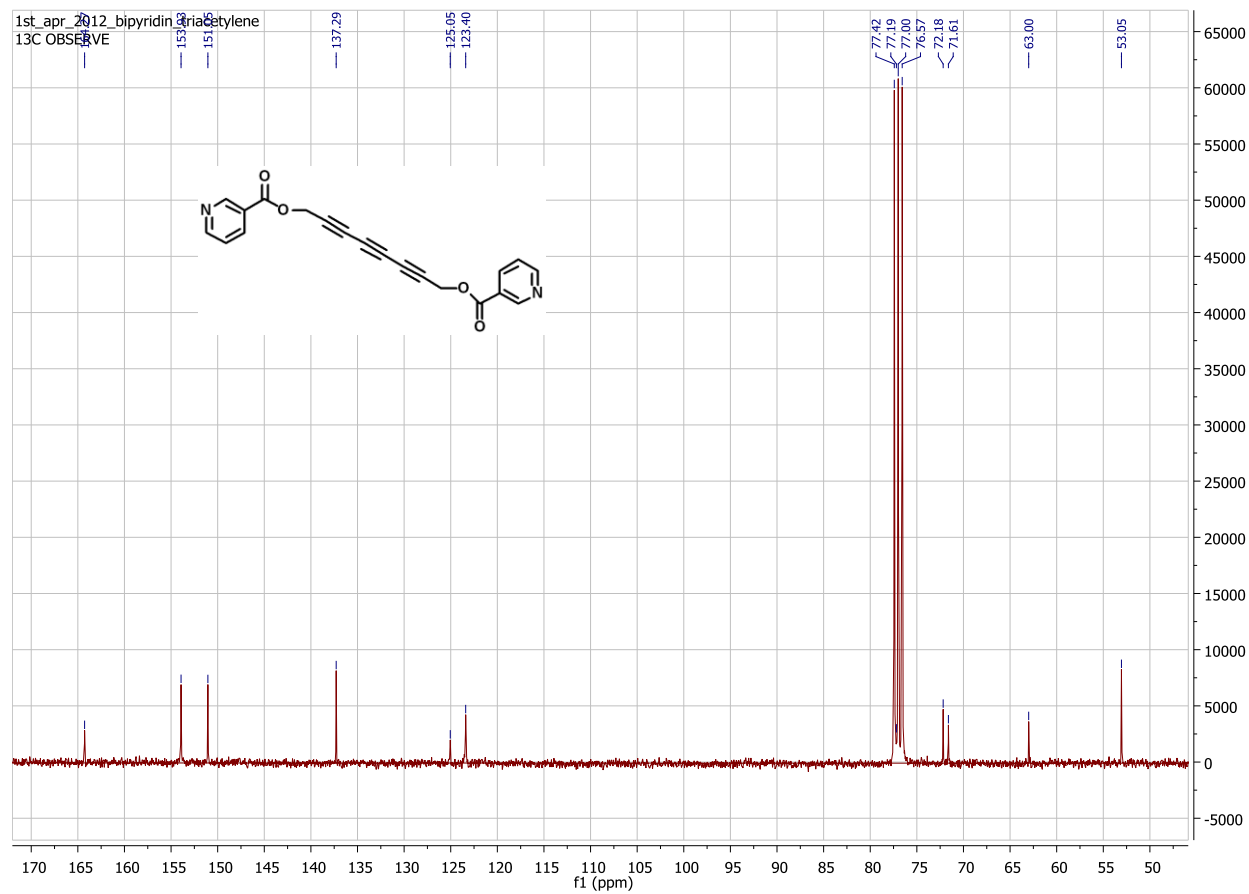
Bond angles[°]

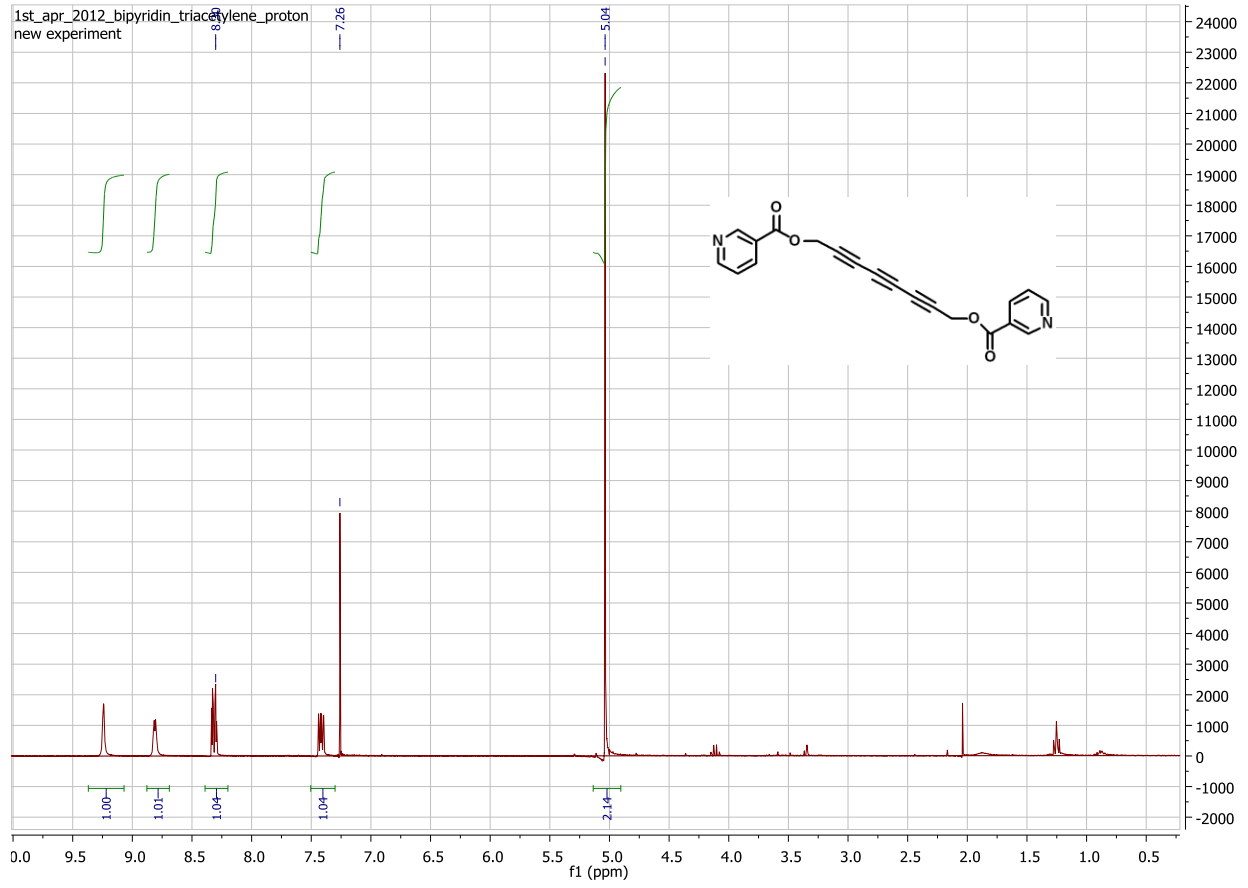
C(4)-N(1)-C(17)	123.2(3)
C(4)-C(2)-C(10)	121.8(3)
N(1)-C(4)-C(2)	122.4(3)
N(1)-C(4)-C(16)	115.9(3)
C(2)-C(4)-C(16)	121.7(3)
C(15)-C(7)-C(7)#1	178.1(6)
C(14)-C(8)-C(24)	114.3(3)
C(12)-C(9)-C(13)	116.3(3)
C(12)-C(9)-C(22)	124.2(3)
C(13)-C(9)-C(22)	119.5(3)
O(3)-C(10)-C(2)	122.2(3)
O(3)-C(10)-C(21)	120.2(3)
C(2)-C(10)-C(21)	117.6(3)
C(18)-N(11)-C(23)	116.7(3)
C(9)-C(12)-C(18)	119.5(3)
C(23)-C(13)-C(9)	120.1(4)
O(6)-C(14)-O(5)	123.5(3)
O(6)-C(14)-C(8)	125.0(3)
O(5)-C(14)-C(8)	111.6(3)
C(7)-C(15)-C(19)	176.0(5)
C(25)-C(16)-C(4)	115.3(3)
N(1)-C(17)-C(20)	112.5(3)
N(11)-C(18)-C(12)	123.6(4)
C(19)#2-C(19)-C(15)	118.3(4)
C(19)#2-C(19)-C(24)	122.9(4)
C(15)-C(19)-C(24)	118.8(3)
C(22)-C(20)-C(17)	113.6(3)
C(25)-C(21)-C(10)	118.2(3)

C(20)-C(22)-C(9)	116.4(3)
N(11)-C(23)-C(13)	123.7(4)
C(19)-C(24)-C(8)	114.5(3)
C(21)-C(25)-C(16)	122.2(4)

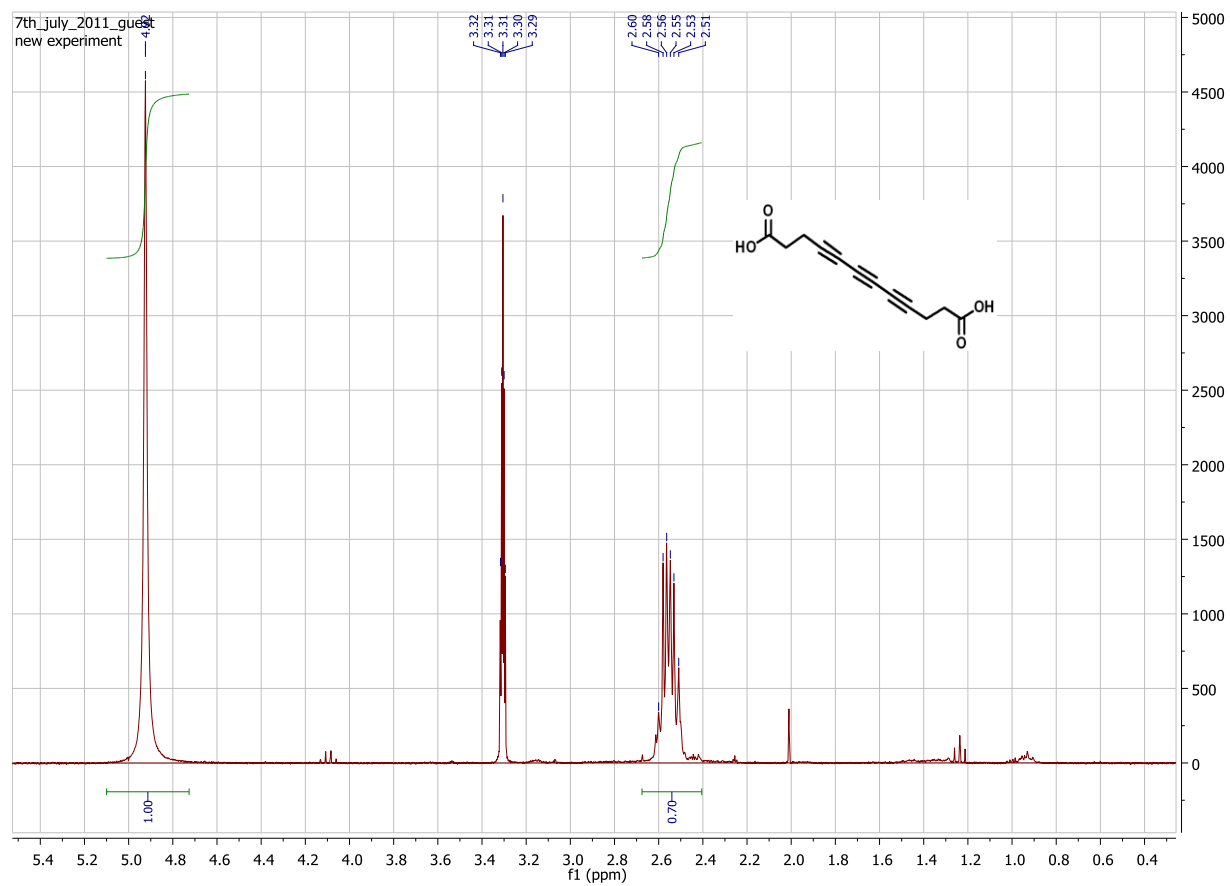
Appendix 2: NMR Spectra Data

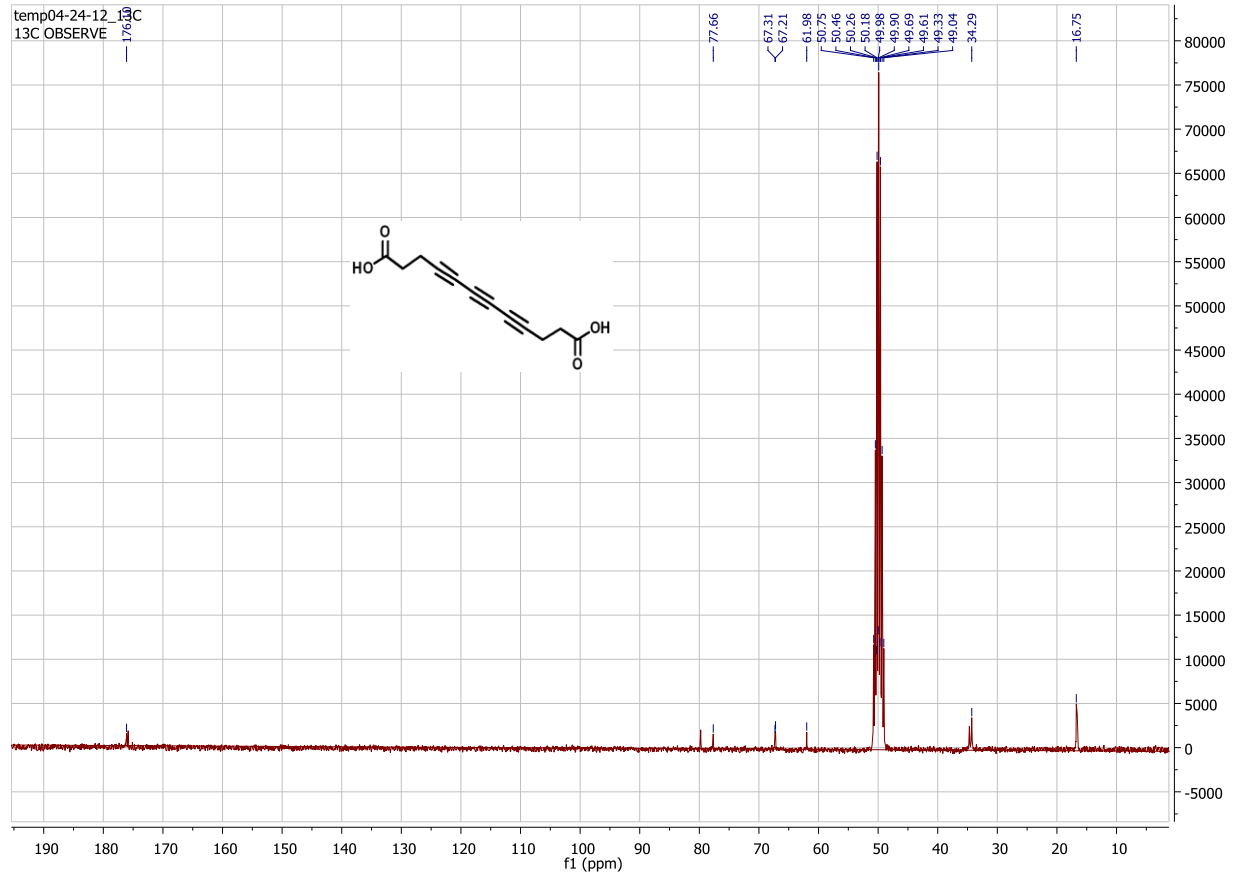
^1H NMR (above) and ^{13}C NMR (below) spectra for product **20b** (CDCl_3)





^1H NMR (above) and ^{13}C NMR (below) spectra for product **7a** (CD_3OD)





^1H NMR (above) and ^{13}C NMR (below) spectra for product **13a** (CDCl_3)

